NASA Contractor Report 158980

INTEGRATED ENERGY MANAGEMENT STUDY

ENERGY EFFICIENT TRANSPORT PROGRAM

BOEING COMMERCIAL AIRPLANE COMPANY,
P.O. BOX 3707, SEATTLE, WA 98124

CONTRACT NAS1-14742, TASK 4.2
MARCH 1979

National Aeronautics and
Space Administration

Langley Research Center
Hampton, Virginia 23665

FOREWORD

This document constitutes the final report for Task 4.2 Integrated Energy Management (IEM), one of five major tasks covered by the Statement of Work for Contract NAS1-14742, Energy Efficient Transport Program. In total, Task 4.2 encompassed five significant areas of investigation (1) collection and reduction of in-flight measurement data of current operating procedures and performance of a 727-200 airplane, (2) selection of typical flights for evaluation, (3) simulation of typical flights in a fast-time simulation, (4) development of energy management algorithms, and (5) algorithm assessment in the simulation. The report covers work conducted from August 1977 through June 1978. The NASA Technical Monitor for all contract tasks was Mr. D. B. Middleton of the Energy Efficient Transport Project Office at Langley Research Center.

The investigations were conducted within the Systems Technology and the Preliminary Design Departments of the Vice President-Engineering organization of the Boeing Commercial Airplane Company. Contractor personnel who participated and their area of contribution are:

G. W. Hanks	Program Manager
R. L. Erwin, Jr.	Task Manager
R. W. Schwab	Algorithm Development and Evaluation
J. McLaren	Aero Performance
M. D. Taylor	Flight Controls
D. A. Hunter	Evaluation Model Development
J. L Thompson	In-Flight Data Reduction
B. F. Itzen	Chebychev Trajectory Optimization

In-flight measurement data were provided by United Airlines. The data were reduced and transmitted to the Contractor by C. H. Humphrey and O. R. Evans, Maintenance Operations, United Airlines, San Francisco.

Principal measurements and calculations used during this study were in customary units.

This Page Intentionally Left Blank

CONTENTS

FIGURES

TABLES

1.0 SUMMARY

The objective of the Integrated Energy Management (IEM) study was to assess the feasibility and practicality of a closed-loop energy management system for transport aircraft. The IEM closed-loop concept involves the on-board sensing of a best energy operating state and the generation and execution of autopilot and autothrottle commands to achieve the best state. The pilot monitors the IEM system output and has a manual override capability, if required. The sensing of the best energy state is through an in-flight sampling process to derive the desired guidance values

The IEM system objective is to minimize trip fuel with direct operating costs, scheduling and air traffic control secondary considerations. The study involved (1) the instrumentation and collection of in-flight data from a United Airlines 727-200 flying 80 revenue flights in the United Airlines network, (2) analysis of the in-flight data to select representative city pairs and establish operational procedures employed in flying a reference flight, (3) simulation of the reference flight profile in a fast-time model to verify the model and establish performance values against which to measure IEM benefits, (4) development of IEM algorithms and (5) assessment of the IEM concept. The basic findings of the study were.

- The IEM techniques investigated provided significant fuel savings, at the expense of increased trip time, for the 727-200 in typical airline operations. Fuel required for the study reference flight of 1087 km (587 nmi) was 5% less than for the same flight using conventional (handbook reference data and pilot control) procedures; however, trip time increased 12% Fuel savings of 4.8% were projected for the spectrum of 80 United Airlines route segments.

- The selected energy guidance technique compared favorably with handbook schedules, optimized calibrated airspeed/Mach techniques and more complex calculus-of-variations optimization techniques. Energy guidance uses the concept of specific energy (the sum of the aircraft kinetic and potential energies divided by the aircraft weight). The climb strategy was to maximize rate of change of energy per unit fuel weight. The cruise strategy was to maximize specific range. The descent strategy was to minimize rate of change of energy per unit fuel weight.

- The concept of an on-board sensed, closed-loop optimization technique for climb and descent was determined infeasible. The mechanization of the IEM guidance algorithms for climb and descent required stored performance values of thrust, drag and fuel flow. The climb and descent algorithms were combined with engine pressure ratio schedules and an airspeed-hold-mode autopilot to automatically control attitude and thrust in climb and descent.

- A closed-loop, on-board sensed mechanization for cruise control was investigated and appears feasible. An assessment indicated a fuel savings of about 3% over conventional cruise procedures. A cruise algorithm, used in conjunction with an airspeed-hold-mode autothrottle and an altitude-hold-mode autopilot, was developed that operates in three modes· search, acquire and monitor. The search mode samples specific range values (using measured velocity, acceleration and fuel flow data). When an optimum is located,

an error signal is generated for the autothrottle. When the optimum velocity is acquired, the IEM logic zeros the error signal to the autothrottle, fixing the thrust-lever position. The algorithm monitors speed, weight and fuel flow. When required, a new search or acquire mode is initiated.

The IEM algorithms were developed to generate minimum fuel trajectories. The IEM fuel saving benefits are referenced against fuel burns in simulations of the actual airline revenue route segments. The 727-200 flying these route segments was conventionally equipped (no on-board performance optimization or autothrottle) and the selected flights were typical in terms of trip length and other operational considerations. Direct operating costs, maintenance costs and various constraints (air traffic control, weather, etc.) also affected flight profiles. The benefits quoted are achievable using an IEM algorithm to provide energy guidance and control to meet the objective of minimizing trip fuel.

A fuel-versus-time cost trade for each airline and flight profile requires evaluation on a case-by-case basis and was outside the scope of this study. The relative cost of fuel, labor, equipment and maintenance requires a continuous review of potential benefits. The economic justification for the implementation of these energy-optimized solutions will depend primarily on the future cost of fuel compared to the other factors.

Various alternatives to IEM can provide a portion of the quoted benefit. The simplest alternative is to select airspeed/Mach schedules approximating best energy schedules. The next step in sophistication involves the use of computing devices with stored data correlating operating conditions (weight, altitude, temperature, etc.) with best operating speeds. These performance computers can provide flight guidance information that theoretically closely approximates best energy guidance.

In addition to fuel savings, the IEM concept provides a number of qualitative benefits such as workload reduction. By providing automatic control through a cruise mode autothrottle and an autopilot, IEM maintains close conformance to optimal speed and thrust schedules. Alternative energy guidance/control concepts provide varying levels of automatic control. Real-time sensing of cruise conditions provides a further capability for assessing off-nominal aircraft performance and ambient conditions, and optimizing for those conditions.

The IEM study determined that a closed-loop energy management system is feasible and practical for transport aircraft, and provides the basis for industry to proceed with development and implementation of the concept. Implementation requires (1) an advanced autopilot providing an airspeed hold mode, (2) an autothrottle with airspeed hold and engine-pressure-ratio hold modes, (3) implementation of the IEM logic in an on-board computing device and (4) improved fuel flow and ground speed sensing. All of these are within the scope of currently available technology, but most are not available to the required level of sophistication in conventionally equipped airplanes now flying

2.0 INTRODUCTION

The increased emphasis on fuel conservation in airline operations has led to many areas of study: improved aircraft design, better operational procedures, advanced control systems, etc. A number of avionics manufacturers have developed performance computing devices that use on-board stored performance data to provide flight profile guidance and control. IEM is a concept for an on-board system in which the real-time aircraft energy state is determined, a new operating state commanded and compared in terms of fuel efficiency with the previous state, and iterated until an optimum operating point is determined. The IEM study objective was to assess the feasibility and practicality of a closed-loop system that sensed, searched and controlled to an optimum operating state. The potential advantages of such a system applied to a transport aircraft include use of real-time data in performance optimization, computational simplicity (little requirement for stored performance data) and operational flexibility. This study was conceived to test the IEM system concept by developing a preliminary set of algorithms, testing the algorithms in a detailed computer model and assessing the potential benefits in terms of conventional (handbook reference data and pilot control) flight profiles being flown today.

As developed in this report, the IEM system is comprised of three elements. 1) a collection of energy guidance algorithms, 2) an autopilot with altitude- and airspeed-hold modes and 3) an autothrottle with engine-pressure ratio and airspeed-hold modes. The energy guidance algorithms determine the optimum operating state (minimum fuel) for fixed ranges of the climb, cruise and descent flight segments. The energy guidance algorithms also compare the desired optimum operating state to the real-time aircraft state to develop error signals for the autopilot and autothrottle. The zeroing of these errors provides automatic control to the optimum state of the aircraft.

Implementation of the IEM algorithms involves the use of stored performance data for climb and descent In cruise, however, determination of the optimum operating state is based on the in-flight sampling process of the closed-loop system. In this sense, the cruise algorithm is a closed-loop system, whereas the climb and descent algorithms are not.

The approach taken to the development of energy management algorithms and their assessment (fig. 1) shows eight areas of study and their interrelationships. An analysis of mid-range transport operations was based on flight data taken on a specially instrumented 727-200 flying revenue passenger routes in airline operations. From a sample of 80 such route segments, data were examined to establish route profile characteristics and flight procedures typically employed in flying the profiles. From this analysis, two flights were selected representing typical medium-range and short-range stage lengths. Data extracted from these two flights were then used to re-create the flight conditions in a computer simulation model and to measure the corresponding performance of the aircraft.

The computer model, a three-degree-of-freedom simulation of the 727-200, was based on the Boeing Standard Simulation Model of that type aircraft. Energy management algorithms and expanded autopilot and autothrottle modes were added to the aerodynamic, engine and atmosphere models and the rigid-body equations of motion in the basic simulation model. The modified model was employed in the study in two modes to establish a performance base

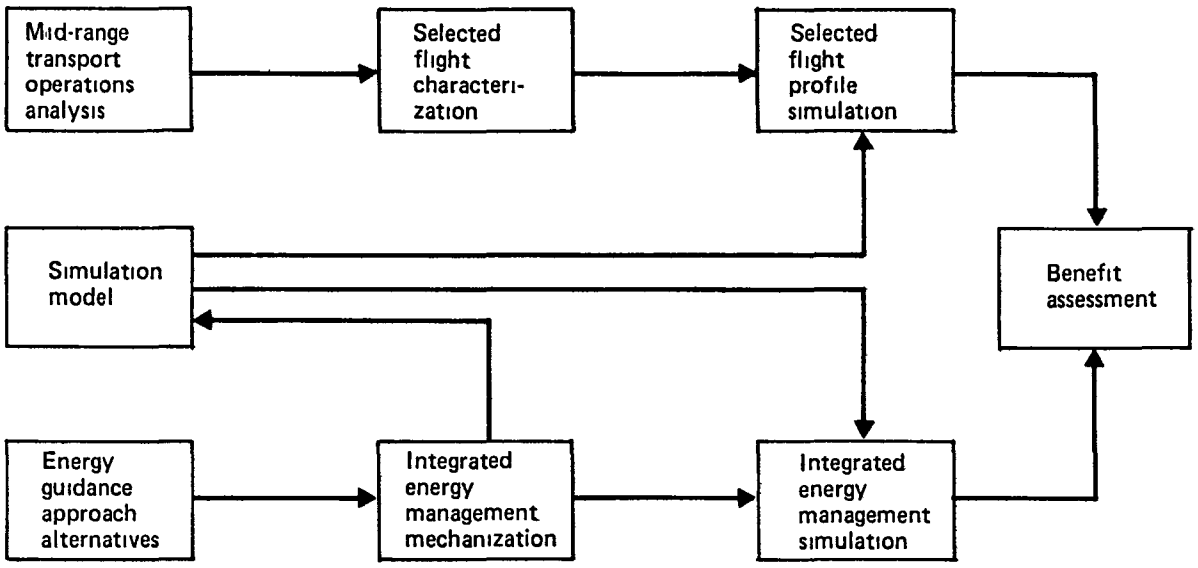

Figure 1. Integrated Energy Management Study Approach

against which to measure energy management algorithm benefits, and to represent the IEM guidance logic.

The development of energy management algorithms was based on an analysis of alternative approaches to the establishment of fuel-efficient procedures. Handbook schedules, optimized airspeed/Mach techniques, specific energy optimization and calculus of variations optimization techniques were reviewed. They were compared in terms of fuel and time efficiency and in terms of their compatibility with IEM objectives. Climb, cruise and descent factors, constraints and performance were analysed. After considering these factors, specific energy optimization was selected as the basis for the algorithm mechanization logic developed. Algorithms for climb, cruise and descent were detailed and associated sensor requirements specified.

The study was concluded with incorporation of the energy management algorithms in the model, followed by assessment of the benefits.

3.0 SYMBOLS AND ABBREVIATIONS

ATC	Air Traffic Control
ALT SEL	altitude select, an autopilot mode
CAS	calibrated airspeed
C_D	coefficient of drag
C_L	coefficient of lift
CTOP	Chebychev Trajectory Optimization Program
D	drag
DME	distance measuring equipment
EAS	equivalent airspeed
EPR	engine pressure ratio
E/W	specific energy, the sum of kinetic and potential energies per unit weight
FAA	Federal Aviation Administration
F_n	net thrust
FORTRAN	formula translation, the standard scientific computing language
g	acceleration of gravity
GMT	Greenwich mean time
h	altitude
$\dot{h}$	altitude rate
IAS	indicated airspeed
IEM	integrated energy management
kcas	kn, calibrated airspeed
ktas	kn, true airspeed

L/D	lift to drag ratio
LRC	long-range cruise
m	mass
M	Mach number
MAC	mean aerodynamic chord
MIMIC	a FORTRAN computer language for solving systems of differential equations
MRC	maximum-range cruise
OAT	outside air temperature
P	atmospheric pressure
R	gas constant for air
S	wing area
SSM	Standard Simulation Model
T_A	absolute temperature
T	thrust
TAT	total air temperature
TSFC	thrust specific fuel consumption
UA	United Airlines
V	velocity
VCAS	velocity, calibrated airspeed
V_p	flight path velocity
$\dot{V}_p$	flight path acceleration
V/S	vertical speed
W	aircraft weight
W_f	fuel weight

Z	altitude
δ	atmospheric pressure ratio
∂	partial derivative
ΔT	excess thrust
π	engine throttle position
σ	specific fuel consumption
ρ	atmospheric density
θ	atmospheric temperature ratio

4.0 STUDY RESULTS

This section of the IEM report details the analyses, modeling, simulation, algorithm development and assessment of the energy management guidance and control concept.

4.1 MID-RANGE TRANSPORT OPERATIONS ANALYSIS

The instrumentation of a United Airlines (UA) 727-200 mid-range aircraft with JT8D-7 engines and collection of both flight planning data and in-flight measurements provided a basis to establish typical flight profiles and procedures. Figure 2 shows the 43 city pairs represented in the 80 flights from which data were obtained.

Two flights were selected as representative of a medium-range and a short-range mission. The selected medium-range flight was designated as the reference flight because it is the most typical of 727-200 operations. By running the airline profile from the selected flights, and then the IEM profile in the simulation of the 727-200, an assessment of the potential benefits of the concept was made. The most detailed analyses and the model calibration were performed for the reference flight. As short-range flights differ substantially in terms of altitude and speed profiles from medium-range flights, a second simulation and benefits assessment was made for the selected short-range flight. A separate long-range flight analysis was not considered

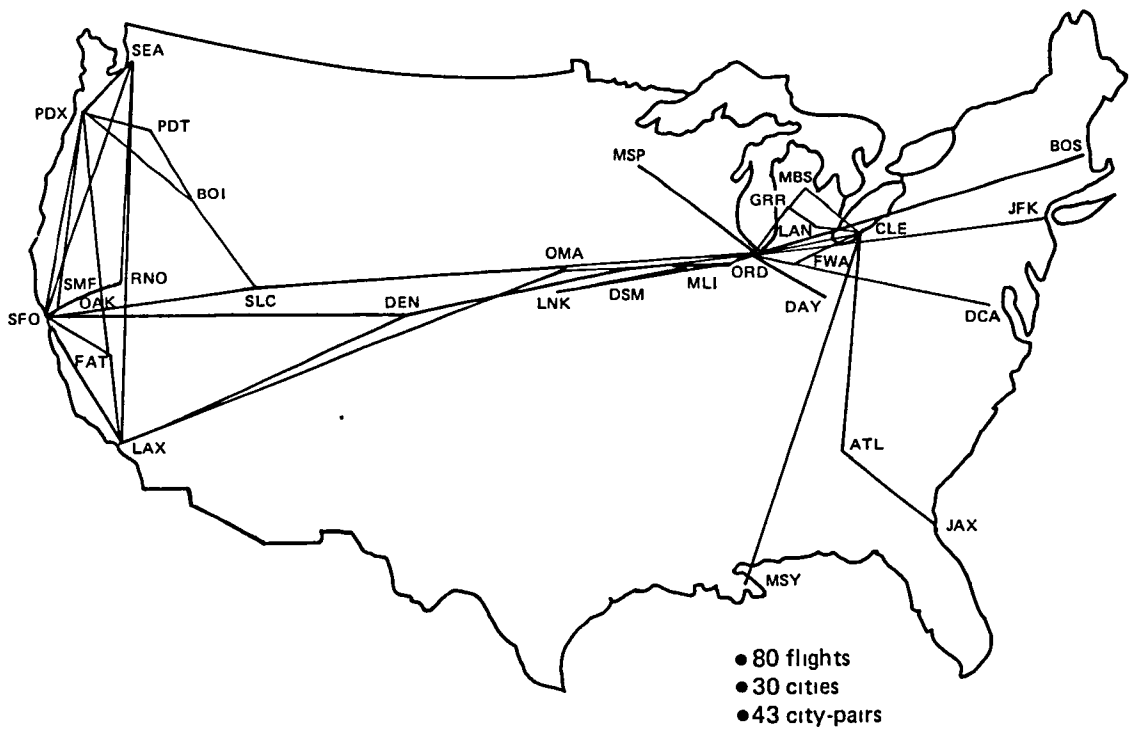

Figure 2. Instrumented 727-200 Route Structure

necessary because extrapolation of reference flight results to longer length flights primarily involves an extension of cruise procedures. The extrapolation of the medium-range IEM flight simulation and benefits assessment to long-range flights is discussed in Section 4.8.3.

4.1.1 United Airlines In-Flight Data Program

This section details the flight planning and in-flight data content of the UA flight measurement program. Flight planning data were supplied for about 50% of the 80 flights, generally those with stage lengths of 648 km (350 nmi) or more. These data included:

- Segment number
- Departure station
- Destination station
- Direction of flight
- Zero fuel weight (manifest)
- Take-off weight (manifest)
- Percent MAC (manifest)
- Time out, GMT
- Time off, GMT
- Time on, GMT
- Time in, GMT
- Planned take-off fuel weight
- Fuel out
- Fuel off
- Fuel in
- Planned flight time
- Planned total burnout
- Reserve and contingency fuel
- Holding/detouring fuel
- Alternate fuel
- Ferried fuel
- Plan code
- Burnout plan
- Total route mileage
- Planned take-off weight
- Deviation from standard temperature
- Head or tail wind component
- Planned zero fuel weight
- Checkpoint
- Segment mileage
- Altitude at checkpoint
- Mach at checkpoint
- Deviation from standard temperature
- True airspeed
- Wind direction/speed
- Head or tail wind component
- Groundspeed
- Segment time
- Segment burnout
- Routing

Flight measurements provided once per second for all of the 80 flights included:

- GMT
- Pressure altitude
- Radio altitude
- Indicated airspeed
- True airspeed
- Magnetic heading
- DME channel
- DME distance
- DME status
- Engine pressure ratio
- Pitch attitude
- Roll attitude
- Angle of attack
- Trailing-edge flap position
- Outside air temperature
- Fuel temperature

The autopilot modes and anti-ice valve position also were included.

4.1.2 Flight Profile Analysis

The UA in-flight data were used to define typical mission profiles. The airspace and environmental factors were compared on the basis of air distance flown, altitude profiles used and outside air temperature. Flight distances were compared in air miles so that the effects of wind speed and direction could be accounted for. The flight profiles also were inspected for evidence of air traffic control (ATC) intervention such as speed control, vectoring or holding. Figure 3 shows the average percentage of flight distance spent in climb, cruise and descent as a function of air miles flown for the UA flights reaching an altitude of 3048m (10 000 ft) or greater. This altitude is referred to throughout the document as the "base altitude." Seventy eight of the 80 flights in the sample reached this altitude. The percentages plotted represented a graphical best fit to the UA flight data. Descents where excessive holding occurred also are noted on the figure and are included in the data used to generate the descent from cruise to base altitude. The specific descent points show the substantial scatter (excessive descent distance) indicative of long delay situations.

Figure 4 shows the altitude-distance envelope for the collection of flights. Specifically noted are those flights where more than one cruise altitude was recorded (12 of the 80 flights). Flights with early descents and holding, and step descents, are a subset of the excessive delay flights noted in the previous figure.

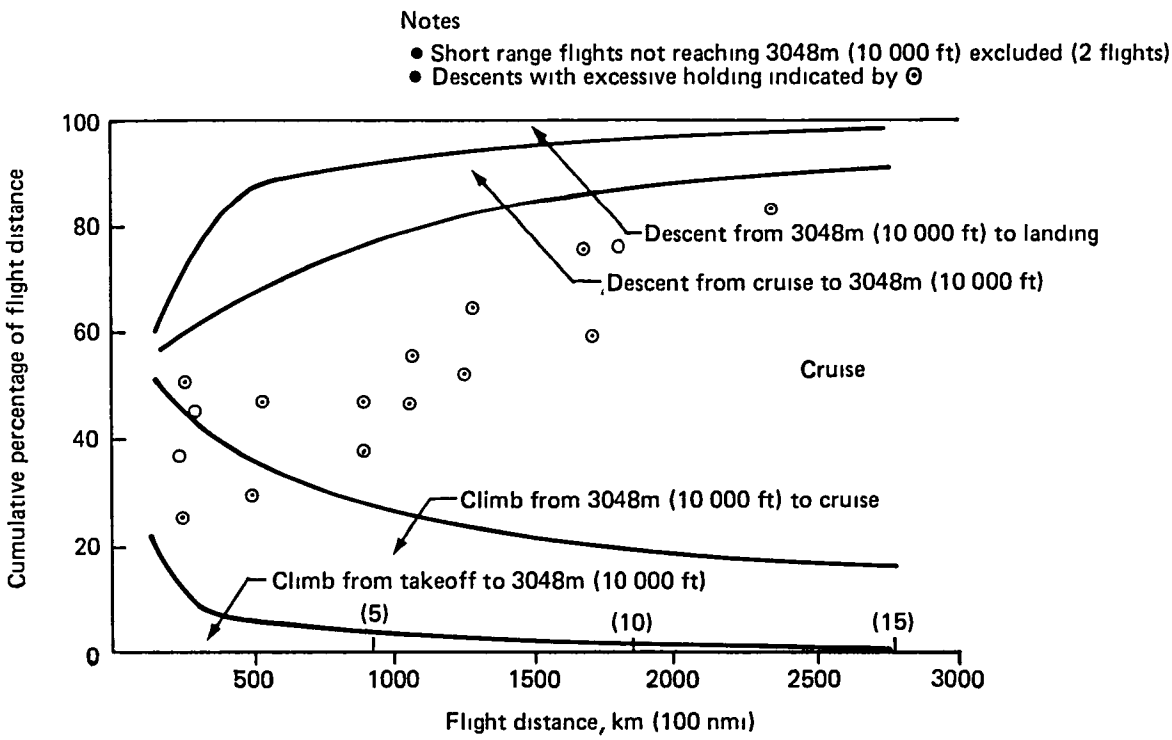

Figure 3. Effect of Total Flight Distance on Flight Phase Percentage

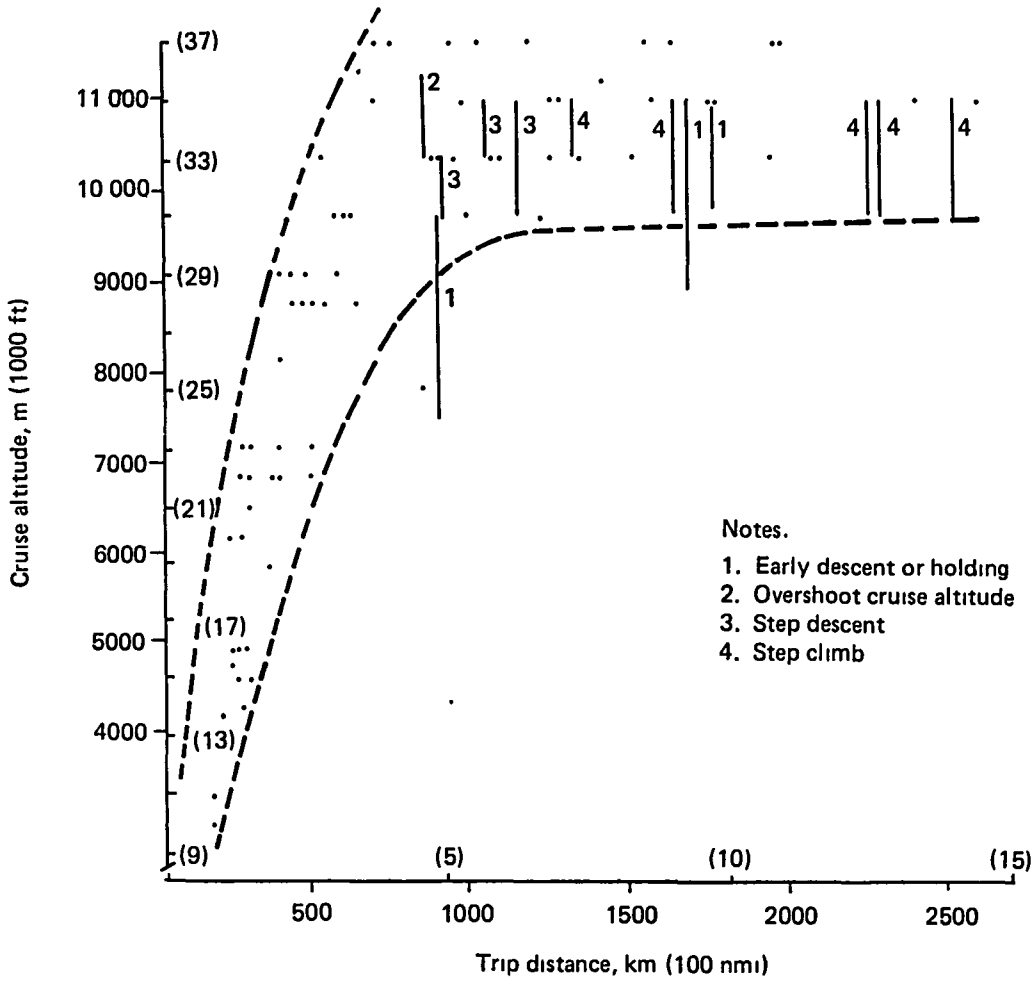

Figure 4. Correlation of Cruise Altitude with Flight Distance

Figure 5 shows the distribution of take-off weights for the collection of flights, and plots for each weight category, the envelope of specific range (kilometers flown per kilogram of fuel consumed) as a function of flight distance. The figure indicates the correlation of weight and flight distance with fuel mileage measured as specific range. The selected flights were checked to ensure that for their respective weights and flight distances they were near the middle of the specific range envelope.

The distribution of flight distances above base altitude with altitude is shown in Figure 6. The flights are grouped into short-range profiles of less than 648 km (350 nmi), medium-range segments of 648 to 1389 km (350 to 750 nmi), and long-range flights of 1389 km (750 nmi) or more.

Approximately 30% of the flights were classified as medium range. These flights were between major terminals with typical city pairs that included: Boston–Chicago, Los Angeles–Denver,

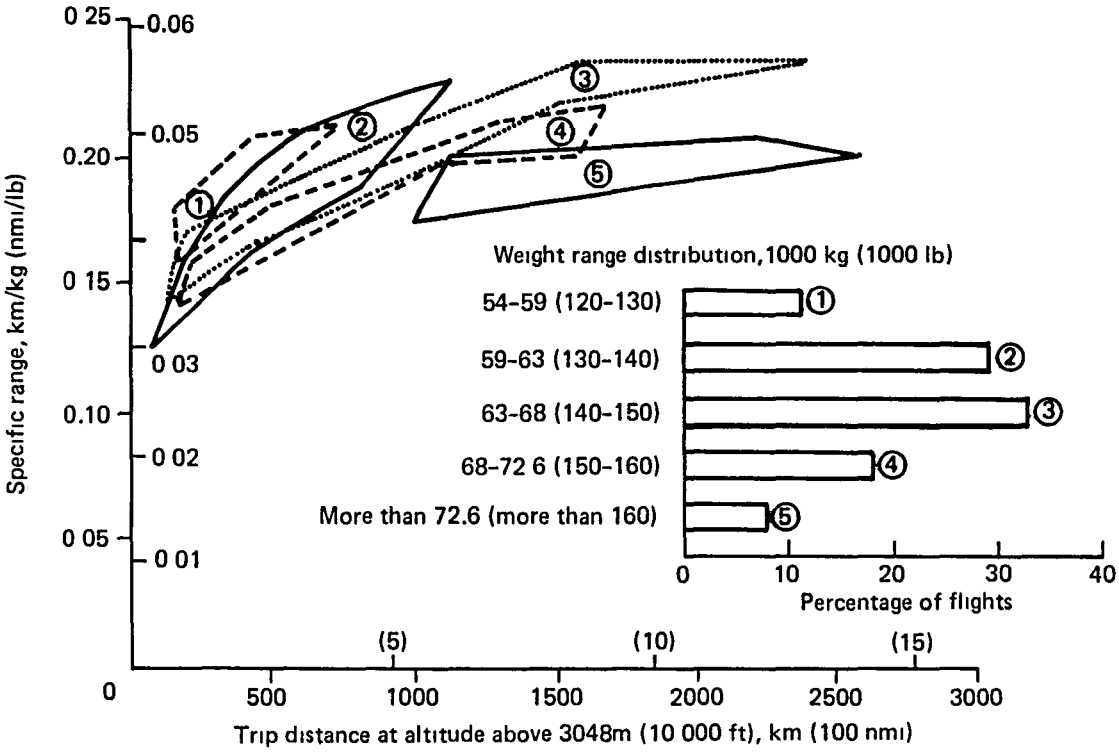

Figure 5. Correlation of Specific Range with Flight Distance.

and Washington, D.C.–Chicago. Table 1 presents characteristics of the reference flight compared to average values for all the medium-range flights.

Approximately 50% of the recorded flights were classified as short-range. Most of these flights connected a feeder airport with a major terminal area. Typical city pairs for the short-range flights included: Chicago–Des Moines, Los Angeles–Fresno, and San Francisco–Fresno. Mean values of flight parameters were calculated for all short-range flights. A typical short-range flight closely approximating these average values was selected from the actual data. Table 2 presents the average and selected flight values used in the comparison.

Both the reference and selected short-range flights were found to be average to above average with respect to trip fuel mileage (given the range and take-off weight of the flights) Both flights also were typical in terms of distribution of climb, cruise and descent segment distances and cruise altitude.

4.1.3 Flight Procedures Analysis

This section examines the airspeeds and engine pressure ratio (EPR) values employed for the airline flights. Of the 80 flights comprising the data sample, only data from those reaching a cruising altitude of 8839m (29 000 ft) or above were extracted for this analysis. Forty-three of the 80 flights are included in this category. Reference flight procedures were compared with the 43 flights to ensure that the airspeed and engine settings used were typical.

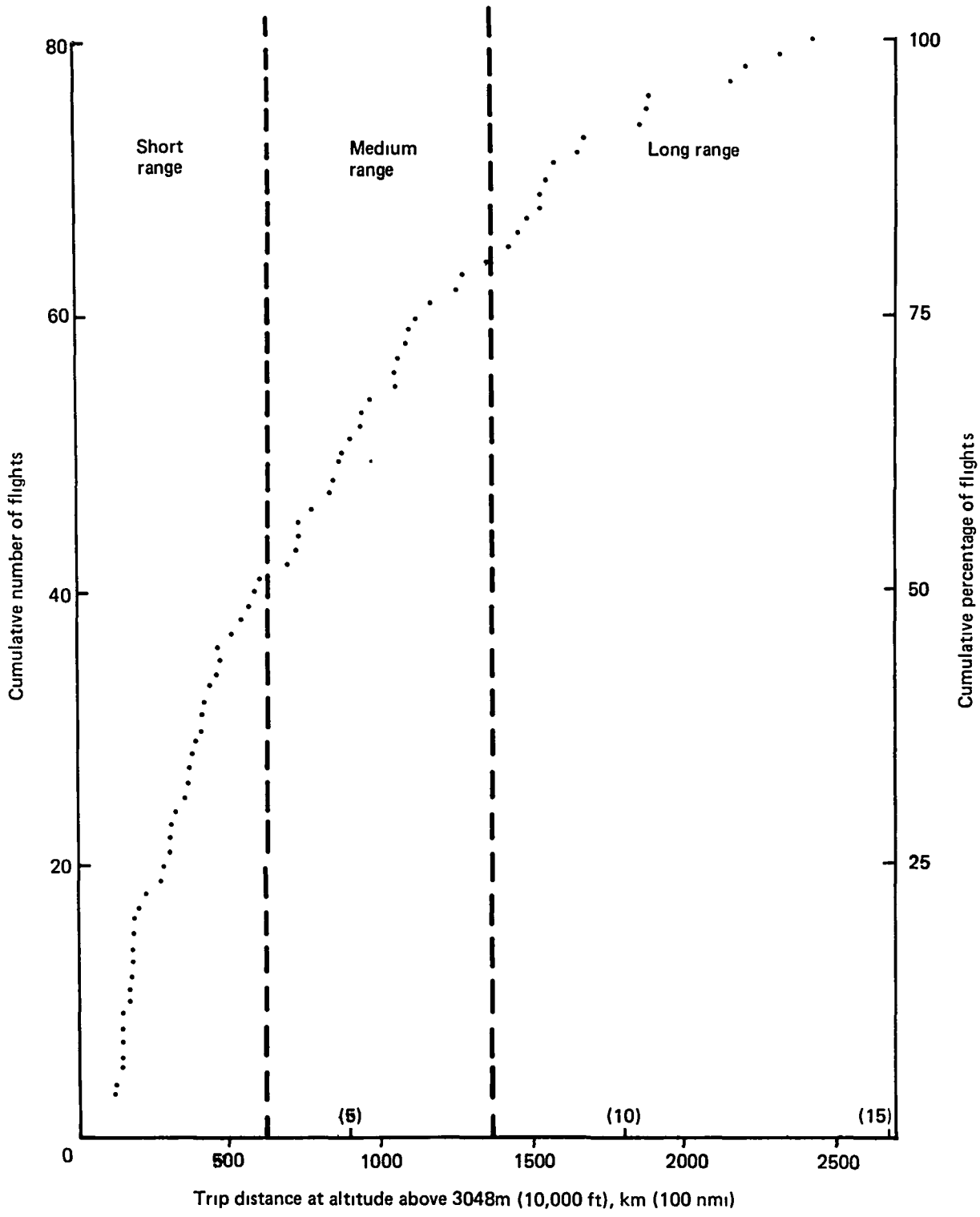

Figure 6. Cumulative Distribution of Flight Distances

Table 1. Comparison of Reference Flight and Average of Medium-Range Flight Parameters

Parameter	Reference flight	Mean value
Cruise distance, km (nmi)	1 087 (587.2)	980 (520.0)
Cruise altitude, m (ft)	10 058 (33 000)	10 226 (33 550)
Planned take-off weight, kg (lb)	65 228 (143 800)	67 722 (149 300)
Planned zero fuel weight kg (lb)	54 024 (119 100)	55 598 (122 570)

Table 2. Comparison of Selected Short-Range Flight and Average of Short-Range Flight Parameters

Parameter	Selected flight	Mean value
Flight distance, km (nmi)	72.7 (160.3)	75.2 (165.7)
Cruise altitude, m (ft)	7 315 (24 000)	7 040 (23 100)
Take-off gross weight, kg (lb)	62 642 (138 100)	62 824 (138 500)
Zero fuel weight, kg (lb)	51 846 (114 300)	52 209 (115 100)

Data on the distribution of airspeeds and of EPR settings were derived as a function of altitude for climb, cruise and descent. The flights cruising at lower altitudes were excluded since their inclusion would obscure, at a given altitude, climb or descent versus cruise values. The 43 flights reaching 8839m (29 000 ft) closely correspond to the medium-range and long-range flights discussed in Section 4.1.2. Climb, cruise and descent procedures employed for both classes of flights were essentially identical; therefore, data from both were combined for comparison with the reference flight.

For the 43 flights the average cruising altitude was 10 211m (33 500 ft) and the average cruise Mach number was 0.81. The average climb speed was about 165 m/s (320 kcas), transitioning to a climb Mach of 0.80. Standard climb and descent profiles employ constant calibrated airspeed schedules (CAS) at low altitudes and constant Mach speed schedules at higher altitudes. Compared with climb, the average descent was somewhat slower, and the mean descent speed schedule not as characteristic of a Mach-to-calibrated airspeed profile. The somewhat irregular descent-speed profile is related to a significant number of very low speed descents into airports typically experiencing substantial delays (Chicago–O'Hare, Cleveland–Hopkins, etc.) The

average speed schedule is summarized in Figure 7 and the corresponding average EPR profile is summarized in Figure 8. For the descent, some power is employed to about 6706 to 7010m (22 000 to 23 000 ft) when the average setting is reduced to near idle.

The climb speed envelope is shown in Figure 9. In this figure, the minimum, mean, and maximum speeds for the 43 flights are shown with the mean plus or minus one standard deviation. The reference flight climb speed schedule also is shown. The reference flight schedule lies between the mean and mean plus one standard deviation in the CAS portion of the climb, and closely approximates the mean speed of the 43 flights in the Mach portion of the climb. The corresponding EPR envelope for climb is shown in Figure 10. Again, the reference flight schedule is shown and lies between the mean and mean-plus-one standard deviation lines. The EPR schedule for the reference flight is the average value for the three engines. Some decrease in the minimum EPR schedule line at altitudes above 7620m (25 000 ft) is seen as some of the flights approach cruise altitude.

The descent speed envelope in Figure 11 shows a substantially greater spread of speeds at all altitudes when compared to the climb envelope. The maximum speeds for descent are approximately the same as those for climb, but the minimum speeds are much slower because of the number of flights with delays included. Sixteen of the flights showed a marked deviation from the average allocation of range to the various flight segments as shown in Figure 3. These

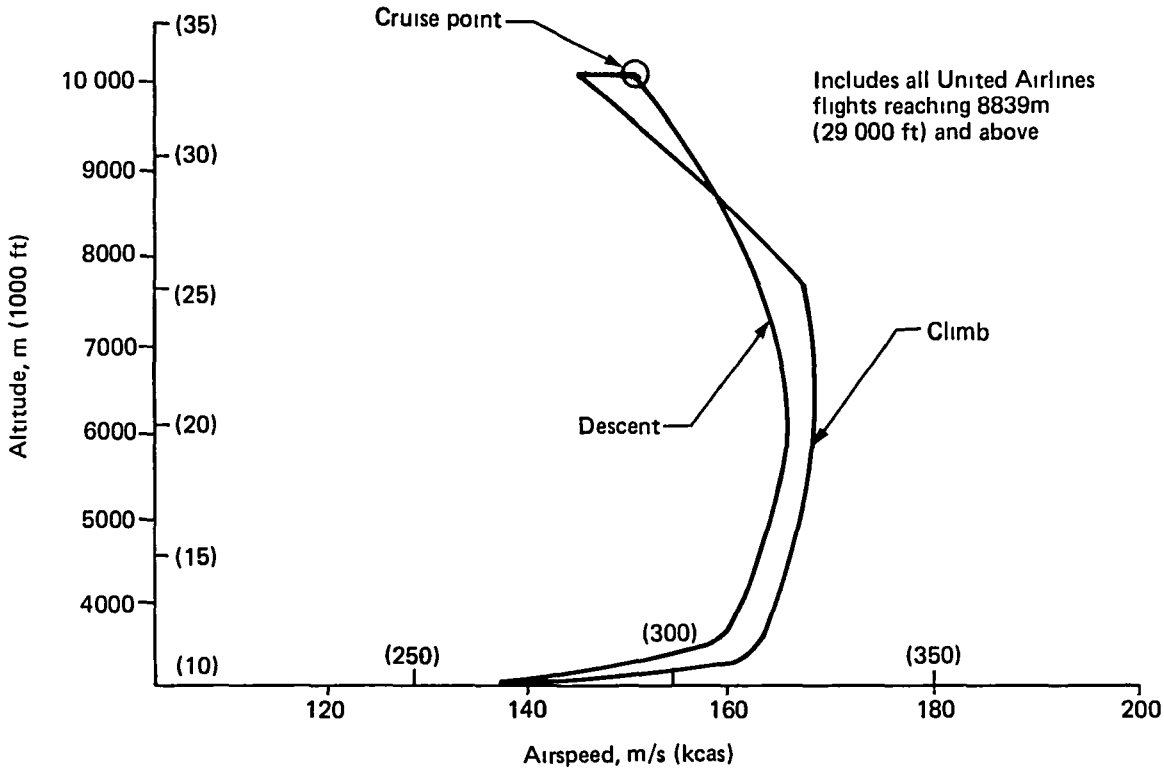

Figure 7. Mean Speed Profile

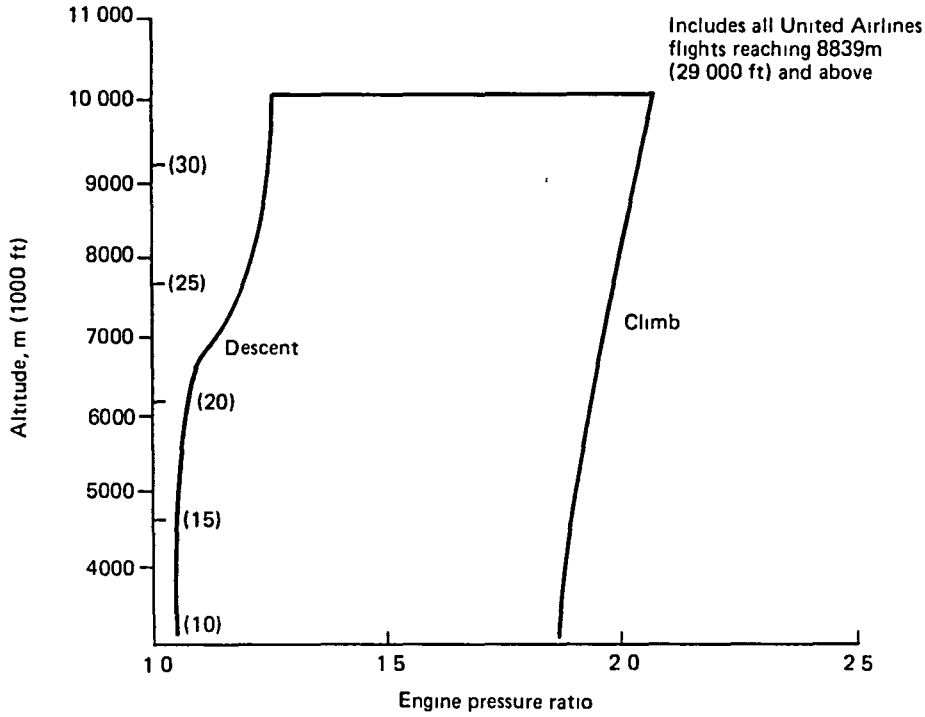

Figure 8. Mean Engine Pressure Ratio Profile

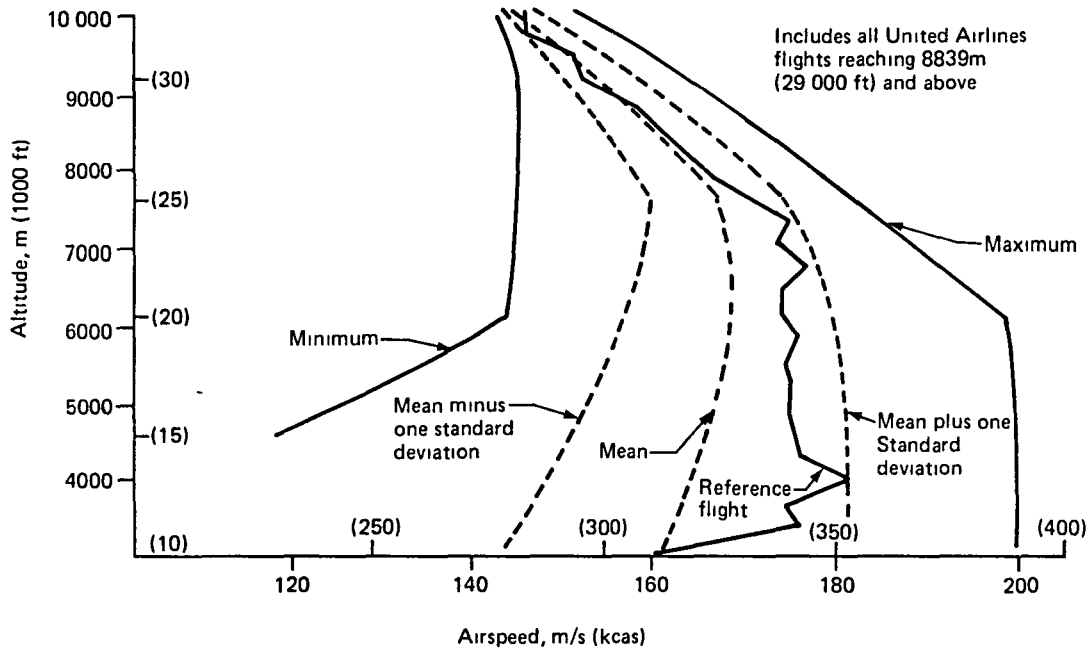

Figure 9. Climb Speed Envelope

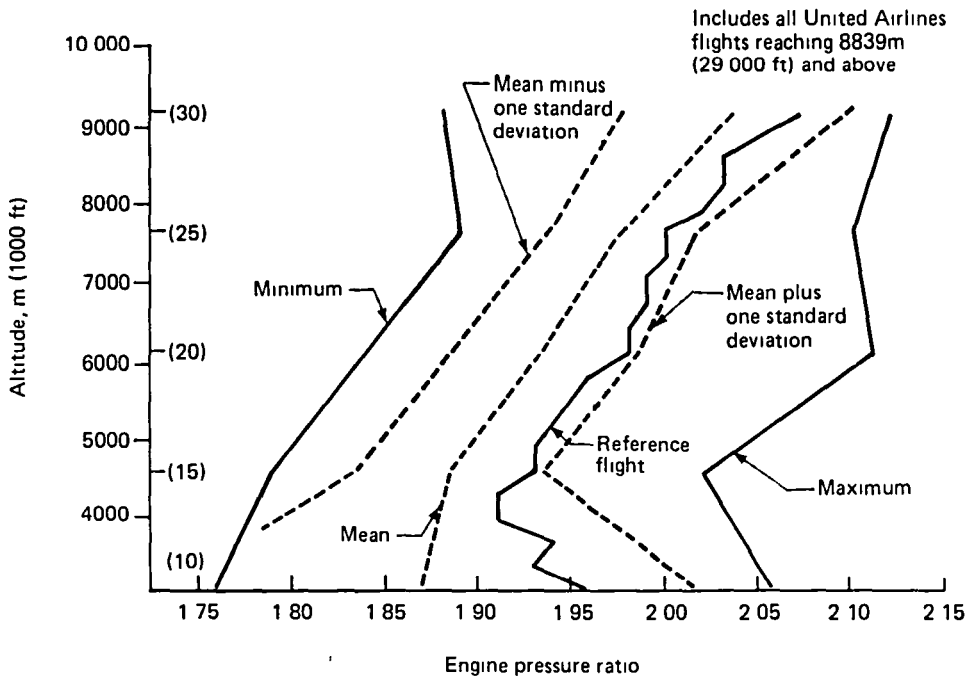

Figure 10. Climb Engine Pressure Ratio Envelope

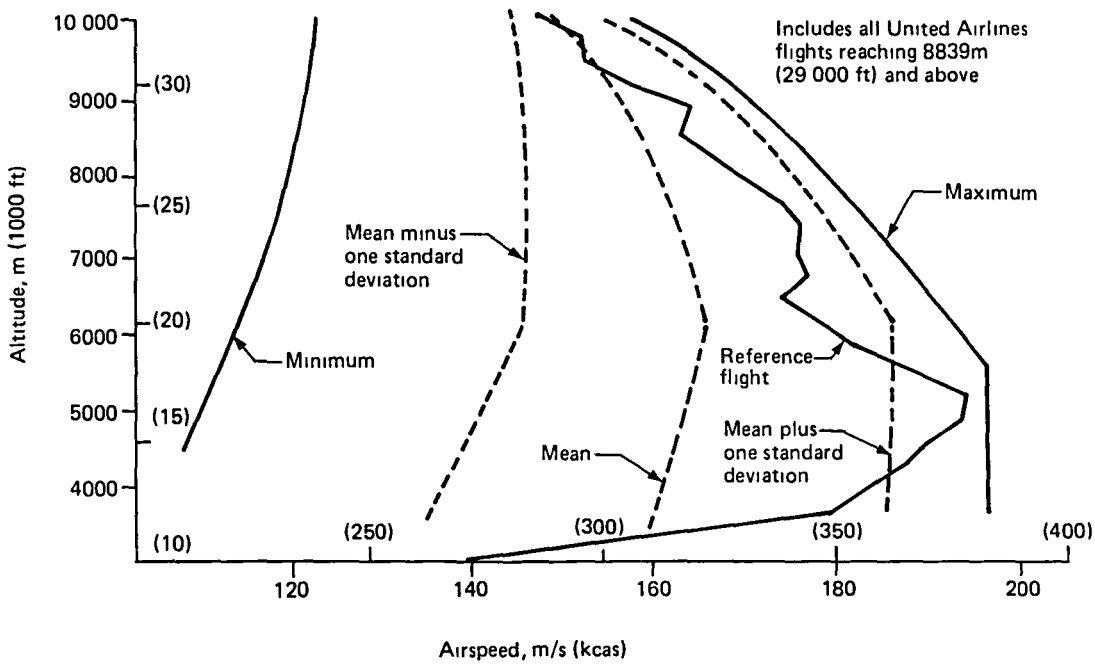

Figure 11. Descent Speed Envelope

16 flights were characterized by early departure from cruise and step descents. The flights were into airports with delay problems (e.g., Chicago–O'Hare). The exclusion of these flights would have caused the mean descent speed for let-down to be higher than the climb speeds, but their inclusion reversed this comparison. The reference flight speed profile lies between the mean and mean-plus-one standard deviation lines, except near 10 058m (33 000 ft) cruise altitude where the speed is slightly lower, and between about 4267 and 5486m (14 000 and 18 000 ft) where the speed increases to near the maximum value of the envelope.

The EPR envelope for descent is shown in Figure 12. The reference flight profile is typical in carrying some power (EPR values of 1.35 to 1.45) from cruise to about 7010m (23 000 ft), then cutting the throttle to idle for the balance of the descent to base altitude.

In summary, the reference flight lies well within the normal range of speed and EPR values (plus or minus one standard deviation), except for a brief speed excursion in descent. The irregularity of the reference profile speed schedule in the CAS portion of the climb and descent was typical of the 43 flights, with the closer adherence to a single Mach line in climb and descent also typical.

4.2 SELECTED FLIGHT DESCRIPTIONS

The following sections describe the reference (medium-range) and selected short-range flights. The altitude, Mach number, EPR values and measured outside ambient temperature are shown

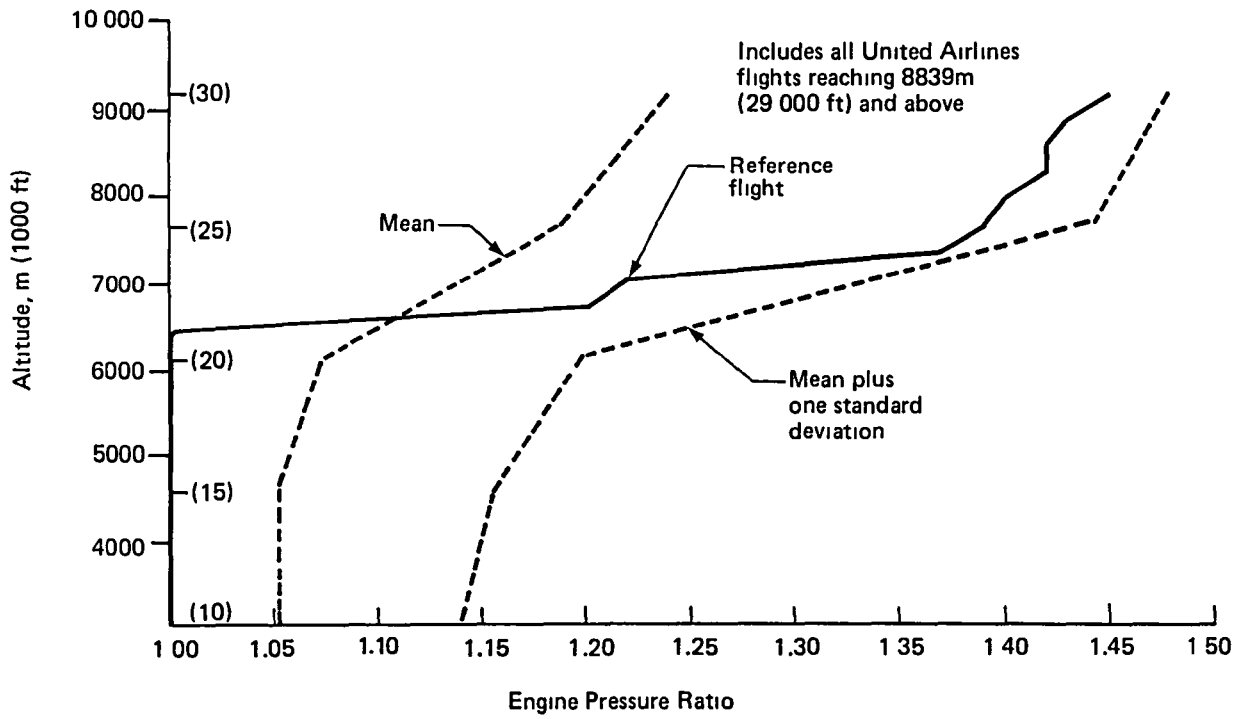

Figure 12. Descent Engine Pressure Ratio Envelope

plotted as a function of elapsed time. Only the portion of the flights above base altitude were included. The summarized flight parameters for the two flights are:

	Time, sec	Distance, km (nmi)	Fuel, kg (lb)
Reference (medium-range) flight	4631	1089 (588.1)	5121 (11 290)
Short-range flight	1310	297 (160.3)	1801 (3 970)

4.2.1 Reference (Medium-Range) Flight Description

Figure 13 shows the altitude-time profile of the reference flight. Climb from base altitude to 10 058m (33 000 ft) took from about 300 to 1200 seconds and descent to base altitude from 4200 to about 4900 seconds. The corresponding Mach number flown is shown in Figure 14. The acceleration to a climb Mach of about 0.80 was followed by cruise at Mach numbers varying between about 0.795 and 0.815. The descent Mach reached almost 0.83 then decreased (with one brief increase at about 4700 sec.) to 0.50 at base altitude. The EPR schedules for the three engines shown in Figure 15 reflect the typical climb, cruise and descent procedures. Some power was maintained on descent for about half of the time. Figure 16 shows that flight temperatures were considerably below standard day: climb averaging 10°C below standard day, and descent about 15°C below. Cruise temperature also showed some variation, ranging from -60°C at the beginning of cruise to -51°C near the end of cruise.

4.2.2 Selected Short-Range Flight Description

Figure 17 shows the altitude profile for the selected short-range flight. The presence of a brief cruise segment in the short-range flight is characteristic of the airline profiles. In this case about 5 minutes cruise was flown out of almost 22 minutes of flight above base altitude. The cruise occupied the elapsed flight time from approximately 900 to 1200 seconds. The Mach number profile is shown in Figure 18. The climb shows generally increasing Mach values with some leveling-off at Mach numbers between 0.60 and 0.65 and between 0.70 and 0.75. A cruise Mach value of about 0.81 was attained sometime before the cruise altitude of 7315m (24 000 ft) was reached and maintained for sometime after leaving cruise altitude. EPR values for the flight shown in Figure 19 reflect typical climb, cruise and descent profiles. In descent, the EPR levels were decreased from a cruise value of 1.7 to about 1.2 and then further decreased to idle. The outside air temperature profile for the flight is shown in Figure 20. The temperature profile for the short-range flight approximated the standard day profile.

4.3 EVALUATION MODEL

The model used to measure benefits of the IEM concept is adapted from the Boeing Standard Simulation Model (SSM) of the 727-200. The model is a modularized engineering simulation of the airplane. It was designed to be broad enough in scope to be used for various engineering analyses, including pilot handling quality studies, flight test data matching for aerodynamic data development, accident investigations, flight profile development analyses, thrust dynamics studies, flight path noise investigations, wind shear studies, etc.

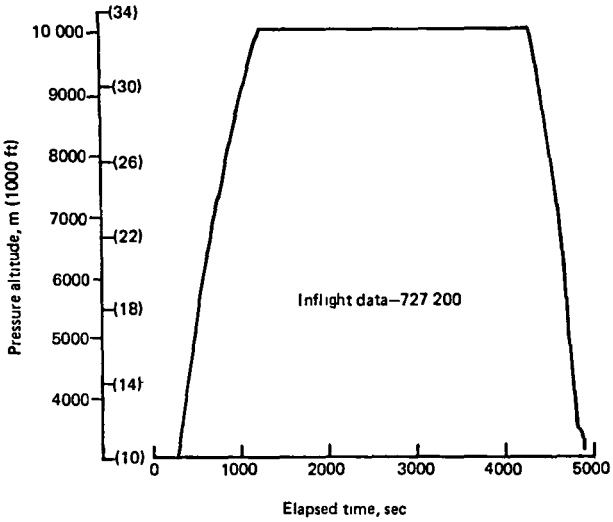

Figure 13. Reference (Medium-Range) Flight Altitude Schedule

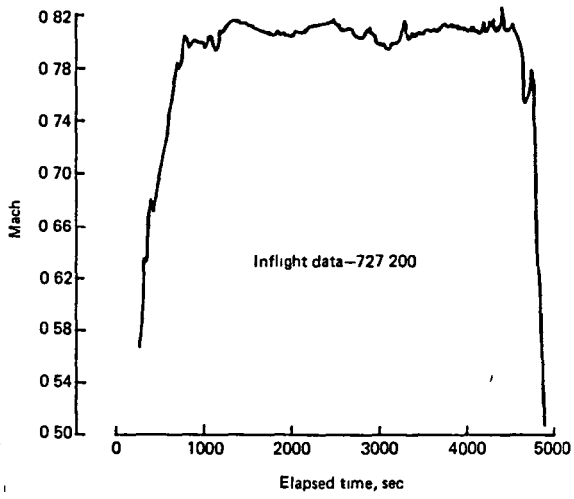

Figure 14. Reference (Medium-Range) Flight Mach Schedule

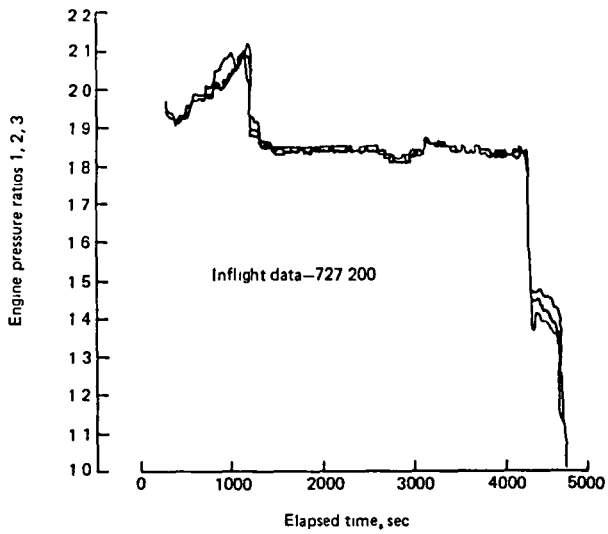

Figure 15. Reference (Medium-Range) Flight Engine Pressure Ratio Schedule

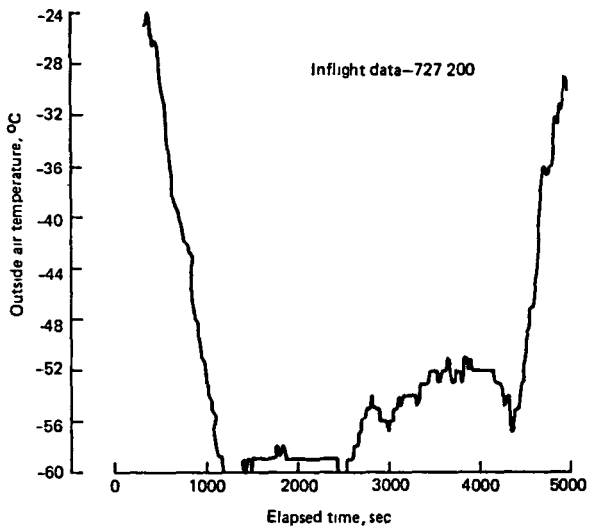

Figure 16. Reference (Medium-Range) Flight Temperature Schedule

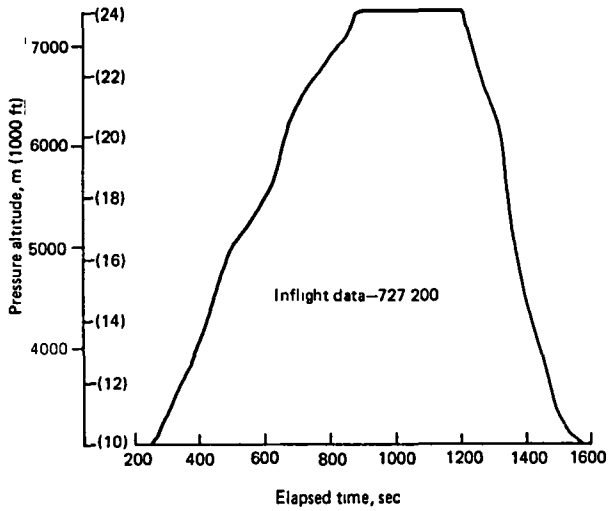

Figure 17. Short-Range Flight Altitude Schedule

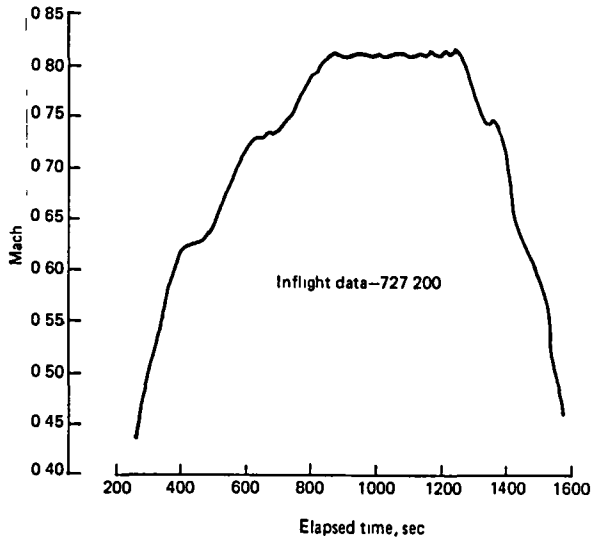

Figure 18. Short-Range Flight Mach Schedule

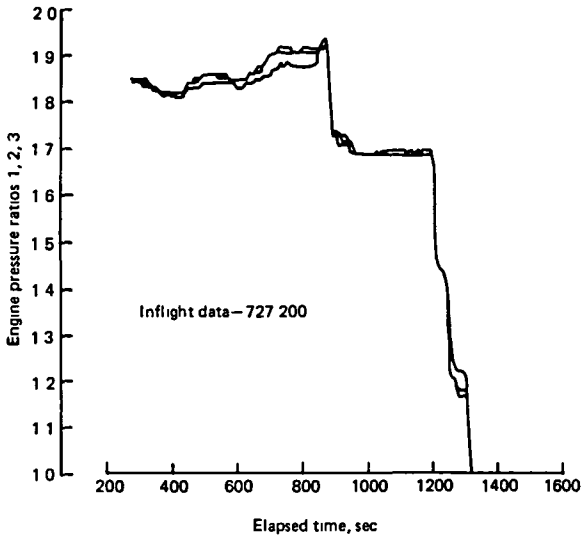

Figure 19. Short-Range Flight Engine Pressure Ratio Schedule

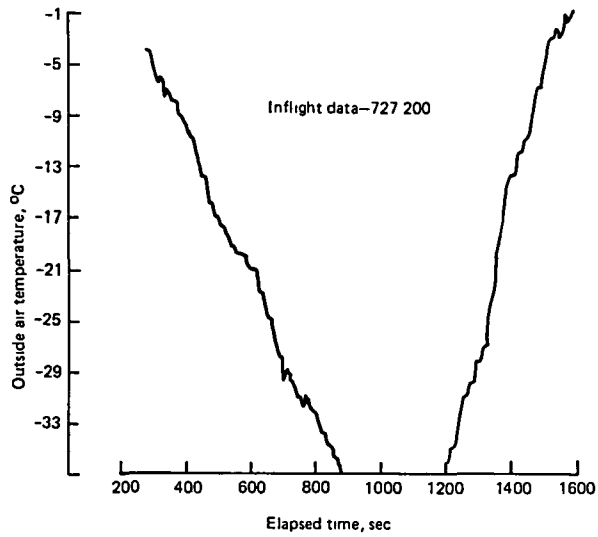

Figure 20. Short-Range Flight Temperature Schedule

The SSM was modified for use in the IEM study in several respects:

- The model was translated into MIMIC, a Fortran IV pre-compiler, used to solve systems of differential equations that may have nonlinearities
- The model runs faster than real time
- The model was simplified to represent 3-degrees-of-freedom
- The pitch-mode autopilot was extended to incorporate additional modes (indicated airspeed hold, vertical speed hold, etc.)
- An equivalent airspeed-hold-mode autothrottle was added
- The IEM guidance algorithms were incorporated

The IEM study SSM consisted of eight basic modules.

1. An atmosphere model
2. An aerodynamic model
3. An engine model
4. The rigid body equations of motion (3-degrees-of-freedom)
5. Trim computation logic
6. Autopilot logic
7. Equivalent airspeed-hold mode autothrottle
8. IEM guidance algorithms

Figure 21 summarizes the basic modules and their interrelationships in the IEM guidance configuration.

A description of each of the model elements (except the IEM mechanization, discussed in sec. 4.6) is included in Appendix A.

4.4 REFERENCE FLIGHT PROFILE SIMULATION

The following is a detailed discussion of simulation of the reference (medium-range) flight segment in the fast-time model of the 727-200. Flight-related inputs to the model included·

- Distance flown above base altitude
- Cruise altitude
- Weight at base altitude
- EPR schedules
- Airspeed schedules
- Atmospheric data

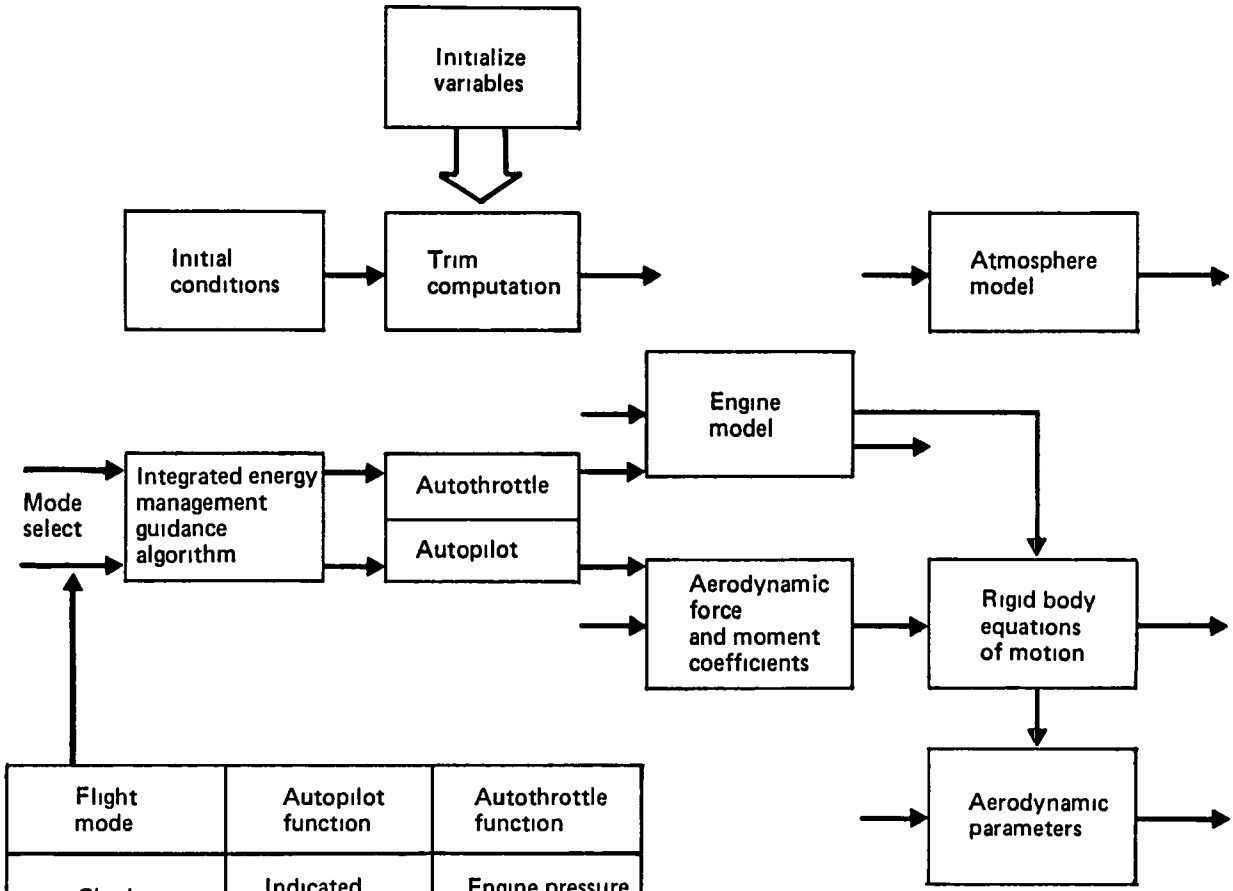

Flight mode	Autopilot function	Autothrottle function
Climb	Indicated airspeed hold	Engine pressure ratio hold
Cruise	Altitude hold	Equivalent airspeed hold
Descent	Indicated airspeed hold	Engine pressure ratio hold

Figure 21. Evaluation Model

The model was run to the specified distance and the resultant time and fuel burns in the model were compared to the in-flight measured data. The output fuel consumption provided a reference against which to measure IEM algorithm benefits. Figure 22 summarizes the reference profile simulation approach. The following sections describe the model inputs for the reference flight (4.4.1) and the model results and validation (4.4.2).

4.4.1 Reference Flight Simulation Inputs

Inputs to the reference flight simulation included climb and descent indicated-airspeed schedules (fig. 23), and climb, cruise and descent EPR schedules (fig. 24, 25 and 26). The airspeed schedules were used in the model as target airspeeds for the autopilot. The EPR

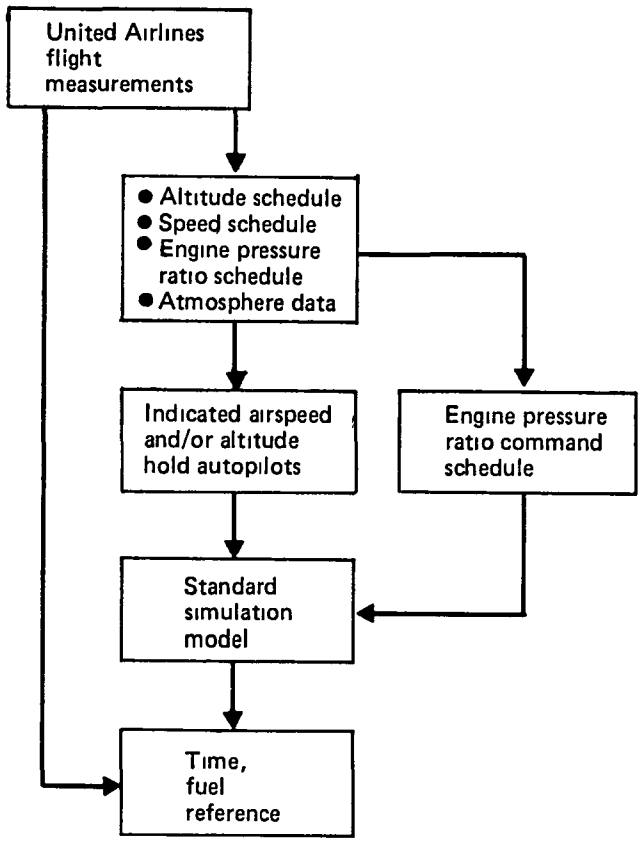

Figure 22. Reference Flight Profile Simulation Approach

schedules were input to the engine model as commanded EPR values. For climb and descent, airspeeds and EPR settings were determined as a function of altitude. In cruise, the EPR schedules were stored as a function of time in cruise. Outside ambient temperature values also were input to the model in table look-up format. The reference flight was flown for a complete climb and descent against the input conditions and for selected portions of the cruise. A complete cruise simulation was not run because of computer processing expense. Instead, representative portions of the cruise were selected and resultant performance and fuel-burn values extrapolated to the total cruise segment.

4.4.2 Reference Flight Results and Validation

A comparison of UA flight-measured parameters of time, distance and fuel to model derived values is summarized in Table 3. The summary comparison shows close agreement with respect to time. Distance values were in exact agreement since the model was run to the measured distance. The fuel values agreed to within 6.5%. Approximately 3% of this discrepancy is attributable to known differences in modeled and actual engine configuration assumptions. The balance of the modeled and measured difference is within the expected performance variance among specific aircraft with the same airframe and engine types. The fuel flow differences between modeled and measured data, while significant when compared to fuel savings

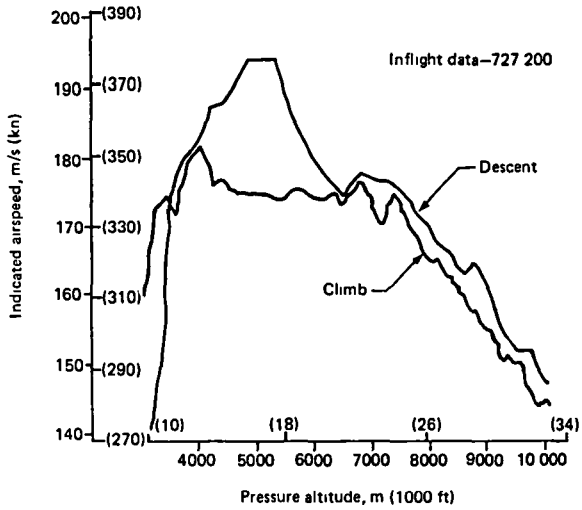

Figure 23. Climb and Descent Airspeed Schedules

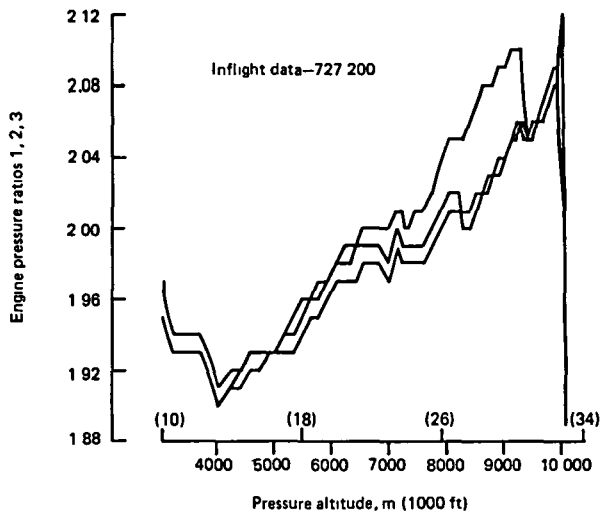

Figure 24. Climb Engine Pressure Ratio Schedule

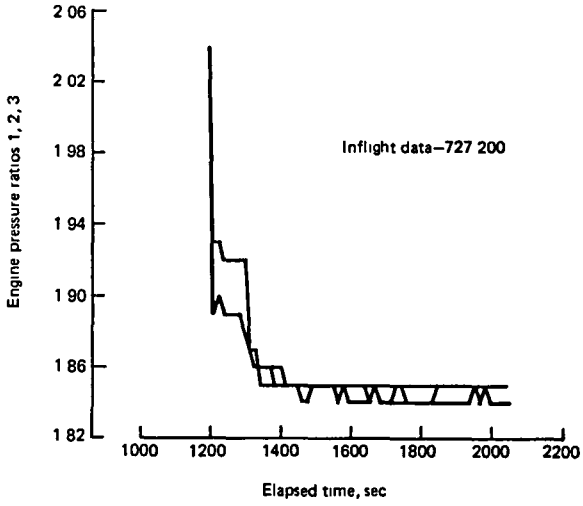

Figure 25. Cruise Engine Pressure Ratio Schedule

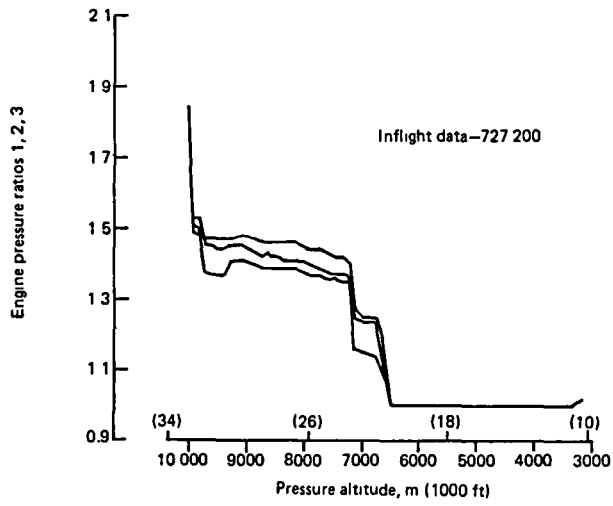

Figure 26. Descent Engine Pressure Ratio Schedule

Table 3. Model Data Versus Flight Measurements

	United Airlines flight measurements			Computed by standard simulation model		
	Time, sec	Distance, km (nmi)	Fuel, kg (lb)	Time, sec	Distance, km (nmi)	Fuel, kg (lb)
Climb	932	213.2 (115.1)	1674 (3 690)	935	212.6 (114 8)	1555 (3 429)
Cruise	3031	722.7 (390.2)	3062 (6 750)	2991	717.8 (387.6)	2872 (6 333)
Descent	668	153.3 (82.8)	386 (850)	700	158.7 (85.7)	361 (795)
Composite	4631	1089.2 (588.1)	5121 (11 290)	4626	1089.2 (588.1)	4787 (10 557)
Error				−0.1%	0.0	−6.5%*

*About 3% of fuel difference attributable to differences in modeled and actual engine bleed assumptions, etc.

for IEM (sec. 4 7), do not invalidate the savings determined. These differences introduce errors primarily of a systematic or fixed-bias type. The IEM benefits were determined by comparing, in the model, airline flight-measured versus IEM profiles and procedures, where the bias errors are self-cancelling.

Climb Profile Comparison—Figure 27 compares climb performance of the model and the actual aircraft and shows some slight difference in initial rate of climb. Overall, the modeled time to climb of 935 sec agreed closely with the measured value of 932 sec.

The modeled rate-of-climb exceeded that of the UA aircraft when the difference between pressure altitude and absolute (energy) altitude was considered. Using the outside air temperature profile measured for the flight and the hydrostatic equation relating atmospheric density to absolute altitude:

$$dp = -\rho g dz$$

$$\text{where } \rho = p/(gRT_A)$$

The absolute altitude was estimated for the reference flight at the cruise pressure altitude of 10 058m (33 000 ft). For the reference flight, the energy altitude was approximately 9693m (31 800 ft). Based on the lower energy altitude for the actual aircraft, the measured and modeled rates of climb compared as·

Flight measured rate-of-climb	7.1 m/s (23.4 ft/s)
Model computed rate-of-climb	7.5 m/s (24.6 ft/s)

Figure 28 shows the close agreement of the target calibrated airspeed values versus those achieved using the calibrated-airspeed hold mode of the autopilot. The airspeed error was less than 2 m/s (4 kn) at all altitudes.

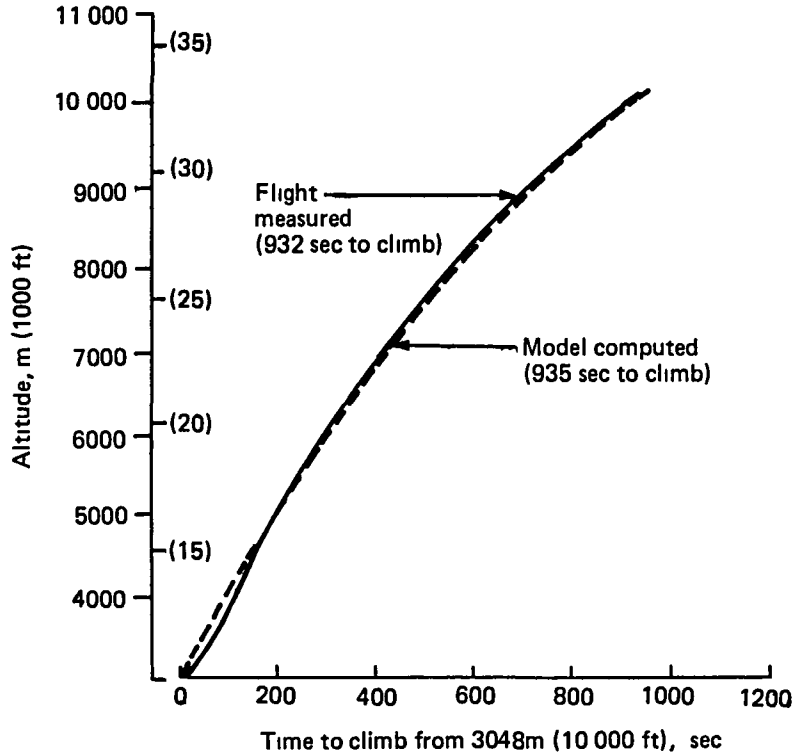

Figure 27. Climb Profile Comparison

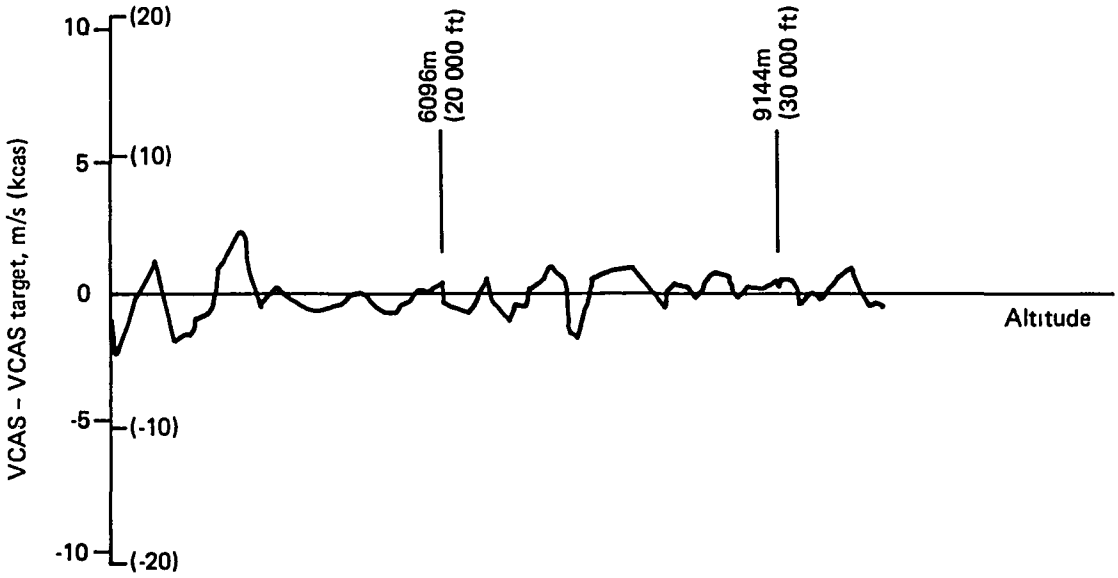

Figure 28. Autopilot Calibrated Airspeed Error for Climb

Figure 29 shows measured and modeled fuel flow rates for all engines as a function of altitude. The computed fuel flow tracks consistently with the measured value, but is about 7% low. Several minor engine differences explain about half of this discrepancy. The UA aircraft has two pod and one center engines, whereas the modeled aircraft in the SSM assumed all pod engines. The UA aircraft probably was operating with normal 8th stage air conditioning airbleed on the pod engines (data not available), whereas the model did not take air-conditioning airbleed into account. Finally, the UA aircraft engines are Pratt & Whitney JT8D-7s, while the model represented JT8D-9s. Performance manual data indicate a difference of about 3% between the reference flight engine configuration and the modeled engine configuration. Fuel flow measurement error for the UA 727-200 is on the order of 0.5%. The remaining fuel flow discrepancy is well within the performance variation in fuel consumption for specific aircraft of the same airframe and engine type.

Cruise Fuel Flow Comparison—For the cruise simulation, measured Mach numbers and airspeeds agreed with modeled values to within 1.5%. Figure 30 compares, for the first minutes of cruise, the measured and modeled values of fuel flow for the three engines. The modeled cruise value was about 6% below the measured value.

Descent Profile Comparison—Figure 31 compares the modeled and measured altitude versus time history for the descent. While the shape of the two curves agrees closely, the magnitude of

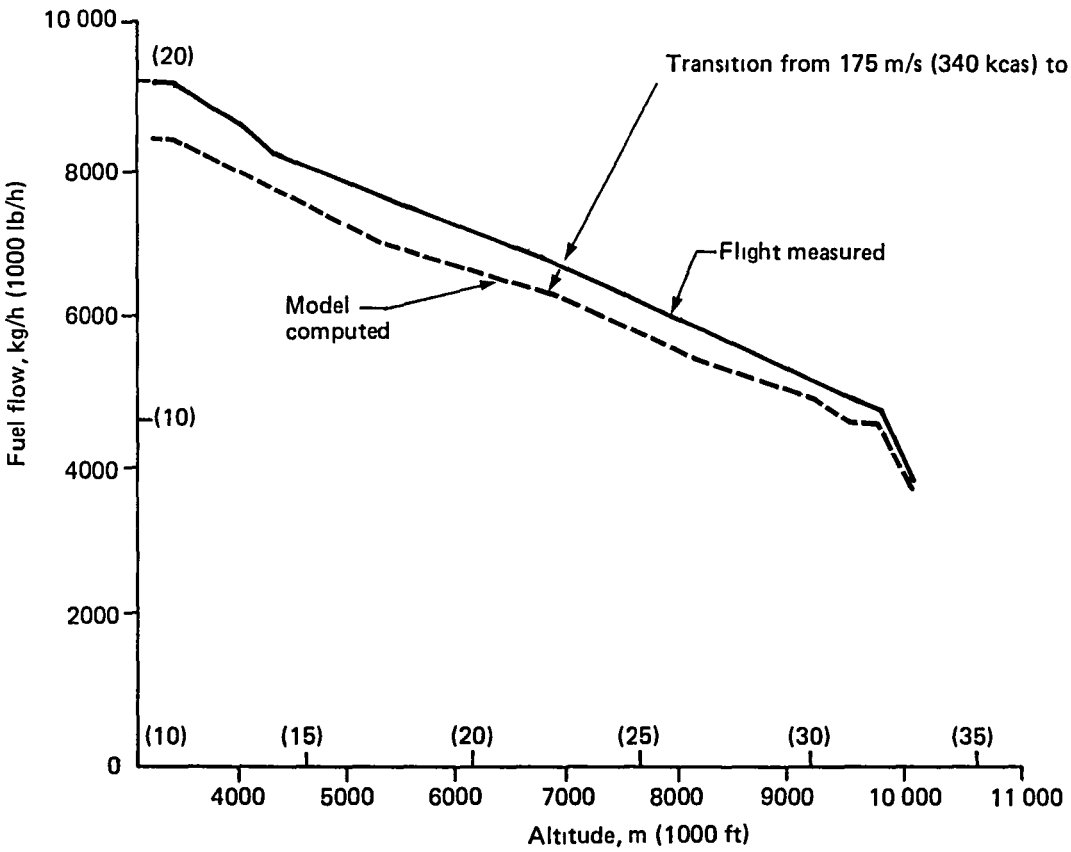

Figure 29. Climb Fuel Flow Comparison

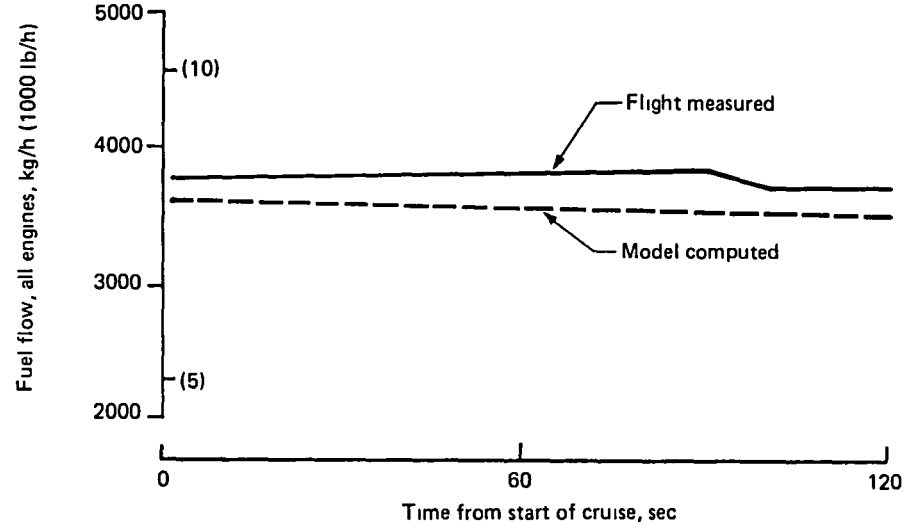

Figure 30. Cruise Fuel Flow Comparison

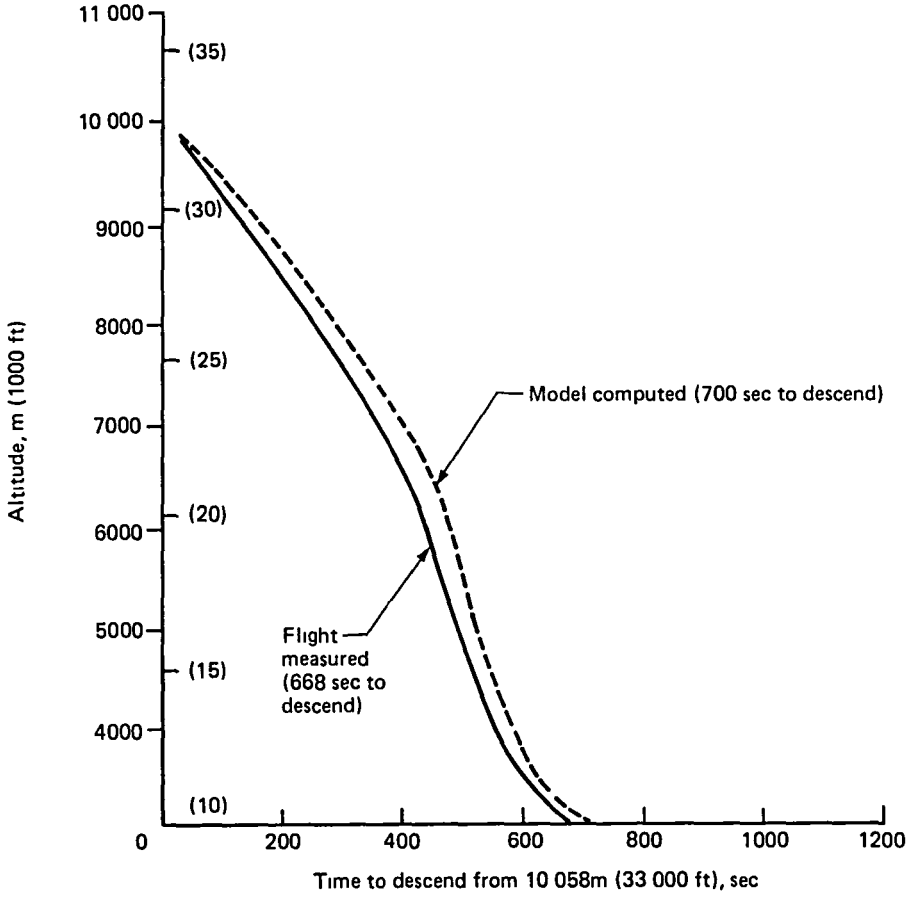

Figure 31. Descent Profile Comparison

the discrepancy in rate of descent is somewhat greater than that for climb. As in climb, the difference between pressure and absolute (or energy) altitude was significant. At top of descent, the pressure altitude of 10 058m (33 000 ft) corresponded to an absolute altitude of about 9632m (31 600 ft). In addition to this discrepancy, spoilers probably were deployed as speed brakes in descent, however data on their use were not available. A third factor, speed tracking error, is shown in Figure 32 as target airspeed minus the actual descent airspeed. The greater airspeed fluctuations in descent created a more difficult schedule for the autopilot to track, resulting in speed errors of almost 5 m/s (10 kn) at one point.

Figure 33 compares the measured and modeled fuel flows for the three engines as a function of descent altitude. As in climb and cruise, the modeled values are lower (about 11%) than the measured values. Causes of this discrepancy (in addition to the differences in bleed assumed and engine type previously discussed for climb validation) include the rate of descent difference and the lack of UA measured EPR values below 1.00. It was assumed for the descent that a read-out of EPR 1.00 was the corresponding idle thrust EPR for the altitude and Mach number. The resultant EPR schedule error due to this assumption is small.

4.5 SELECTED ENERGY GUIDANCE APPROACH: SPECIFIC ENERGY

This section describes the approach used for the development of an energy guidance algorithm and includes an overview of the development of the concept of specific energy, a summary of the guidance equations for each flight phase and a discussion of the advantages and limitations of the selected approach using the concept of specific energy as a parameter.

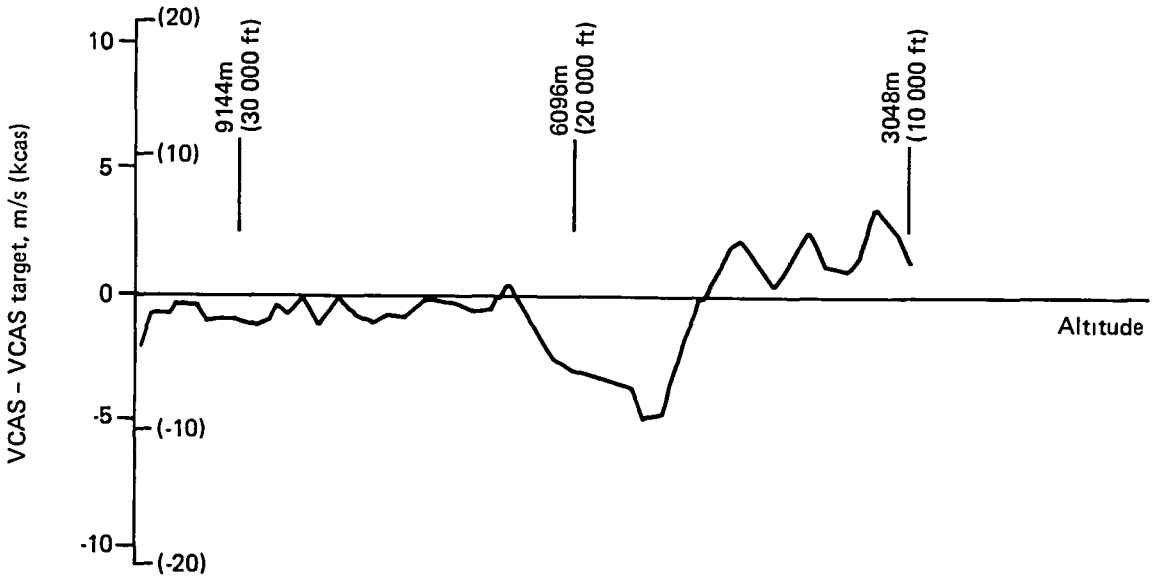

Figure 32. Autopilot Calibrated Airspeed Error for Descent

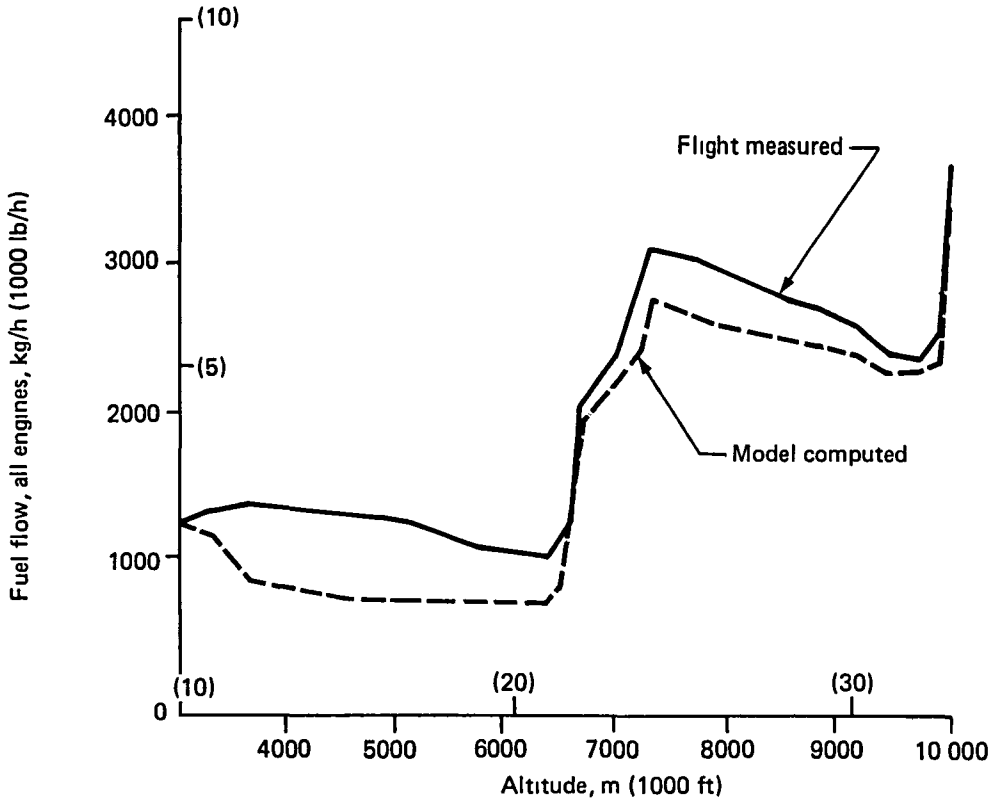

Figure 33. Descent Fuel Flow Comparison

4.5.1 Specific Energy Concept Development

The classical point mass, steady state solution to the equations of motion of an airplane relates rate of climb (or descent) to thrust, drag and weight terms (assuming the angle of climb is small):

$$\frac{dh}{dt} = \frac{V}{W}\,(T - D)\left(1 + \frac{V}{g} \cdot \frac{dV}{dh}\right)$$

where h = aircraft altitude
t = time
V = velocity
W = weight
T = thrust
D = drag
g = acceleration of gravity

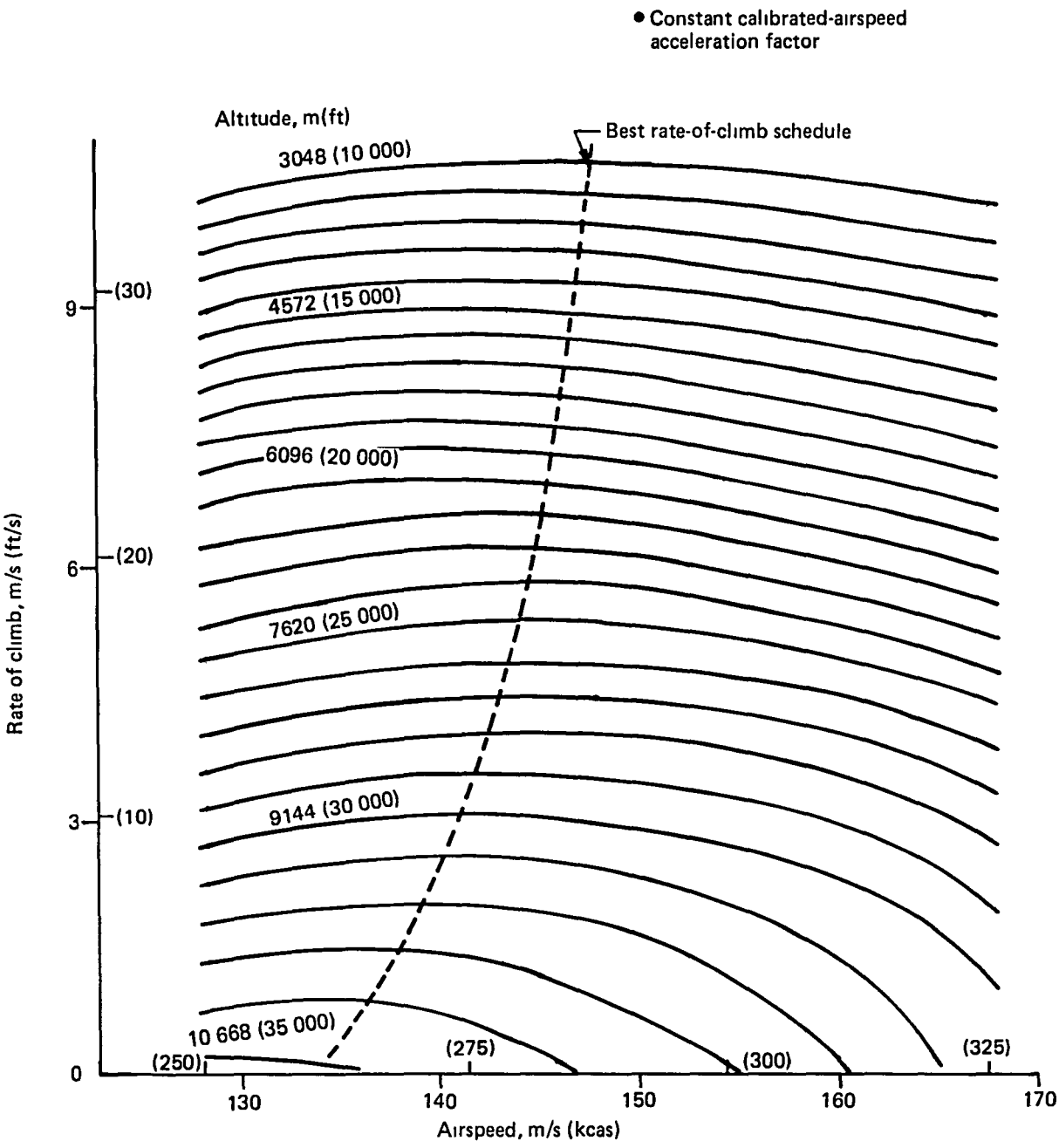

Figure 34. Effect of Airspeed and Altitude on Rate of Climb

Figure 34 shows rate of climb (dh/dt) versus calibrated airspeed for a 727-200 under standard day conditions. These data were generated from a point-mass, steady-state model employing performance manual values for aircraft thrust and drag. A standard approach to minimizing fuel in climb is to maximize rate of climb so that time spent at low, fuel-inefficient altitudes is minimized. Maximum rate of climb is found by determining, at every altitude, the airspeed that gives the largest value of dh/dt (shown by a dashed line). The maximum rate-of-climb concept is analogous to a minimum-angle (maximum-range) descent concept.

Rutowski, in 1954, formulated the equations of motion of aircraft in terms of specific energy (ref 1). Specific energy is defined as the sum of the potential and kinetic energies of the aircraft divided by aircraft weight.

$$E/W = h + V^2/2g$$

where E/W is the aircraft specific energy

A formulation analogous to rate of climb then can be derived for specific energy rate of change.

$$\frac{d}{dt} E/W = \frac{V}{W}(T - D)$$

which is a simple form of the previous expression for $\frac{dh}{dt}$ (implicitly incorporating the acceleration factor $\frac{V}{g}\frac{dv}{dh}$). Rutowski also formulated an expression to maximize rate of change of specific energy per pound of fuel expended, as.

$$\frac{d}{dW_f}(E/W) = \frac{V}{W}(T - D)/\, T \cdot \sigma$$

where W_f = fuel weight
σ = thrust specific fuel consumption

Figure 35 shows contours of constant rate of change of specific energy per pound of fuel expended for a 727-200. The dotted line indicates the maximal (with respect to energy state, not altitude) rate of change of energy per pound of fuel. Flying the airspeed schedule indicated will provide a minimum fuel trajectory between two energy states. The airspeed schedule will not, however, provide minimum fuel to a fixed range.

4.5.2 Summary of Guidance Equations

Zagalsky and others (ref 2), in 1971 formulated the solution to the problem of minimum fuel to a fixed range. Using optimum control techniques, an equation was derived based on specific energy. This formulation involved maximization of the function:

$$\frac{T - D}{W} \Big/ \left[\left(\frac{\sigma \cdot T}{V}\right)_{CL} - \left(\frac{\sigma \cdot T}{V}\right)_{CR}\right] \quad \text{at a given energy state}$$

where $\left(\frac{\sigma \cdot T}{V}\right)_{CL}$ is the climb fuel efficiency factor in fuel weight per unit distance

and $\left(\frac{\sigma \cdot T}{V}\right)_{CR}$ is the corresponding cruise efficiency factor.

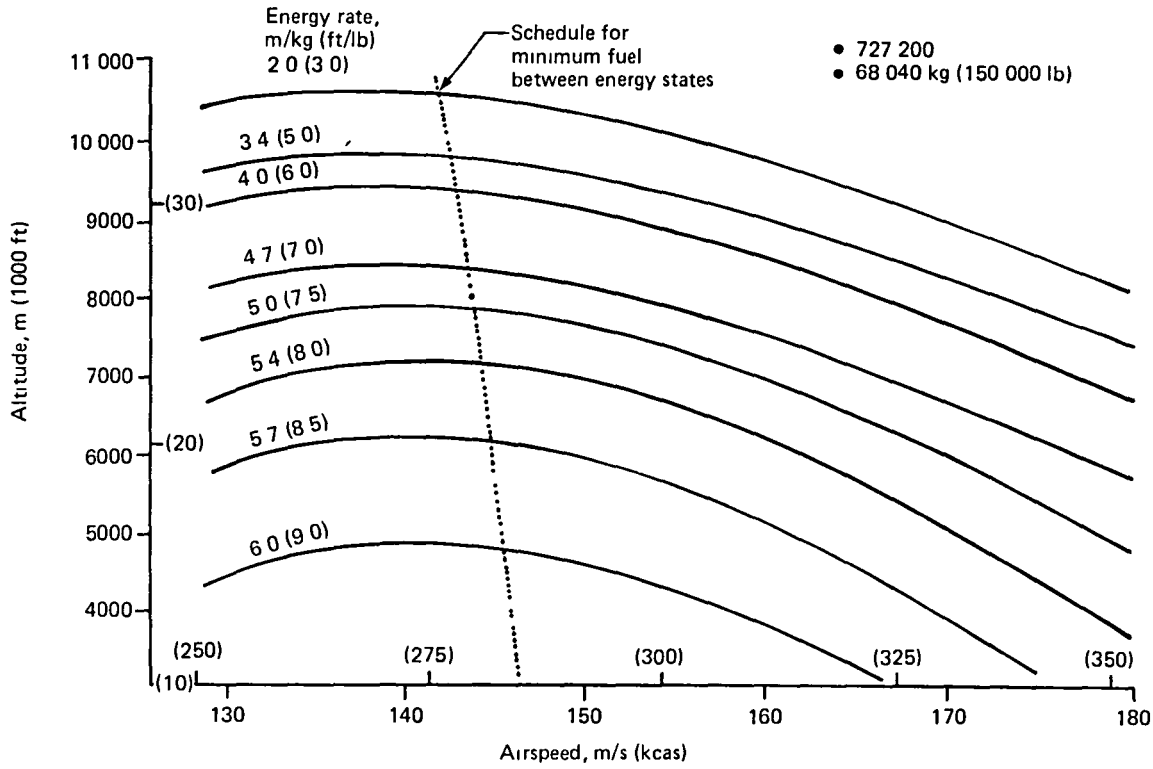

Figure 35. Contours of Constant Rate of Change of Energy per Pound of Fuel

The resulting contours of constant rate of change of specific energy per pound of fuel, with the cruise efficiency factor incorporated, are shown in Figure 36. The dotted line is the calibrated airspeed schedule for minimum fuel to a fixed range trajectory. The evaluation of this trajectory in a point-mass 727-200 performance model verifies the fuel minimization to a fixed range, compared with parametrically optimized constant calibrated airspeed/constant Mach climbs, as discussed in Appendix B.

Analagous techniques can be used to determine the cruise minimization method. For cruise, the airspeed schedule is determined by minimizing $\frac{\sigma \cdot D}{V}$ at cruise altitude. Similarly, the minimum fuel descent is obtained by minimizing the function:

$$\frac{(D - T)}{W} \Big/ \left[\left(\frac{\sigma \cdot T}{V} \right)_{CR} - \left(\frac{\sigma \cdot T}{V} \right)_{DS} \right]$$ where $\left(\frac{\sigma \cdot T}{V} \right)_{DS}$ is the descent fuel efficiency factor.

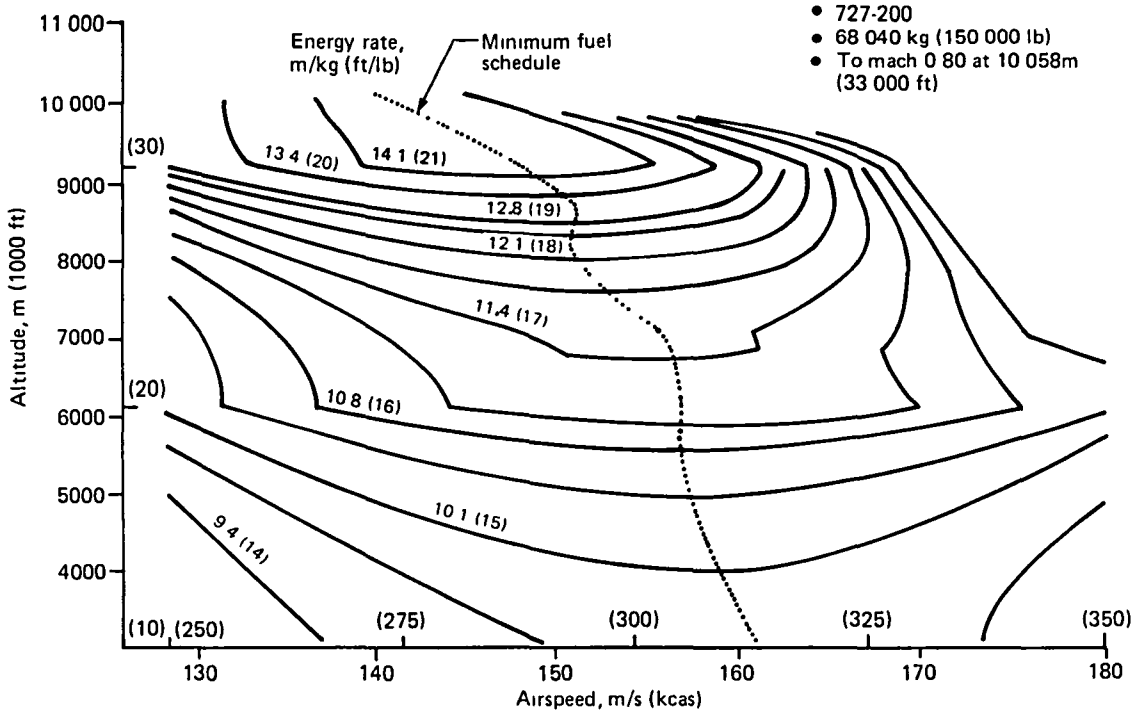

Figure 36. Contours of Constant Rate of Change of Energy per Pound of Fuel with Cruise Efficiency Factor

For these formulations, the climb throttle setting corresponds to the maximum climb engine pressure ratio schedule; cruise throttle thrust setting provides operation at the airspeed minimizing the cruise function, and the descent throttle setting is at idle Recent work by Erzberger (ref. 3) and others has extended the specific energy optimization techniques to minimum cost trajectories and to throttle optimization schedules for climb-to-cruise and cruise-to-descent transitions. For the development of IEM algorithms, the climb, cruise and descent specific energy functions to minimize fuel consumption to a fixed range were selected for mechanization. The maximum climb, partial cruise and minimum throttle schedules also were assumed. Details of the algorithms developed are discussed in Section 4.6.

4.5.3 Advantages and Limitations of the Specific Energy Concept

The specific energy guidance formulation is compared with alternative energy guidance techniques in Appendix B. An evaluation is made of the alternatives in terms of fuel burn and flight time by flight phase. Alternative techniques considered include handbook schedules and optimized airspeed/Mach and calculus-of-variations schedules. The handbook schedules

contain recommended airspeed/Mach values for climb, cruise and descent to be used as a guide to airline flight planning. The specific energy approach was selected since it provided:

- Fuel performance as good as, or better than, that of any of the other techniques investigated
- An energy-state based formulation
- A formulation compatible with the real-time, aircraft-derived guidance objectives of IEM
- A method combining relative computational simplicity and operational flexibility

As indicated in Appendix B, the specific energy optimized trajectories consistently provided minimum fuel to a fixed range. Significant gains were shown compared to handbook schedules, but only slight fuel savings (0.1–0.2%) compared to optimized airspeed/Mach schedules. Figures 37 and 38 compare the optimal rates of change of specific energy per pound of fuel for climb and descent versus various constant calibrated airspeed/Mach schedules. The figures indicate the approximation to an optimum energy schedule by selected constant calibrated airspeed/Mach schedules. The figures also indicate the substantial energy penalty in climb imposed by the 129 m/s (250 kn) speed restriction below base altitude. The FAA restriction limits speed in the high density airspace region as a safety measure.

Rate of change of energy as an optimization parameter is compatible with the aircraft state sensing objective of IEM. The determination of altitude, speed, mass and fuel flow allows aircraft-sensed estimates of rate of change of energy per pound of fuel flow. However, the implementation of a closed-loop on-board state sensing and control algorithm was concluded to be feasible only in the cruise state, as discussed in Section 4.6. For climb and descent, the rate of change of optimal energy state with altitude does not allow sufficient time for on-board determination of best speed schedule. Therefore, energy climb and descent algorithms were derived employing stored performance data. These algorithms require thrust, drag and fuel flow information, as specified in Section 4.6.

The use of stored basic performance data to derive trajectories results in both computational and operational simplicity and flexibility. By specifying basic aircraft performance, the best schedule can be computed for given flight conditions, and the ability to alter the performance allows assessment of off-nominal performance. As an example, Table 4 compares three climb schedules. The first assumed full thrust to generate the energy schedule. The second, a 5% de-rated climb, required 20 lb of additional fuel. The third, a re-optimized climb schedule, used only one additional pound over the original schedule (at a cost of 55 sec.). This example illustrates the potential for operational flexibility of the specific energy approach over pre-computed trajectories, for which it is difficult to evaluate strategies for off-nominal performance.

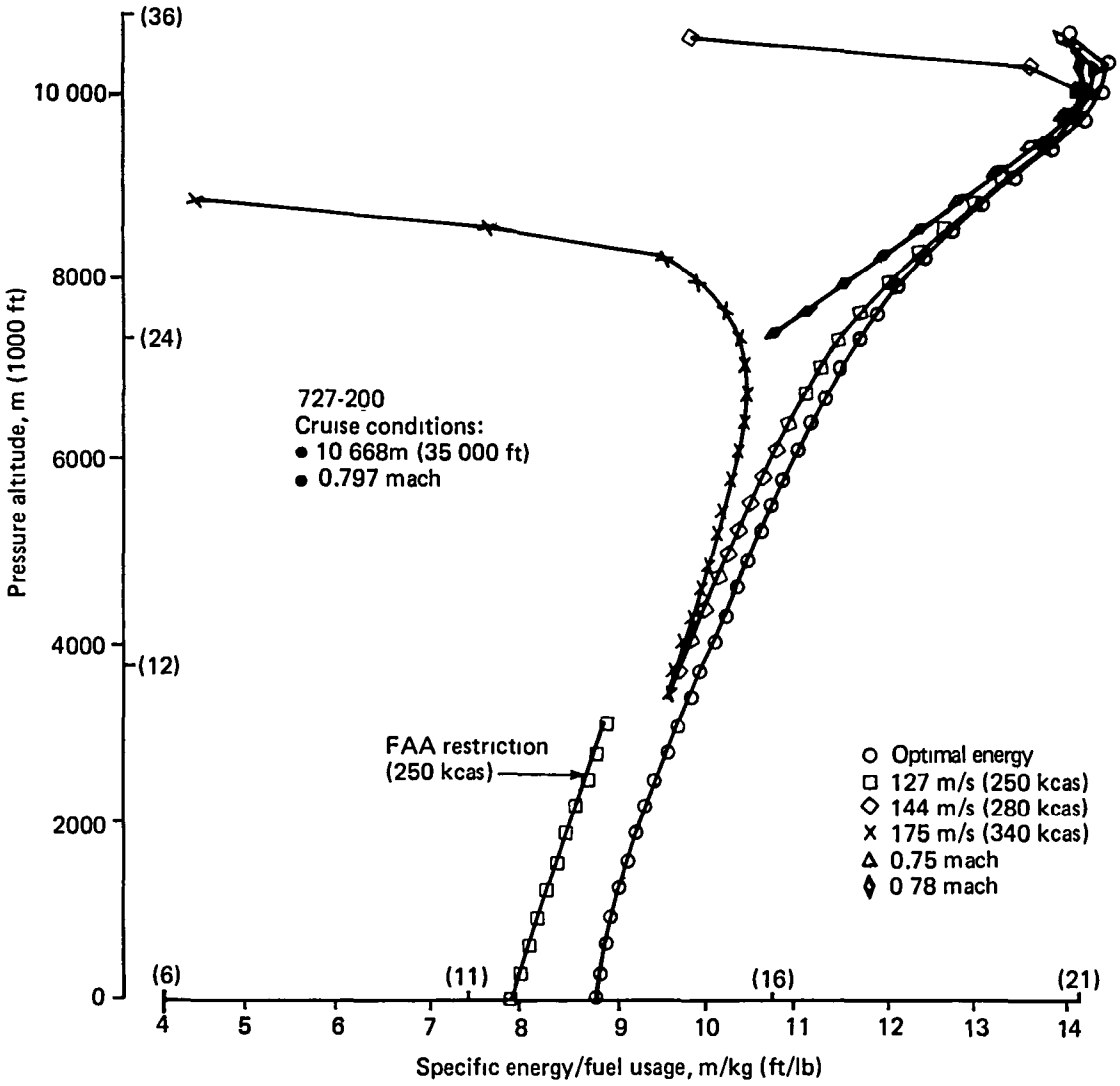

Figure 37. Effect of Climb Schedules on Specific Energy per Pound of Fuel

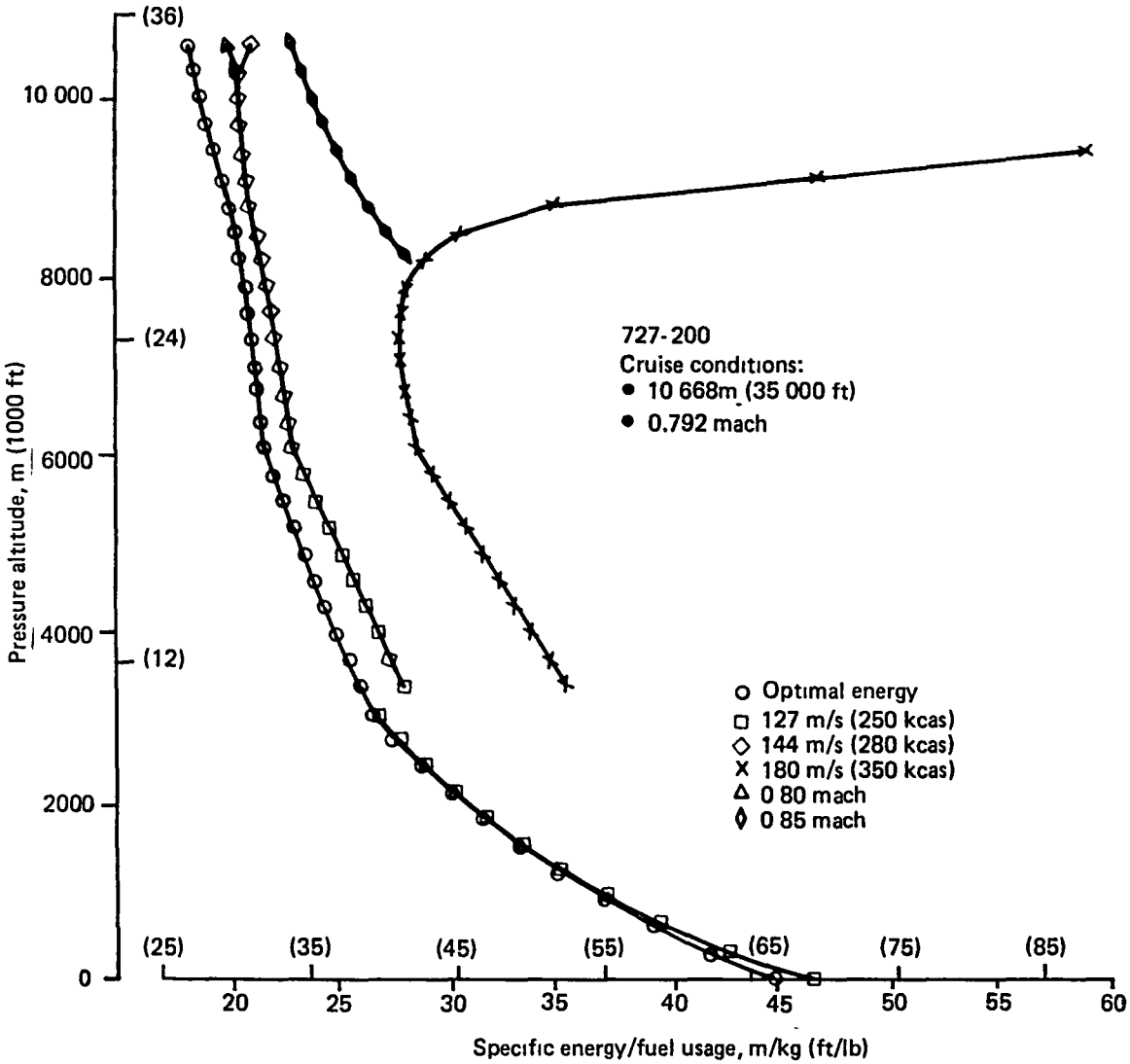

Figure 38. Effect of Descent Schedules on Specific Energy per Pound of Fuel

Table 4. Potential Benefits of Thrust Derating

Energy schedule assumption	Climb thrust used	Fuel, kg (lb)	Time, sec	Delta fuel, %
100% EPR	100% EPR	2479 (5466)	1662	—
100% EPR	95% EPR	2488 (5486)	1696	0 4
95% EPR	95% EPR	2480 (5467)	1717	0.0

Assumptions:
- 68 040 kg (150 000 lb) gross weight
- Climb to 10 668m (35 000 ft) at long-range cruise mach (0.797)
- 370 km (200 nmi) distance

The specific energy approach also accomodates to extension of best climb and descent strategies below base altitude, as shown in Figures 39 and 40. Best climb speed varies from almost 179 m/s (330 kcas) at low altitude to 134 m/s (260 kcas) at cruise. Best descent speed ranges from 121 to 137 m/s (235 to 265 kcas). Especially for climb, the FAA speed restriction represents an energy cost. Also, the greater the CAS variation in climb or descent, the less satisfactorily a single CAS or Mach/CAS schedule will be able to approximate the energy schedule

The specific energy approach selected for the development of the IEM algorithms represents a good compromise between fuel minimization, operational flexibility and airborne computing burden. The development of IEM algorithms for a 727-200 is readily generalized to other aircraft models, only the stored climb and descent performance data would need to be re-programmed. The specific energy optimized trajectories are based on simplifying assumptions:

- The lift in climb and descent is assumed equal to the aircraft weight
- Fuel burned while climbing or descending is neglected in the weight term
- Throttles are assumed maximum in climb and minimum in descent
- The cruise boundary condition is considered in the climb and descent formulation, but the base altitude condition is not

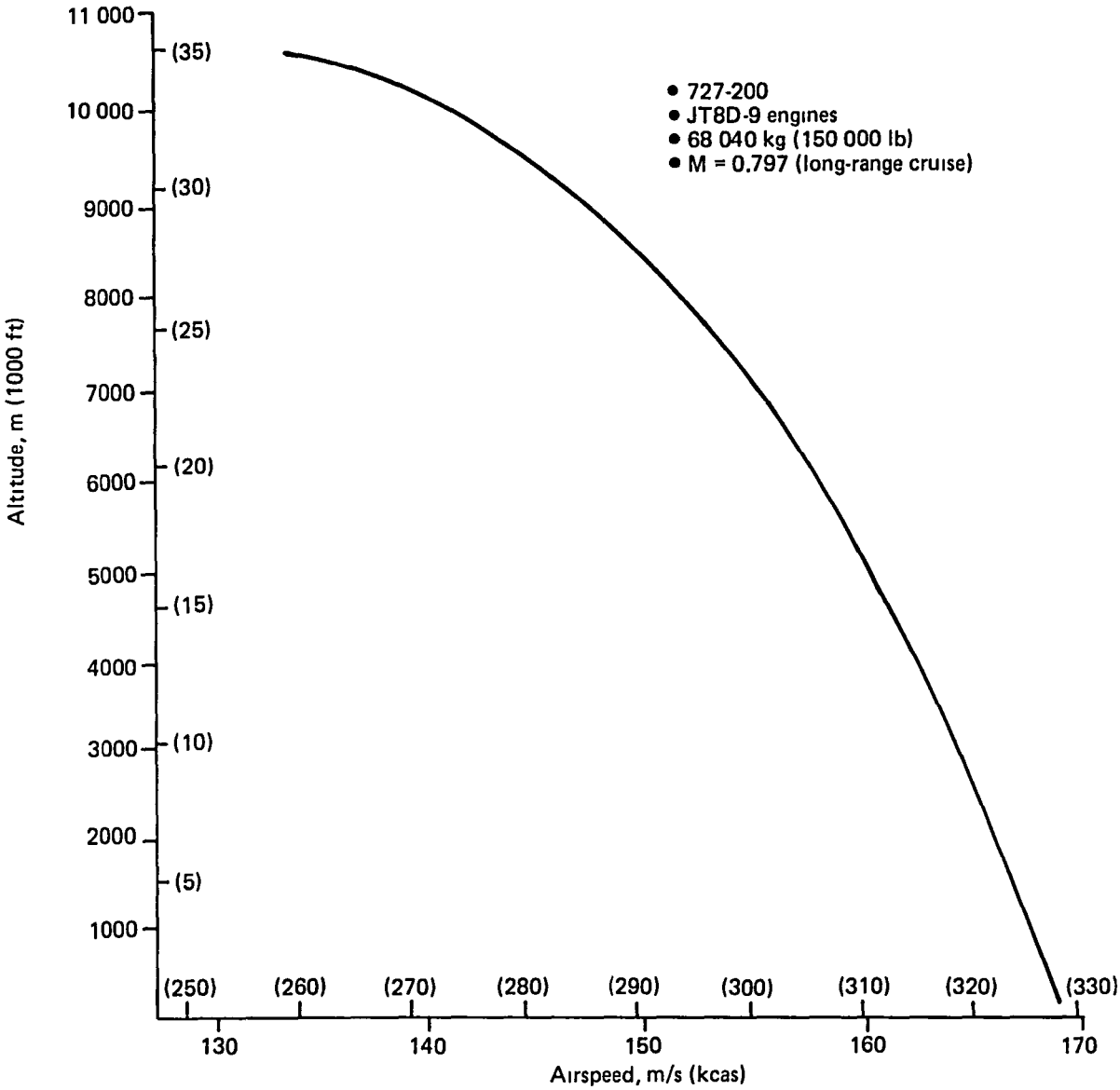

Figure 39. Optimized Speed Schedule for Climb Specific Energy

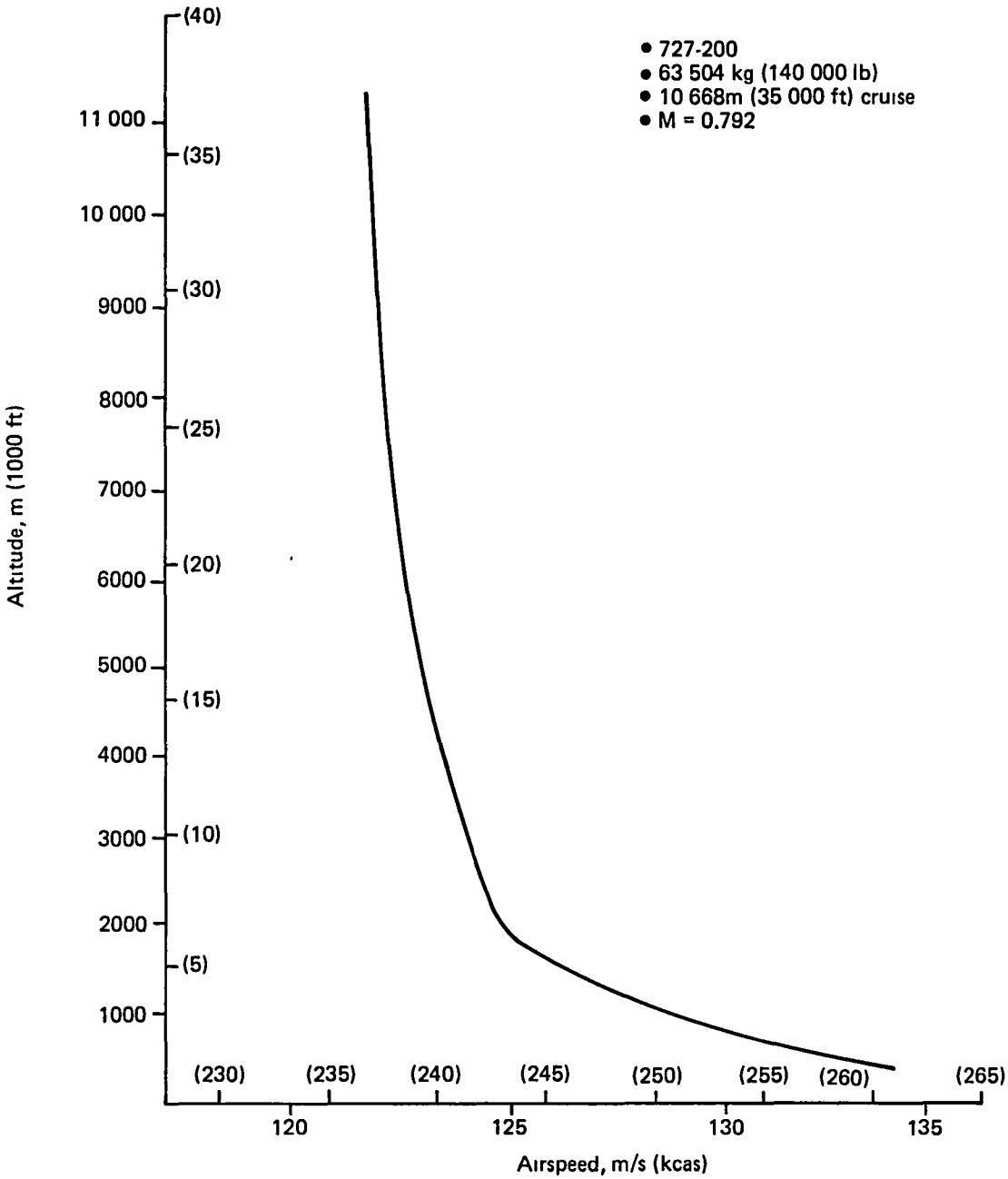

Figure 40. Optimized Speed Schedule for Descent Specific Energy

The Chebychev Trajectory Optimization Program (CTOP) discussed in Appendix B provided a first iteration appraisal of an angle-of-attack optimum climb schedule. The results of the Chebychev optimization were not significantly better than the specific energy trajectory results, although continued development of the technique should provide some gains. Probably the most critical factor neglected in the IEM formulation was the throttle transition between climb and cruise, and cruise and descent. Recent studies (ref 3 and 4) indicate further fuel savings of approximately 1% when both airspeed and throttle are included as controls. With such techniques, optimal throttle schedules from climb-to-cruise and from cruise-to-descent transitions can be derived at the cost of increased complexity in the mechanization of the energy guidance algorithms.

4.6 INTEGRATED ENERGY MANAGEMENT ALGORITHMS

This section details the climb, cruise and descent algorithms that were developed to generate the energy guidance instructions. Table 5 provides an overview of the IEM guidance function, the data required to evaluate the guidance function, and the associated autopilot and throttle modes. Mechanization of the climb and descent functions was through commands generated in an open-loop mode based on initial conditions and stored performance data. For cruise, however, an algorithm to maximize specific range was developed based on aircraft sensed speed, acceleration, weight and fuel flow parameters.

4.6.1 Climb and Descent Algorithms

The original IEM study concept for climb optimization was maximization of rate of climb. This concept was found to be impractical, for reasons discussed below, and was replaced by the open-loop concept utilizing stored performance data. The original concept was to seek the optimum climb rate by measuring rate of climb while varying the aircraft pitch angle. Several difficulties were encountered. The rate of climb parameter does not optimize climb fuel to a fixed range, although it is a fair approximation for optimizing climb fuel between two altitudes.

Table 5. Mechanization Overview of Integrated Energy Management Algorithm

Flight mode	Integrated energy management guidance	Data required	Autopilot mode	Throttle
Climb	Maximum rate of change of specific energy per unit weight of fuel	Thrust Drag Fuel flow	Indicated airspeed hold	Maximum climb engine pressure ratio schedule
Cruise	Maximize specific range	Airspeed Acceleration Fuel flow	Altitude hold	Equivalent airspeed hold autothrottle
Descent	Minimize rate of change of specific energy per unit weight of fuel	Thrust Drag Fuel flow	Indicated airspeed hold	Idle engine pressure ratio schedule

A second difficulty involved sensing the maximum rate of climb in real-time. Figure 34 shows the rate of climb for a maximum climb EPR schedule for the 727-200. The figure indicates the relative insensitivity of rate of climb to airspeed (achieved by varying pitch angle) compared to change in altitude. For climb rates typical of the 727-200, and time required for the aircraft to stabilize at a new climb speed, an energy controller would be unable to achieve the successive samples of rate of climb (even with the incorporation of acceleration terms) necessary to converge to a maximum rate at a given altitude.

The same difficulty is intrinsic in a closed-loop specific energy mechanization. Figure 35 shows contours of constant rate of change of energy per pound of fuel flow, with best climb track shown as a dotted line. The rate of change of energy varies from almost 10 energy feet $(h + v^2/2g)$ per pound of fuel at base altitude to about 3 energy feet per pound at 12 668m (35 000 ft) for the conditions noted. In climb and descent, energy changes are small for changes in airspeed and time would not be available to obtain multiple samples.

When range factor is incorporated into the energy formulation, the inclusion of the cruise range term further complicates the problem of on-board sensing of an optimal condition. Figure 36 shows climb energy contours with the range factor considered. The figure shows the flat energy gradient minima with respect to airspeed at a given delta-energy, delta-fuel level.

The climb algorithm formulated in the IEM study used stored performance information to generate the climb guidance trajectory. Figure 41 summarizes the climb guidance logic developed for IEM in 10 basic computational steps. Climb initialization, Step 1, provides

- Input of initial altitude and velocity
- Estimated initial weight input
- Computation of initial specific energy
- Input of planned cruise altitude and velocity
- Computation of final specific energy

Step 2 involves iteration of the specific energy state of the aircraft from initial to final (cruise condition) value. At each value of specific energy, a sequence of computations (Steps 3 through 8) are performed to determine the combination of altitude and velocity for which the climb function is to be maximized.

Within Step 2, a velocity iteration, Step 3, is performed from a minimum to a maximum value. At each velocity (given the energy state) the corresponding altitude (Step 4) and required atmosphere parameters (Step 5) are computed:

- Determine $h = E/W - V^2/2g$
- Compute temperature ratio
- Compute pressure ratio
- Compute density
- Compute total temperature

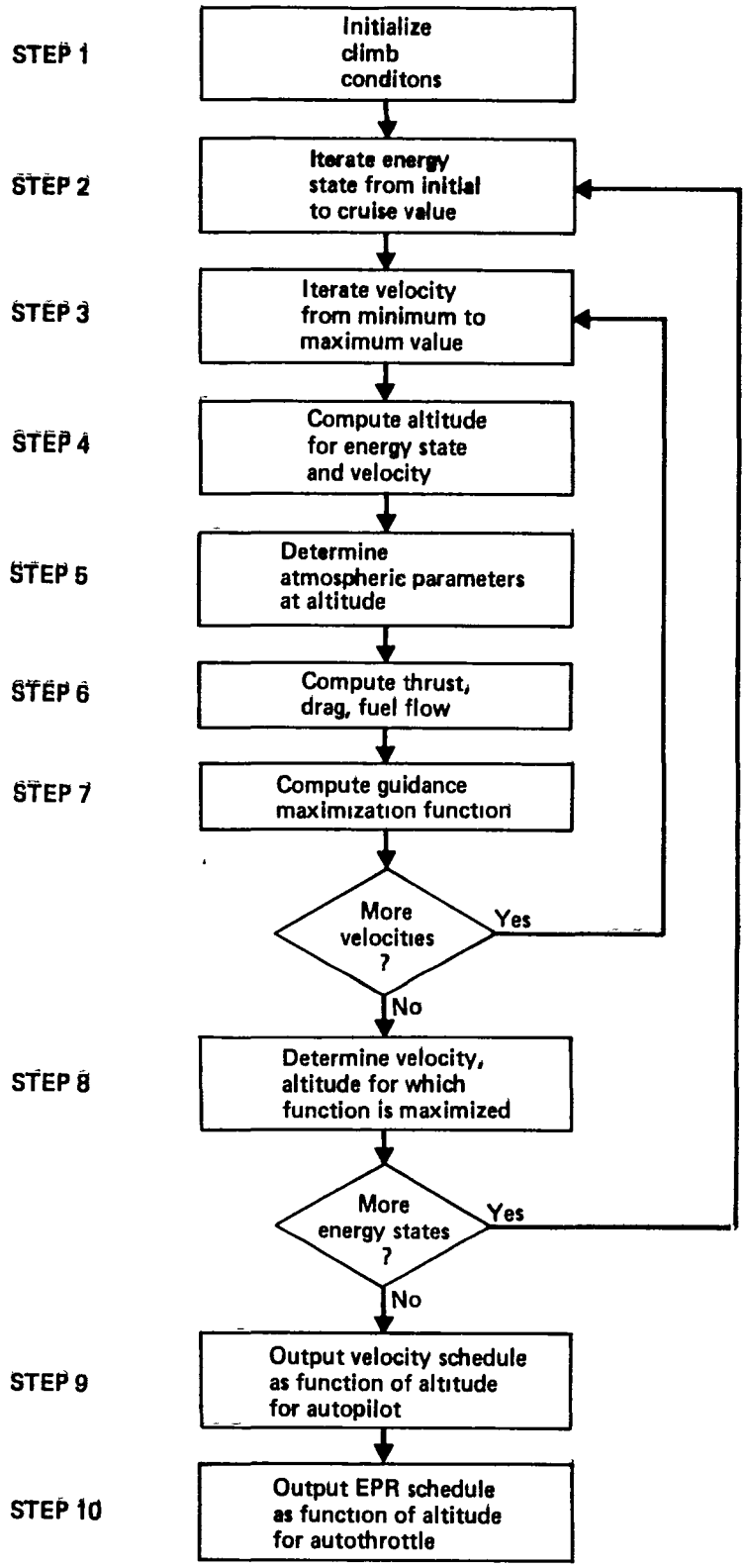

Figure 41. Functional Logic for Climb Guidance Mode

The next computation, Step 6, involves the determination of thrust, drag and fuel flow values for the altitude and velocity being considered:

- Compute $C_L = W/\frac{1}{2}\rho V^2 S$ where S is the wing area
- Determine $C_D = f(C_L, \text{Mach})$
- Compute $D = \frac{1}{2} C_D \rho V^2 S$
- Determine EPR = f (total temperature); $\Delta EPR = f(\text{altitude})$
- Determine $T/_\delta = f(\text{Mach}, EPR, \Delta EPR)$
- Compute $T = T/_\delta \times \delta$
- Determine $\sigma = f(T/_\delta, \text{Mach, altitude})$

The numerical value of the specific energy maximization function (Step 7)

$$\frac{T-D}{W} \Big/ \left[\left(\frac{T \cdot \sigma}{V}\right) - \left(\frac{T \cdot \sigma}{V}\right)_{CR}\right]$$ is evaluated,

where $\left(\frac{T \cdot \sigma}{V}\right)_{CR}$ is the cruise fuel per distance factor.

The current value of the function is saved. When all velocities have been evaluated, the largest of the computed values is determined (Step 8), with the associated velocity, altitude and engine pressure ratios. These values are used to construct tables of velocity versus altitude and engine pressure ratio versus altitude as the successive energy states are evaluated. The final two algorithm steps (9 and 10) involve the output of the velocity versus altitude schedule to the autopilot to provide a ΔV_{IAS} error signal in the IAS-hold mode and an EPR versus altitude schedule to the autothrottle to provide an EPR error signal in the EPR-hold mode.

The descent guidance logic developed for IEM is summarized in two figures. The logic to provide the specific energy optimized airspeed and engine pressure ratio schedules as a function of altitude is shown in Figure 42 The additional logic to predict the point of descent is summarized in Figure 43.

The descent energy guidance functional logic of Figure 42 contains 10 steps, as in the climb logic process. Two steps differ from those of the climb logic the use of idle descent thrust instead of maximum climb thrust (Step 6), and the replacement of the climb maximization function by the descent minimization function (Step 7).

The descent thrust, drag and fuel flow calculation step involves·

- Compute C_L as in climb
- Determine C_D as in climb
- Compute drag as in climb
- Determine idle EPR = f (total temperature, Mach)
- Determine idle T = f (Mach, altitude)
- Determine idle $\sigma = f(\text{Mach, altitude})$

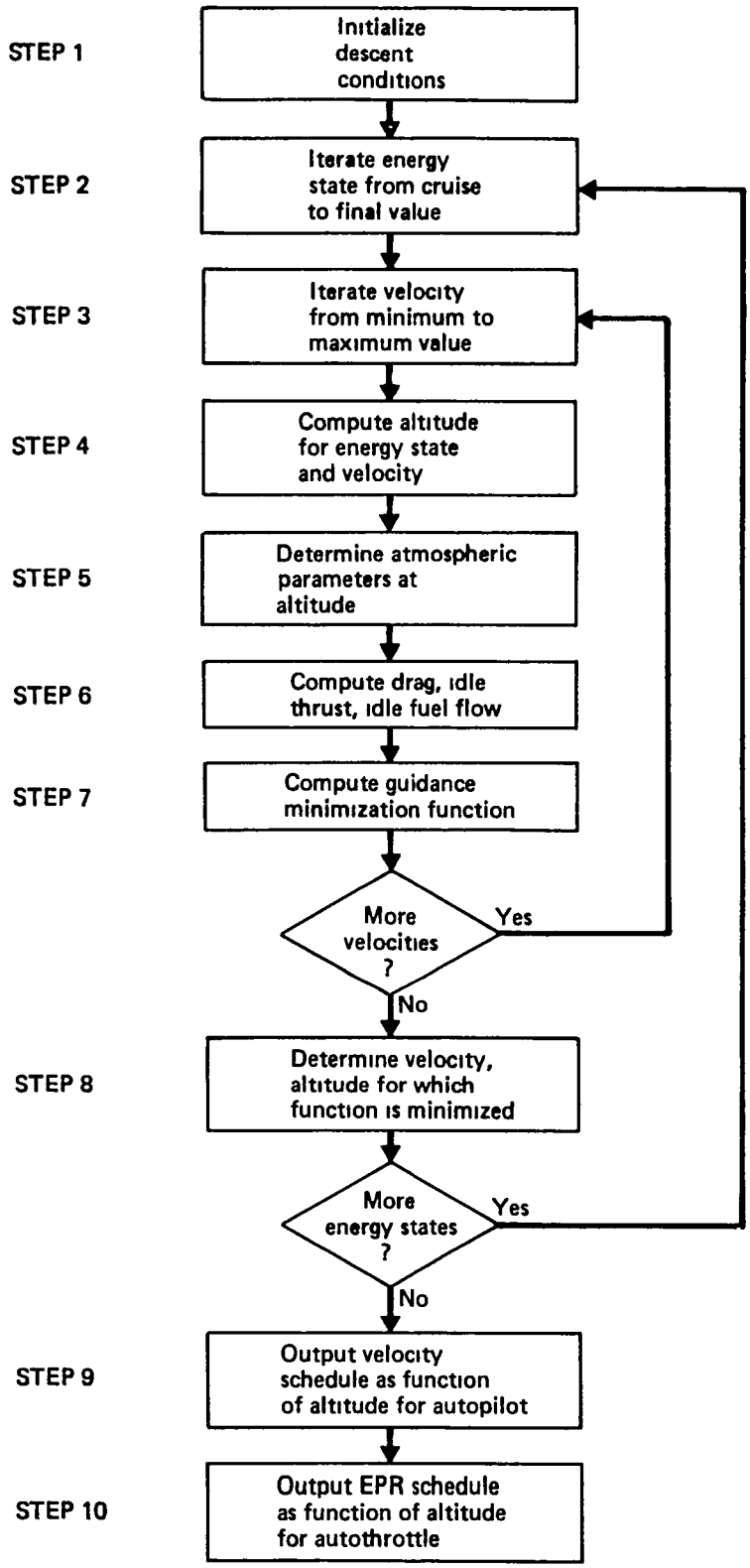

Figure 42. Functional Logic for Descent Guidance Mode

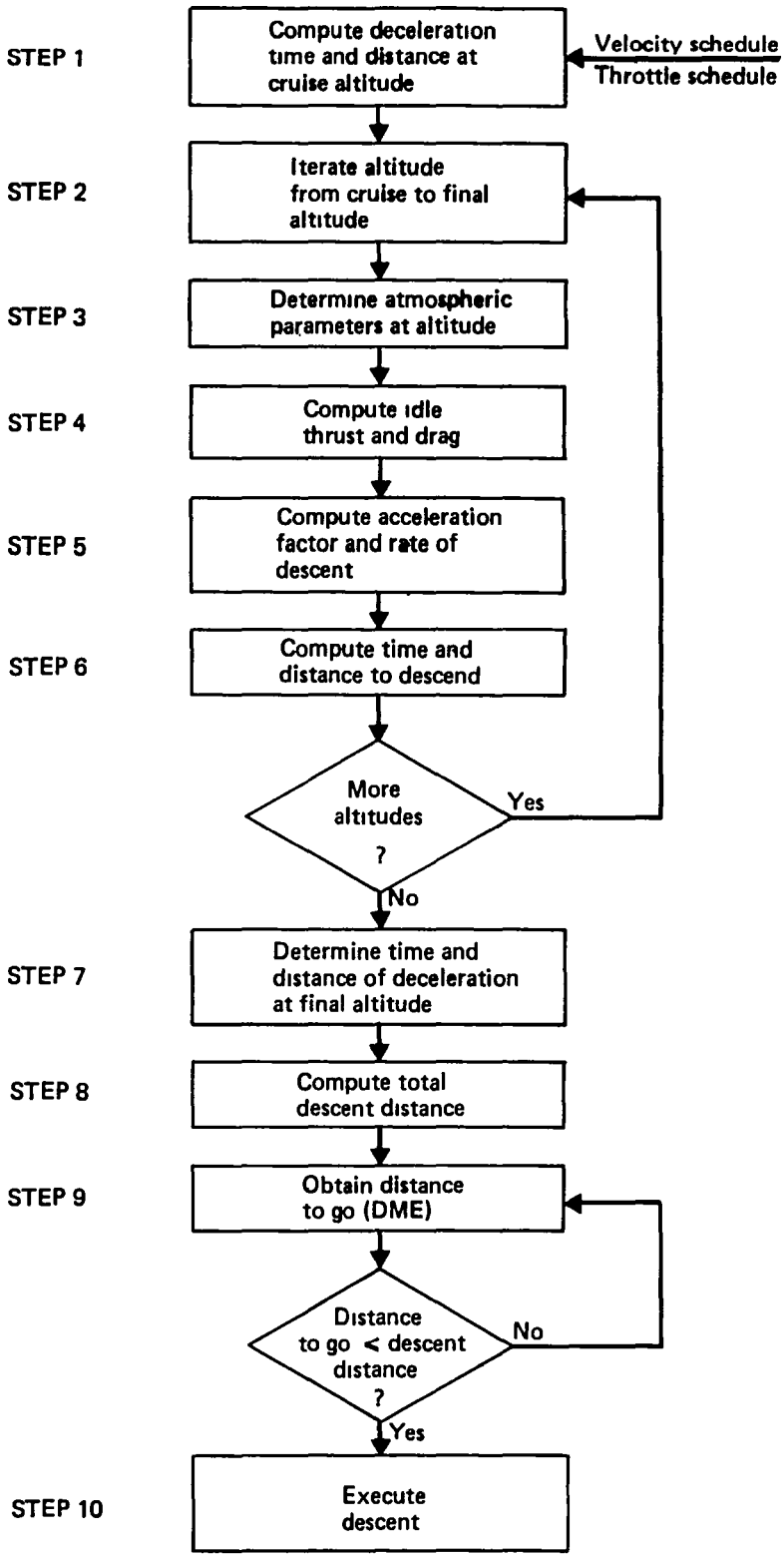

Figure 43. Functional Logic for Point of Descent

The numerical value of the specific energy function to be minimized in descent

$$\frac{D-T}{W}\Big/\left[\left(\frac{T\cdot\sigma}{V}\right)_{CR}-\left(\frac{T\cdot\sigma}{V}\right)\right]$$

where $\left(\frac{T\cdot\sigma}{V}\right)_{CR}$ is the cruise fuel per distance factor.

In addition to the guidance functional logic, provisions for point-of-descent prediction are incorporated in the descent algorithm as shown in Figure 43. The point-of-descent prediction involves the determination of the descent trajectory in the algorithm. The computed distance to descent is then compared to the distance to go, to determine the point at which the descent should be initiated. Nine steps are involved in the determination of the required let-down distance. The time and distance to decelerate (or accelerate) from cruise velocity to the initial value of the descent speed schedule is determined, assuming idle deceleration or maximum cruise thrust acceleration (Step 1). The altitude is iterated by 152m (500 ft) steps from cruise altitude to the base altitude for the IEM flights (Step 2). For each altitude interval, the required atmosphere parameters (density and total temperature) are computed (Step 3). The drag and thrust forces are computed as in the analagous descent energy guidance computation (Step 4).

The computation of acceleration factor and rate of descent (Step 5) used the standard point-mass, steady-state descent equations.

$$\frac{dh}{dt}=\frac{V(D-T)}{W}\Big/\left[1+\frac{V}{g}\cdot\frac{dV}{dh}\right]$$

where $\frac{V}{g}\cdot\frac{dV}{dh}$ is the acceleration factor.

The time to descend the altitude interval is computed by dividing the interval by the rate of descent (Step 6). A deceleration (or acceleration) calculation at the final altitude ends the descent with the aircraft at the specified energy state (Step 7). The total distance to decelerate, descend, and again decelerate is computed (Step 8) and compared to the distance to go (Step 9). The algorithm assumes the availability of DME or an equivalent capability to determine when to start the descent. The mechanization logic can incorporate wind profile effects, although zero wind was assumed for the IEM applications.

4.6.2 Cruise Algorithm

The development of an automatic energy manager to locate and acquire a best cruise operating state required consideration of four basic problems

1. Speed/thrust instability near maximum range cruise speeds
2. Airspeed/groundspeed optimization
3. Engine dynamics fuel penalties
4. Aircraft acceleration response time constant

Figure 44 shows the relationship between thrust required and thrust available for one altitude and weight condition, as a function of Mach number, and for one value of engine pressure ratio. For the given thrust level there exist two steady-state operating Mach numbers. The higher Mach number has positive speed-thrust stability. Any disturbance (wind gust, etc.) will be compensated by the aircraft and the original Mach number will tend to be restored. At the lower intersection point, the original operating condition will not tend to be restored. Once the aircraft thrust is less than the thrust required, the difference (deceleration) will tend to increase. The minimum thrust required Mach number is the maximum endurance operating point. The maximum range cruise point occurs at a higher Mach number (maximum Mach L/D). The Mach number for long-range cruise is defined as occuring where a 1% fuel penalty (in terms of range) is accepted in order to provide more positive speed stability and decrease trip time. The IEM cruise algorithm investigates operation at the maximum range cruising point and provides an automatic monitor/thrust controller to operate near the minimum fuel speed.

Since the objective of the optimization process in cruise is to maximize ground miles per pound of fuel burn, wind effects should be considered. Figure 45 shows the change in maximum range cruise Mach as a function of headwind. The effect of a headwind on fuel minimization is to require a higher operating airspeed. Conversely, in a tailwind, the best fuel strategy is to reduce the airspeed. However, the speed stability considerations at airspeeds below the zero-wind

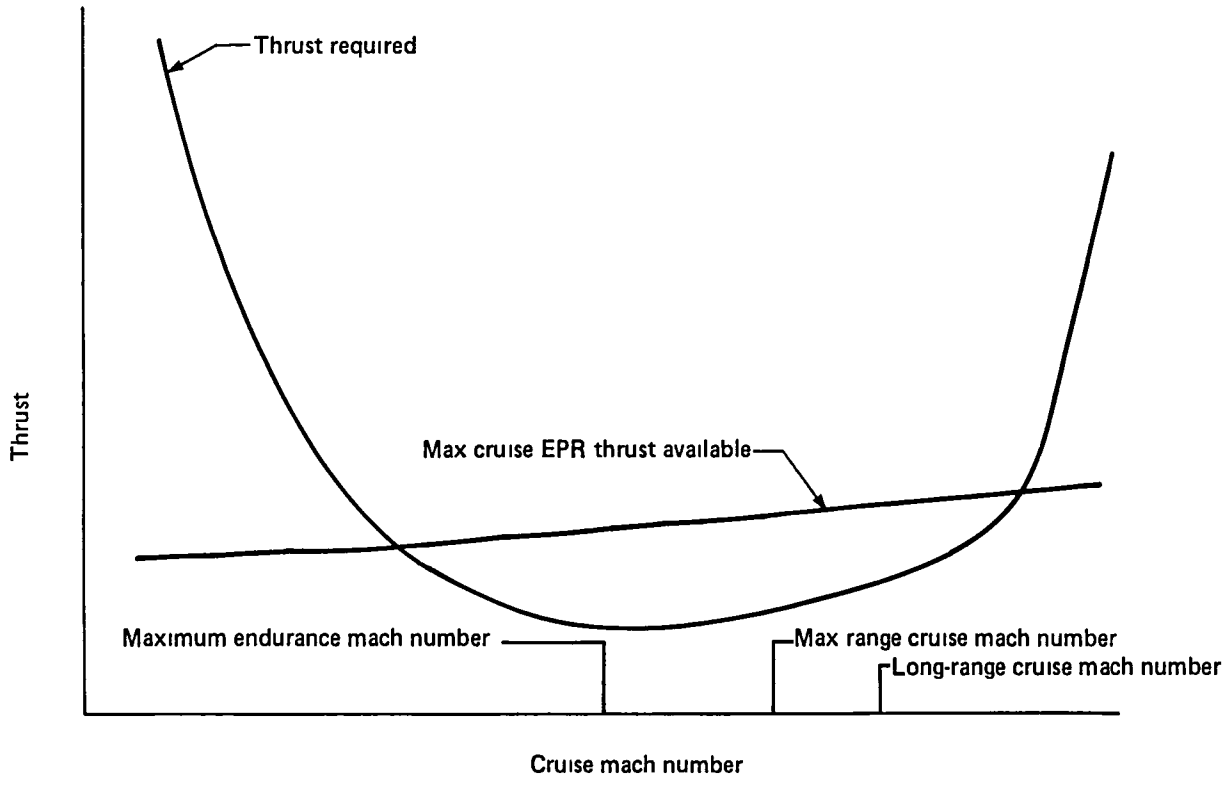

Figure 44. Available Thrust Versus Required Thrust in Cruise

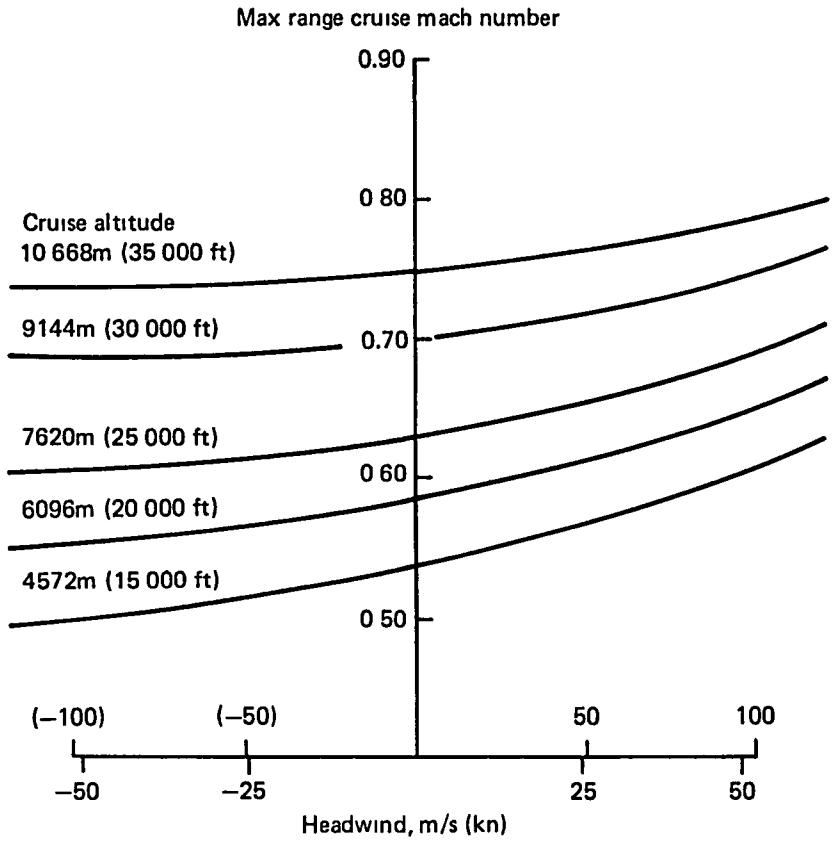

Figure 45. Wind Effects on Max Range Cruise Mach Number

maximum range cruise Mach number tend to prohibit operation. As an example of the impact of winds on fuel mileage, consider a 63 504 kg (140 000 lb) 727-200 cruising at 10 668m (35 000 ft). The maximum range cruise Mach number is about 0 75. In the presence of a 51.4 m/s (100 kn) headwind, increasing the cruise Mach number to 0 785 will result in an improvement in fuel mileage of about 0.7%. In the still air case, increasing the Mach number from 0.75 to 0.785 would have decreased the fuel mileage by about 0.7%. The estimated average savings per flight would require an analysis of wind frequencies for various cruise altitudes and the corresponding fuel penalties.

Because ground speed was not obtained from the airline measured data due to processing complexity, the original algorithm development assumed a zero wind environment and optimized with respect to nautical air miles. The extension of the algorithm to incorporate wind data (if available on-board the aircraft) would be straight-forward. In the case of a tail-wind, speed reduction probably would be limited to the maximum range (zero wind) airspeed value.

Figure 46 shows how fuel flow varies for one altitude as a function of engine pressure ratio and Mach number. Three engine operating states are considered· engine accelerating, steady-state

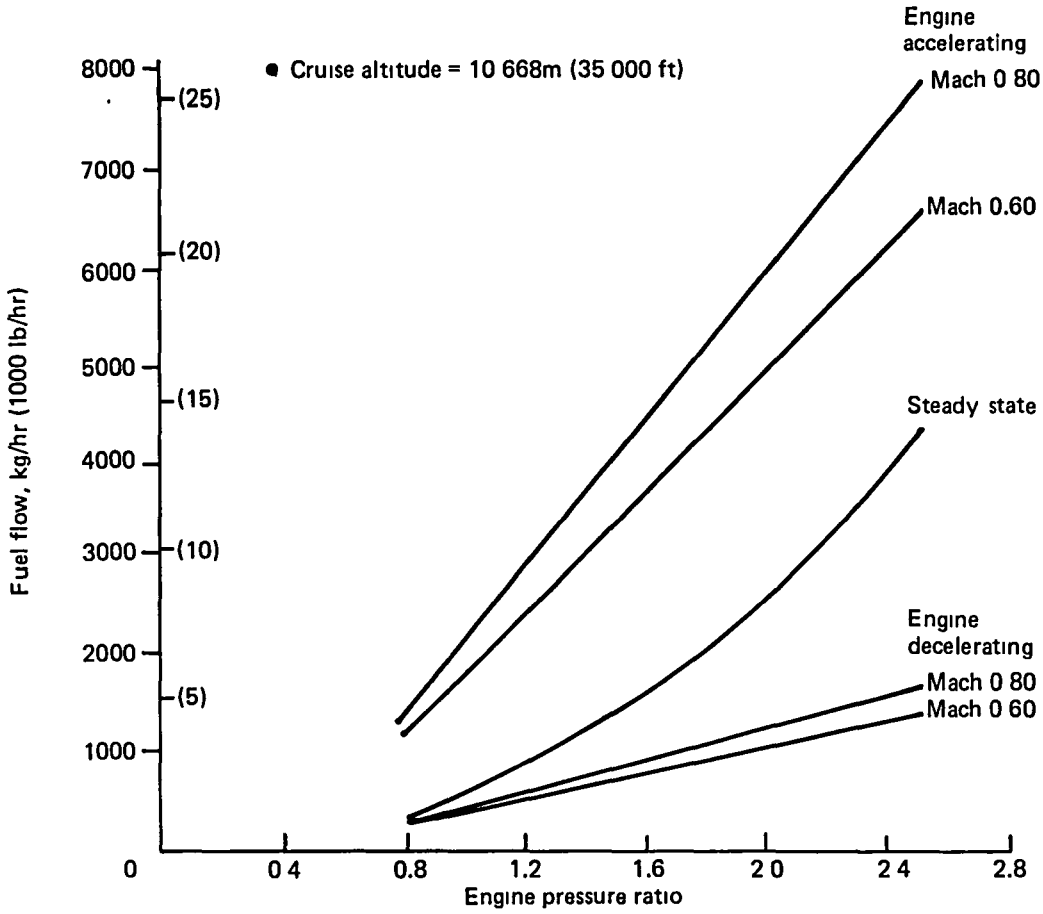

Figure 46. Effect of Engine Operating State on Fuel Flow

and decelerating. The development of a fuel-efficient cruise algorithm should provide most operation in the steady-state condition because rapid accelerations tend to produce fuel penalties The IEM cruise algorithm, once locating the optimum operating point, zeros the autothrottle error signal. As long as the aircraft speed remains within an acceptable airspeed dead zone, no corrections are made.

The next consideration in the development of the IEM cruise algorithm is the time taken by the aircraft to reach an airspeed corresponding to a given thrust available. Figure 47 indicates the relatively long response time required by the aircraft to reach an unaccelerated operating speed. The engine acceleration/deceleration time for the small changes in commanded EPR during cruise is only a few seconds; the aircraft, however, requires several minutes to stabilize.

The technique developed for the IEM algorithm was to maximize V/w_f where

V = true airspeed
w_f = fuel flow

Instead of waiting for the aircraft to stabilize at an unaccelerated airspeed, the IEM search for best range occurs while thrust is not equal to drag. The difference, measurable as an acceleration, is converted into a fuel flow correction term by applying the thrust specific fuel consumption (TSFC). Thus, the fuel flow value used is the measured fuel flow plus a correction term:

$$\Delta T = T - D = ma$$

$$\Delta w_f = TSFC \cdot \Delta T = TSFC \left(\dot{V}_p \cdot \frac{W}{g} + \frac{\dot{h}W}{V_p}\right)$$

where:

ΔT	=	excess thrust
T	=	thrust component of force
D	=	drag component of force
$TSFC$	=	thrust specific fuel consumption
$\dot{V}_p$	=	flight path acceleration
W	=	aircraft weight
g	=	acceleration of gravity
$\dot{h}$	=	altitude rate, and
V_p	=	flight path velocity.

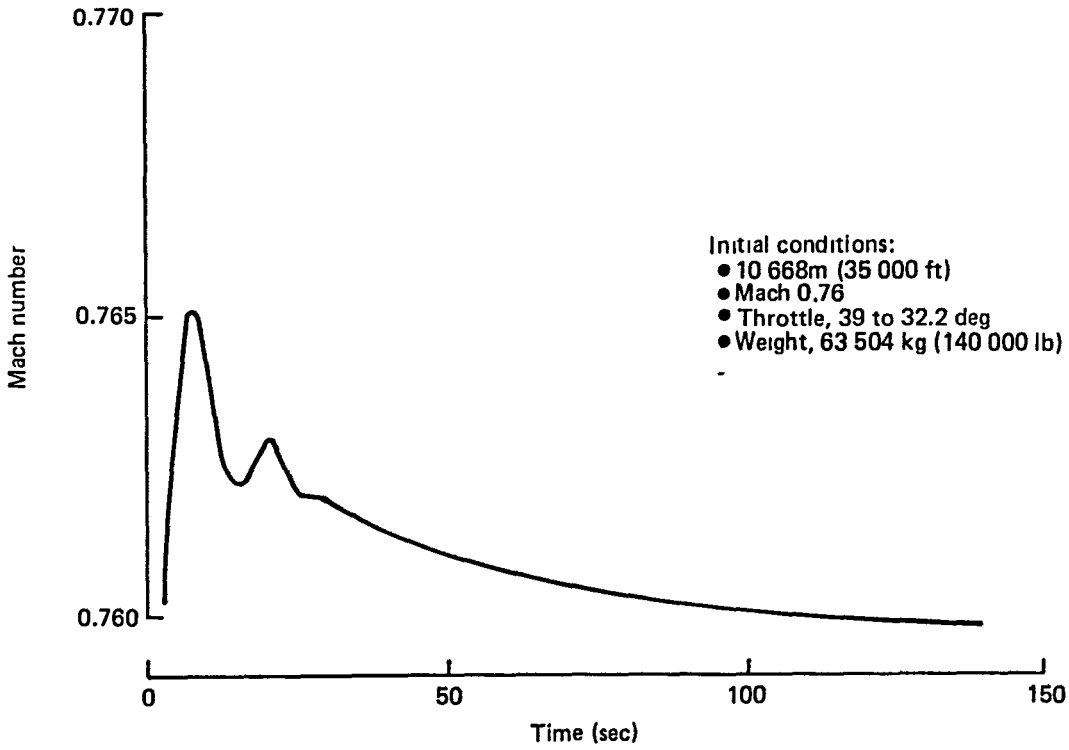

Figure 47. Velocity Convergence to Max Range Cruise Mach Number

An example of one specific range search is shown in Figures 48 through 50. These figures show the resultant Mach number, fuel flow and adjusted (steady-state) fuel flow, and sampled specific range for one altitude, weight and throttle setting. For the case shown, the aircraft was accelerated from Mach 0.70 through the target maximum range cruise Mach number (about 0.757). The resultant estimates of specific range were based on a 5-sec sampling interval, with several successively decreasing specific range values required to indicate a minimum. The sampling interval and multiple values were used as a simple smoothing technique. Some short-term oscillations in measured specific range were encountered due to thrust changes, stabilizer movement, etc. No atmospheric turbulence was assumed for the modeling. The presence of moderate turbulence might require development of a more sophisticated sampling technique. In the presence of heavy turbulence the target (handbook) cruise Mach value might prove more reliable than a sampled value. Further study also would be required to establish airspeed decay times at maximum range cruise Mach for various turbulence levels.

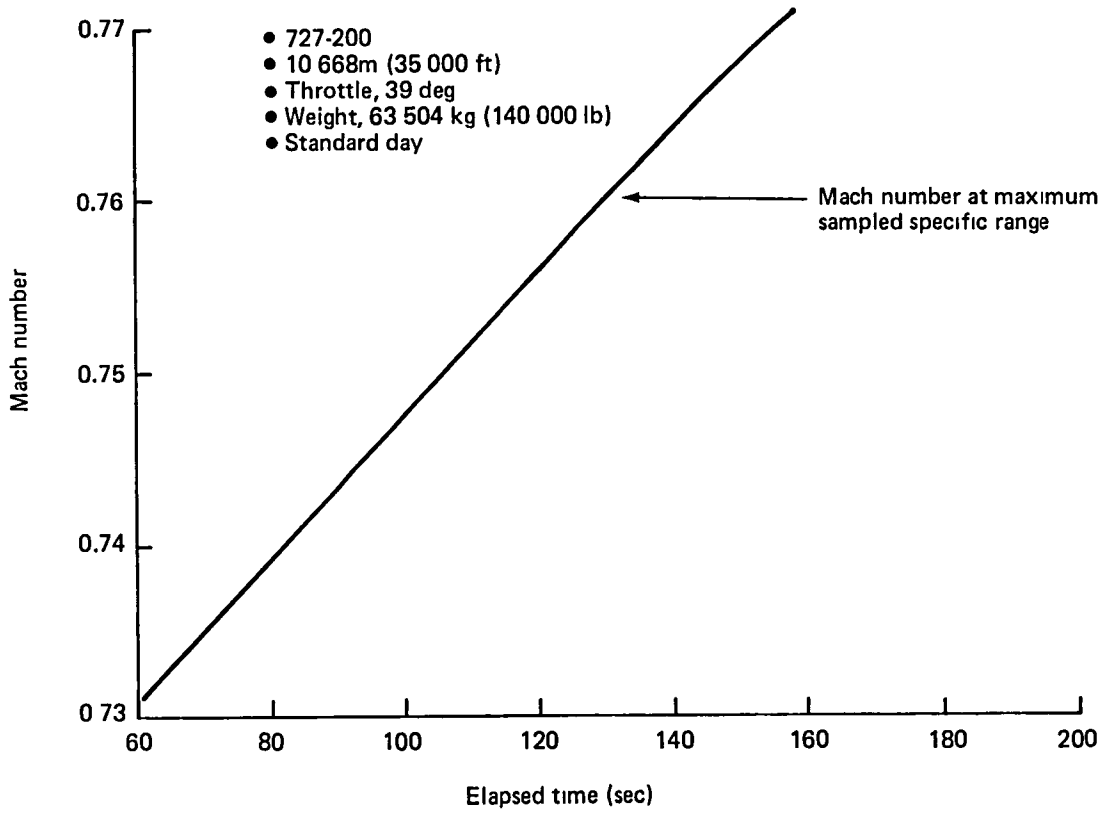

Figure 48. Airspeed During Cruise Sampling

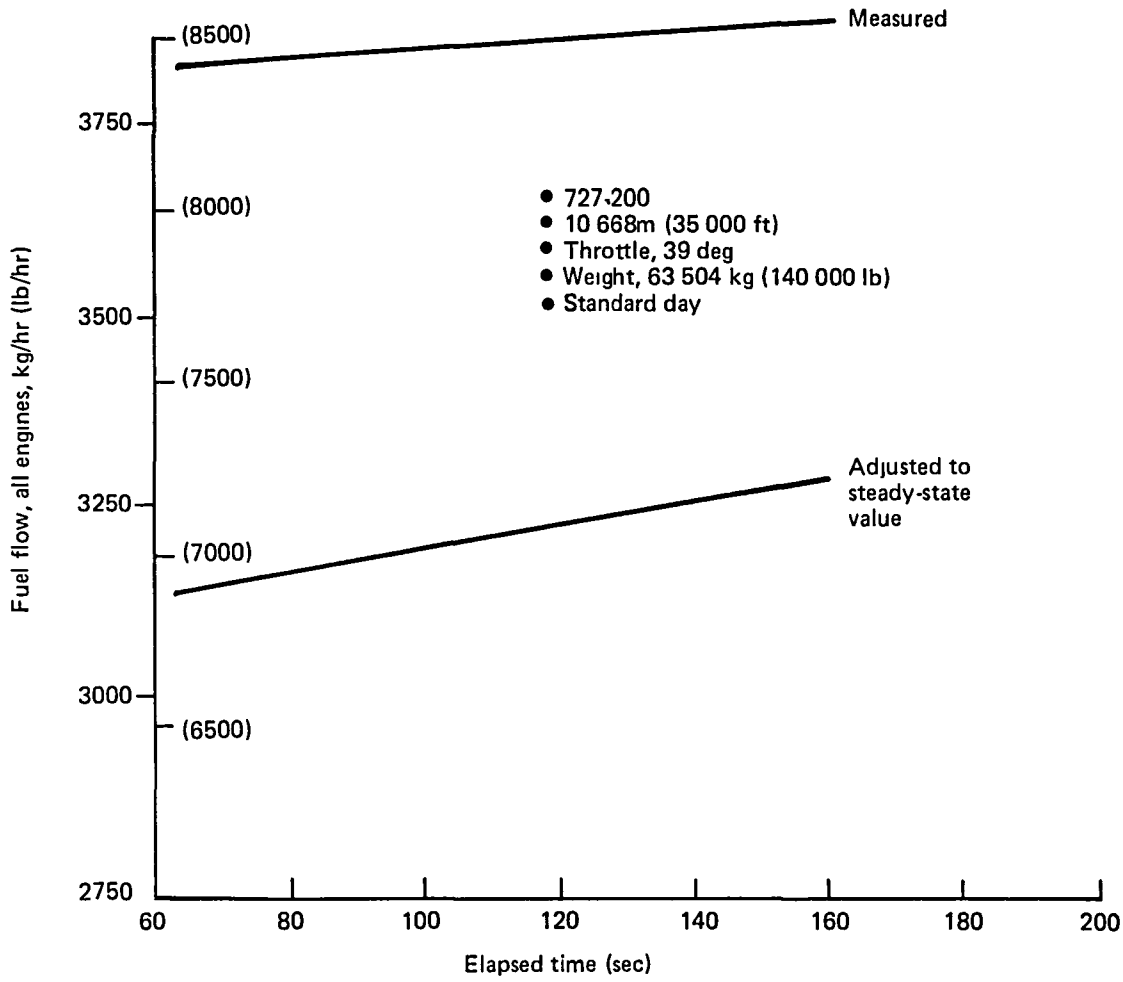

Figure 49. Fuel Flow During Cruise Sampling

The detailed logic flow developed for the IEM cruise algorithm and a variable glossary are included as Appendix C. The logic was incorporated into the evaluation model and used to provide error signals to the autopilot and authrottle for the cruise test cases. The IEM cruise logic is summarized in four steps.

1. Search for the maximum range cruise Mach at an assigned altitude and employing real-time values of velocity, acceleration and fuel flow from airplane sensors (Mode 1)

2. Engage the autothrottle to attain the optimum speed throttle position (Mode 2)

3. Fix the throttles at the optimum position monitoring airspeed and weight (Mode 3)

4. Reinitialize to Mode 1 or 2 as required

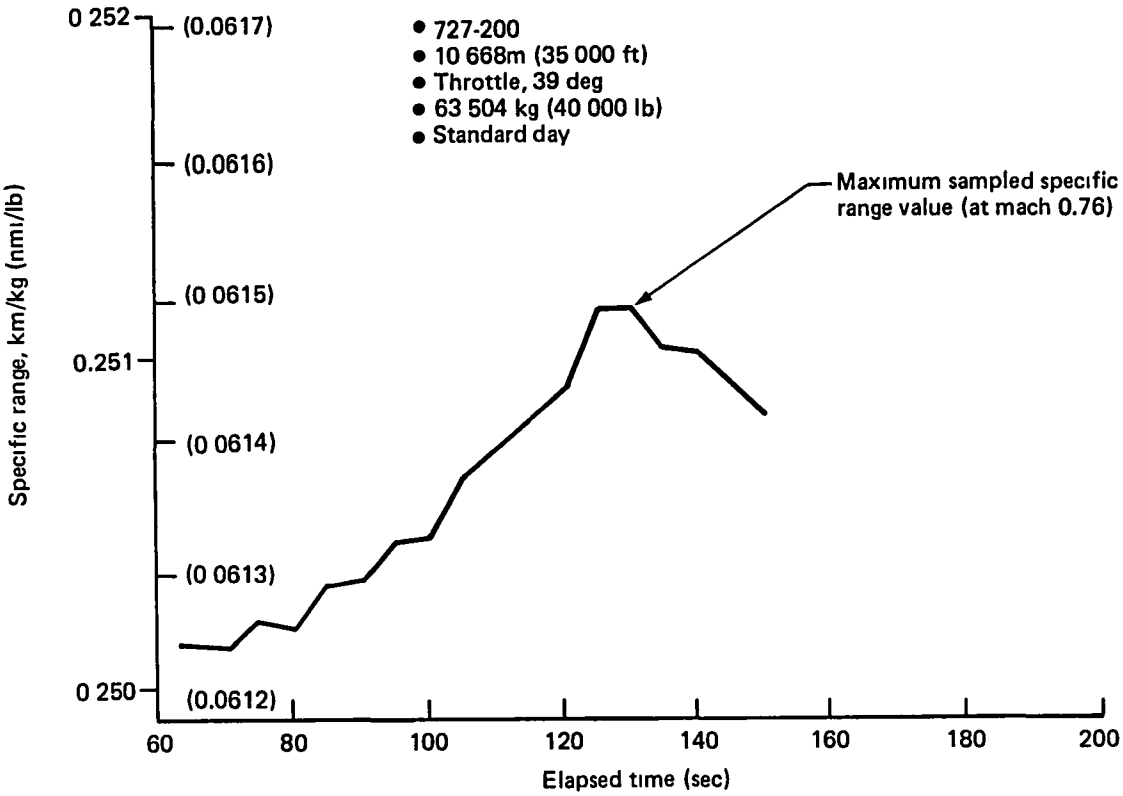

Figure 50. Estimated Specific Range

4.6.3 Cruise Algorithm Sensor Requirements

Figure 51 summarizes the inputs required for the IEM cruise algorithm mechanization: measured values of Mach number, equivalent airspeed, true airspeed, flight path acceleration, altitude, altitude rate, fuel flow and weight. Tabular values of specific fuel consumption and target Mach numbers are required. The IEM processes and output signals also are indicated.

4.7 IEM SIMULATION OF REFERENCE FLIGHT CONDITIONS

This section describes the application of the IEM algorithms to the reference flight conditions in the Boeing SSM. The basic conditions of the reference flight imposed on the IEM simulation were reference flight range above base altitude, cruise altitude, takeoff weight, and climb, cruise and descent temperature profiles. The IEM algorithms described in Section 4.6 then were used to generate airspeed and engine pressure ratio commands to minimize fuel to a specific range. The resultant time and fuel values were determined in the SSM and compared with the reference flight results (described in sec. 4.4).

The fixed range value was based on integrated true airspeeds of the reference flight. As groundspeeds were not available, a zero-wind condition was assumed for both the reference flight simulation and the IEM simulation. A cruise altitude of 10 058m (33 000 ft) was used, although this altitude is not optimal for fuel consumption at the reference flight weight. Flight distance at cruise altitude was adjusted for the IEM profile climb and descent distances.

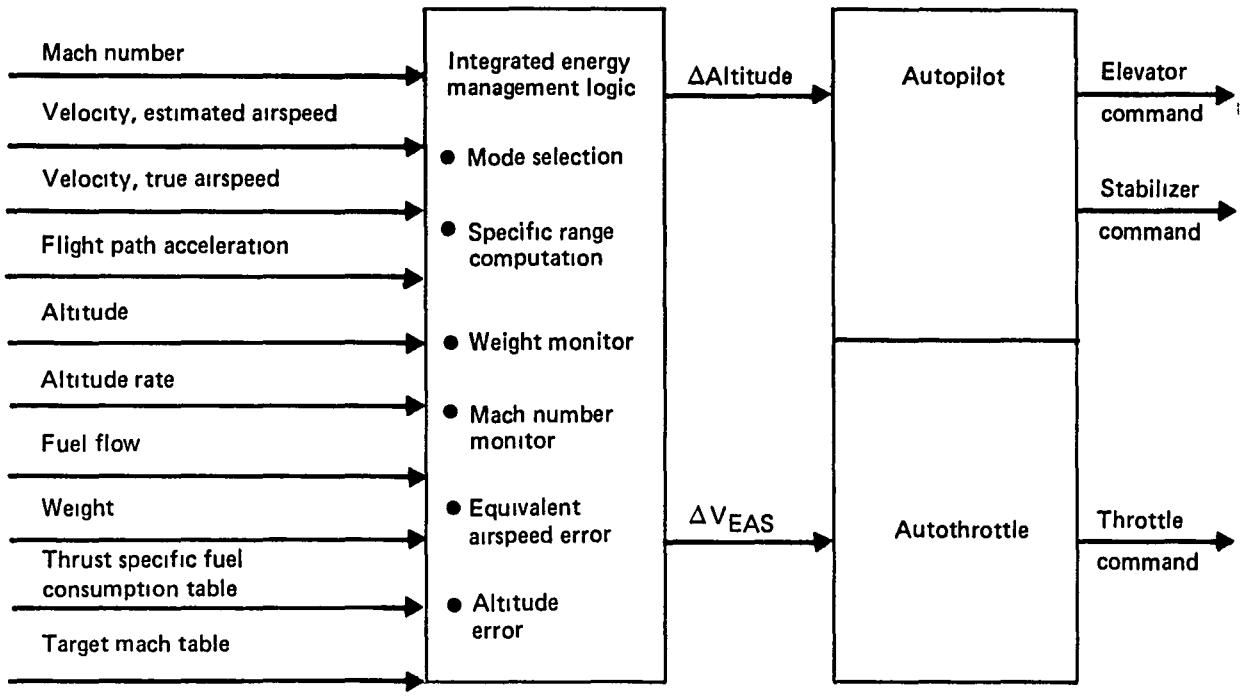

Figure 51. Mechanization for Integrated Energy Management Cruise Algorithm

The IEM profile was divided into climb, cruise and descent segments. Weight was set to the comparable reference flight weight at the beginning of each segment to ensure comparability of performance of each segment. The weight discrepancy thus introduced was small, but resulted in the IEM simulation carrying a slight fuel weight penalty.

Complete climb and descent simulations, and selected portions (about 700 sec.) of the cruise segment were run. The cruise sampled results were extrapolated to the total cruise flight to reduce computer execution time and cost.

4.7.1 IEM Profile for the Reference Flight Conditions

Climb and descent energy profiles generated by the IEM guidance algorithm are contained in Figures 52 and 53. They are based on reference flight weight, cruise altitude and temperatures. The resultant energy airspeed tracking error is shown as a function of altitude for climb and descent in Figures 54 and 55. Except for initialization error, the target and actual airspeeds were generally within one knot. The resultant climb and descent profiles are shown in Figures 56 and 57. Cruise altitude was reached in 640 sec. from base altitude, compared to the reference profile time to climb of 935 sec. Descent required 839 sec. for the IEM profile versus 700 sec. for the modeled reference profile. Fuel flow values for climb and descent for the IEM profile are shown in Figures 58 and 59.

One complete cycle of search, acquire, throttle lock/monitor, re-acquire and lock/monitor was simulated for the initial cruise conditions of the reference flight. Also, a cycle of search,

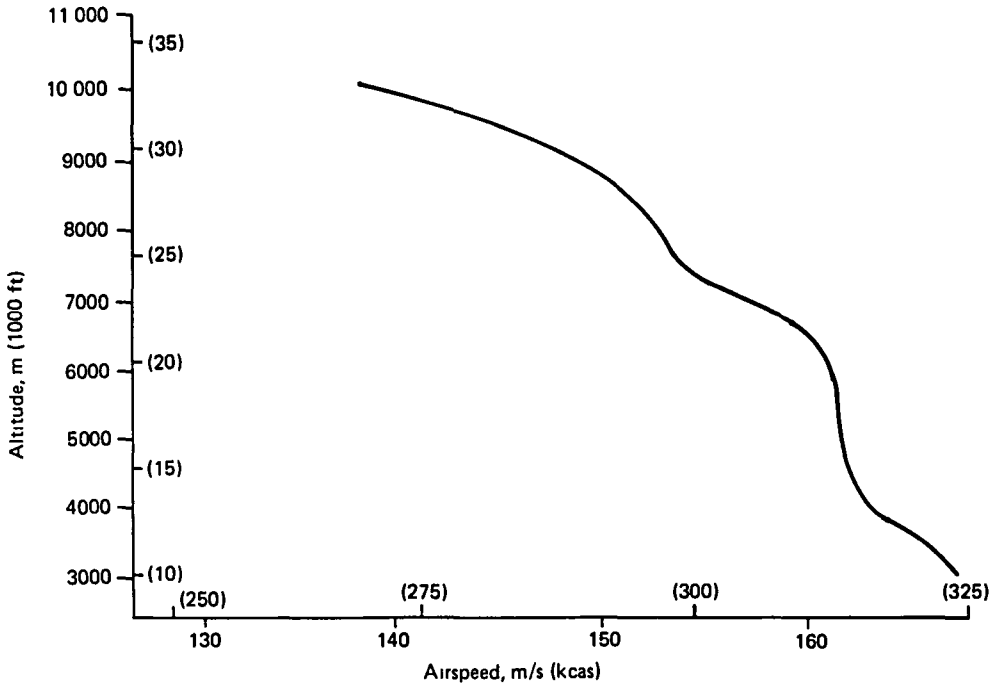

Figure 52. Integrated Energy Management Climb Schedule

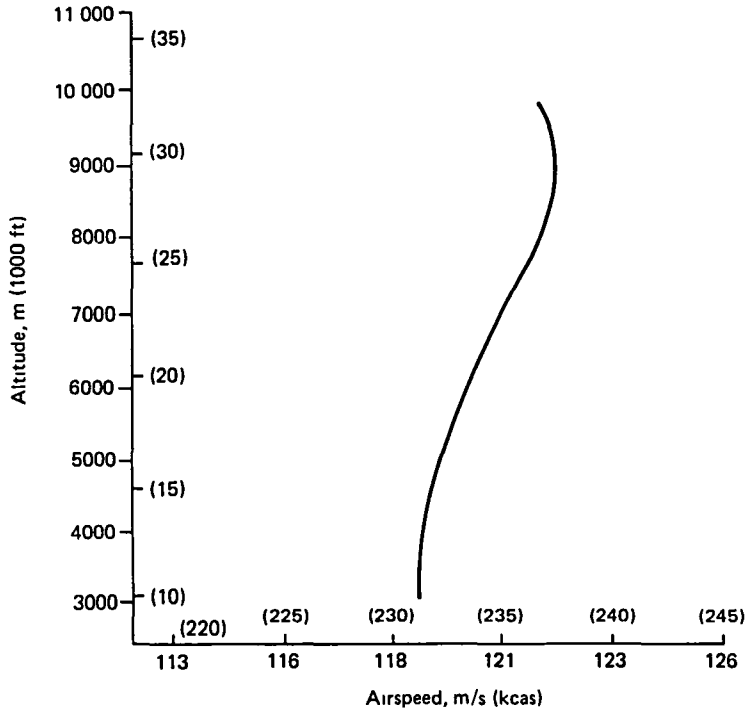

Figure 53. Integrated Energy Management Descent Schedule

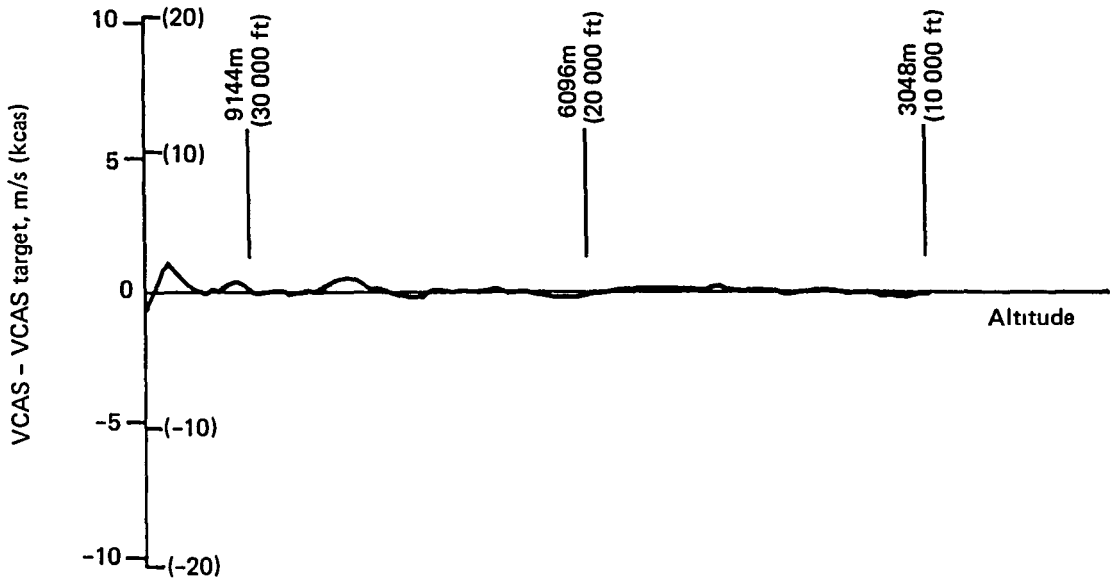

Figure 54. Airspeed Tracking Error for Energy Climb

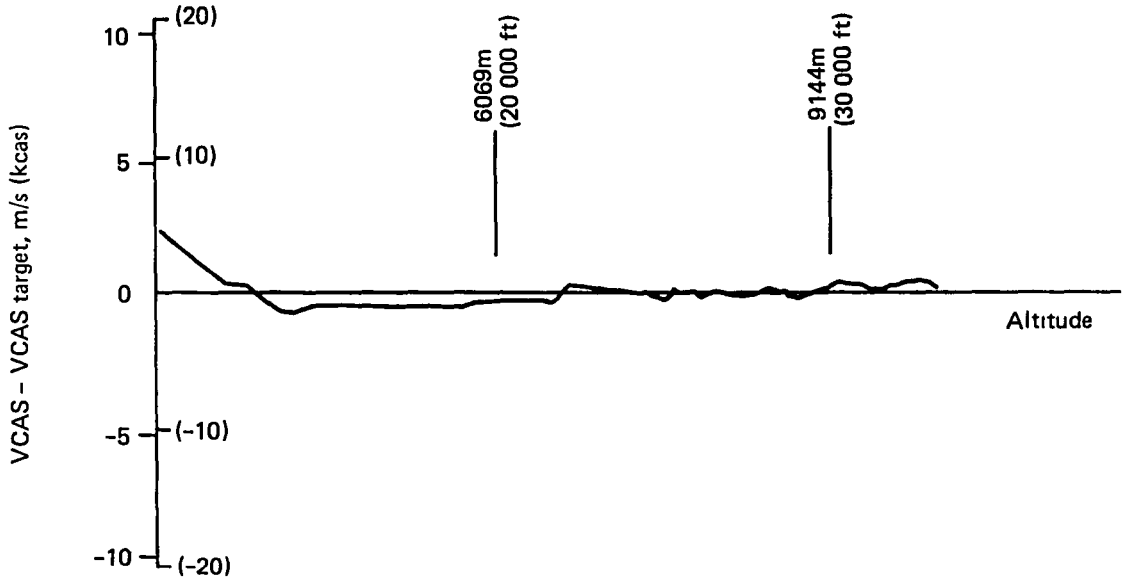

Figure 55. Airspeed Tracking Error for Energy Descent

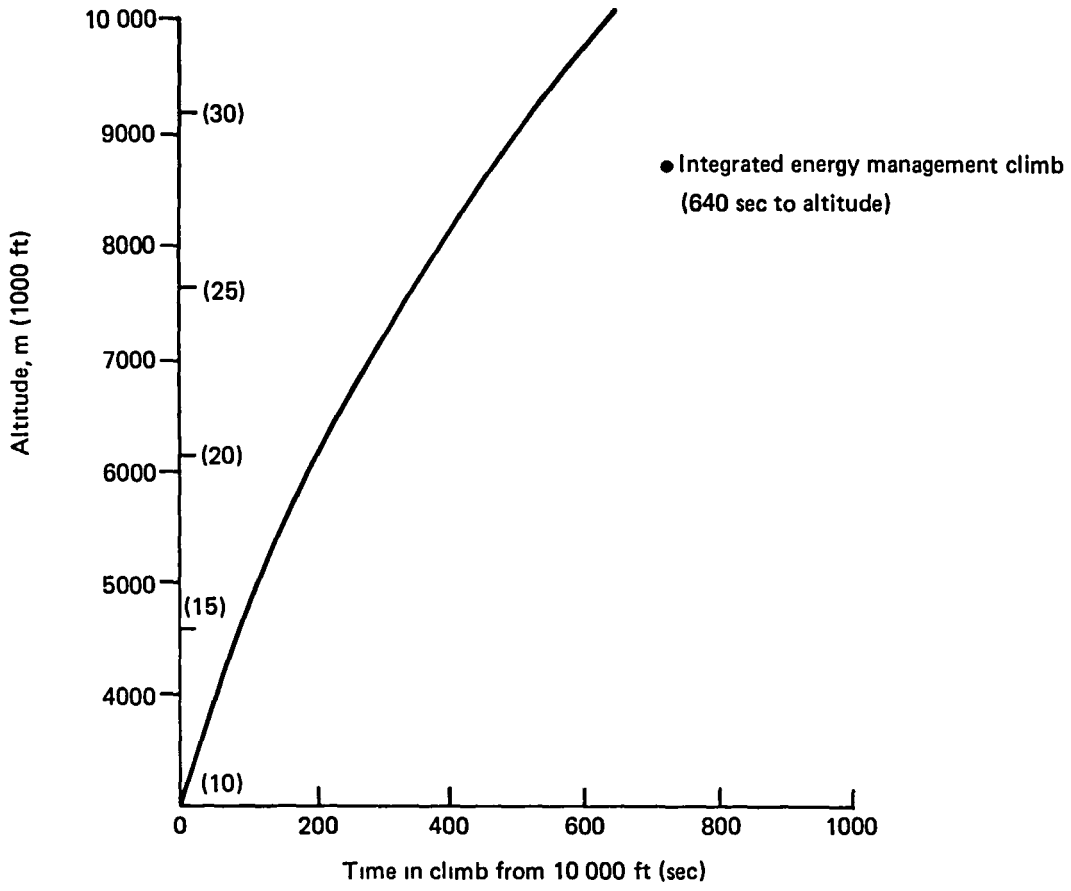

Figure 56. Integrated Energy Management Climb Profile

acquire and lock/monitor was simulated for the final cruise conditions. Mach number for 200 sec. of initial cruise is shown in Figure 60, increasing in the search mode and stabilizing at the sampled maximum range Mach number. The equivalent airspeed error signal input to the auto-throttle is shown over the same interval in Figure 61. The corresponding IEM modes (search, acquire and monitor) also are indicated. The resultant throttle lever angle position is shown in Figure 62 for the same time interval.

4.7.2 IEM Simulation Results

The resultant IEM medium-range flight parameters of time, distance and fuel total are compared with the reference flight simulation results in Table 6. The flights were adjusted by an acceleration to climb speed and a deceleration at the end of descent at base altitude to guarantee that both flights had the same starting and ending energy states. The cruise distance for the energy flight was adjusted to guarantee a common range.

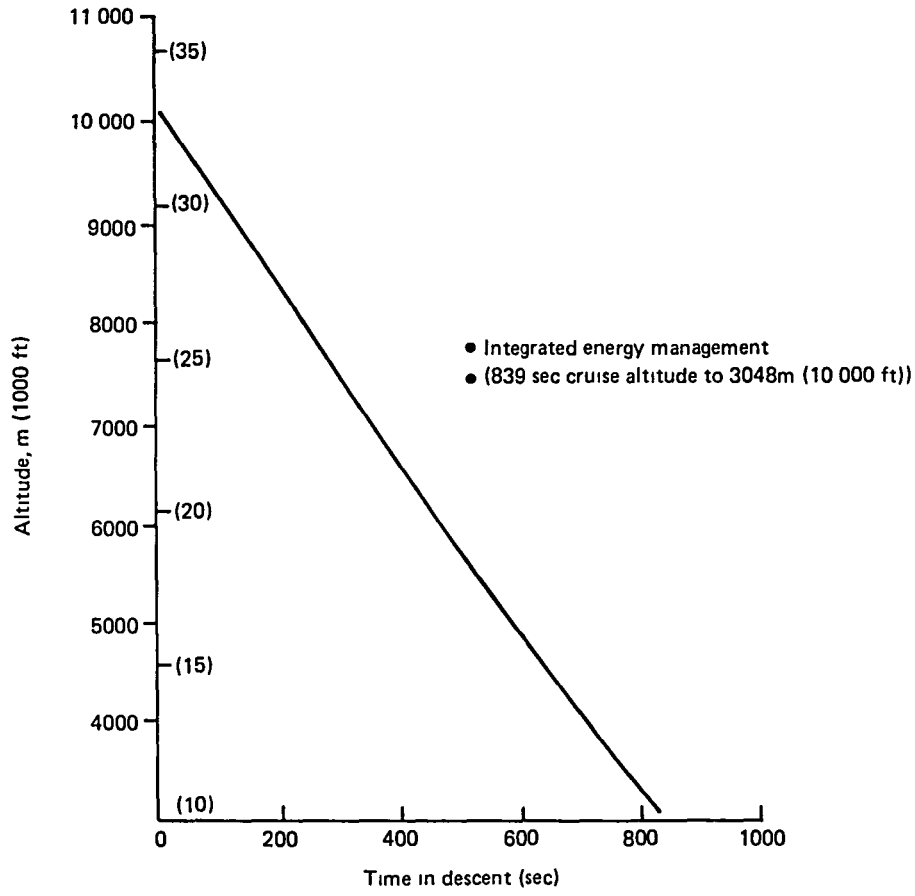

Figure 57. Integrated Energy Management Descent Profile

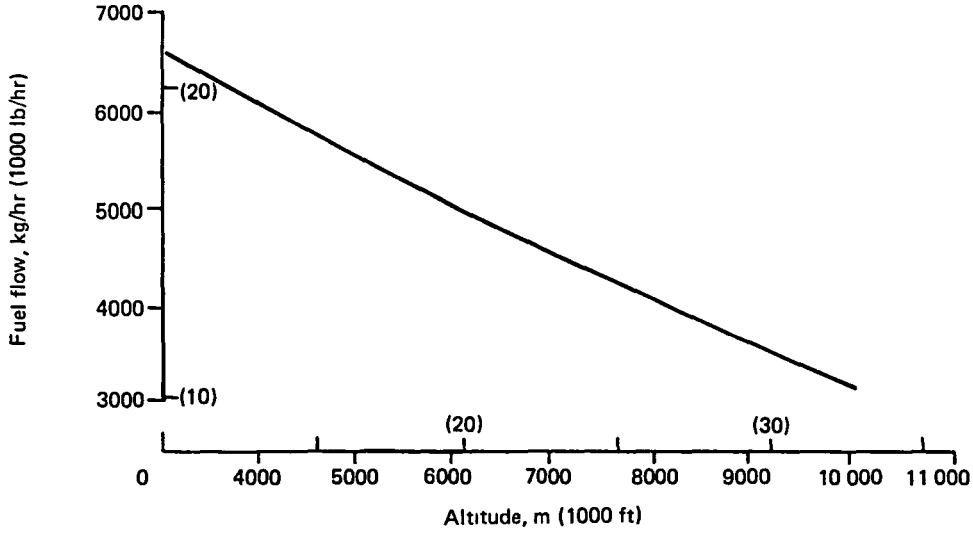

Figure 58. Integrated Energy Management Climb Fuel Flow

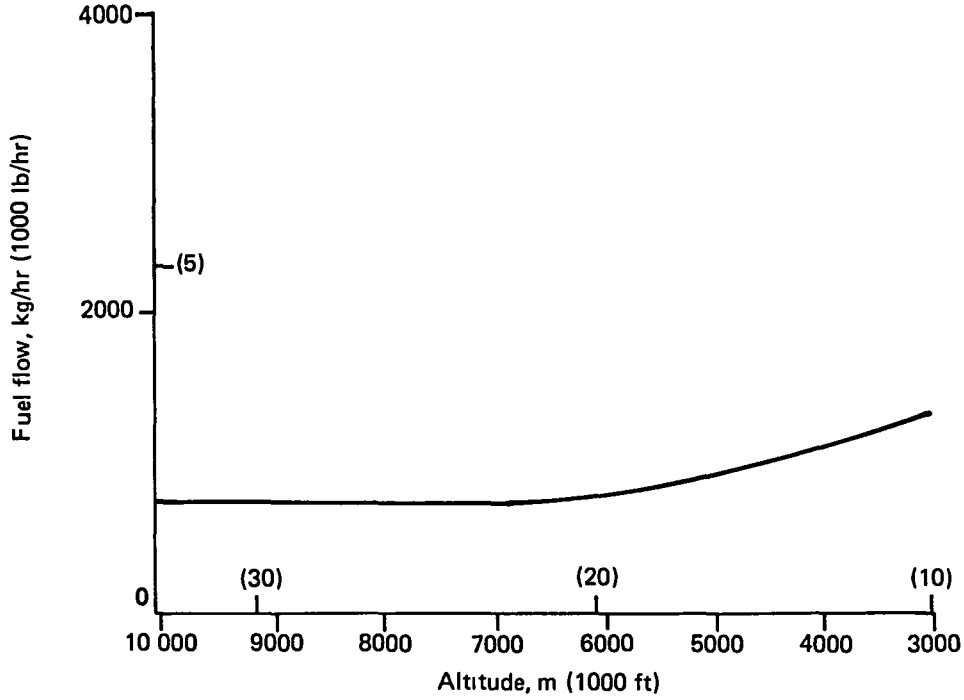

Figure 59. Integrated Energy Management Descent Fuel Flow

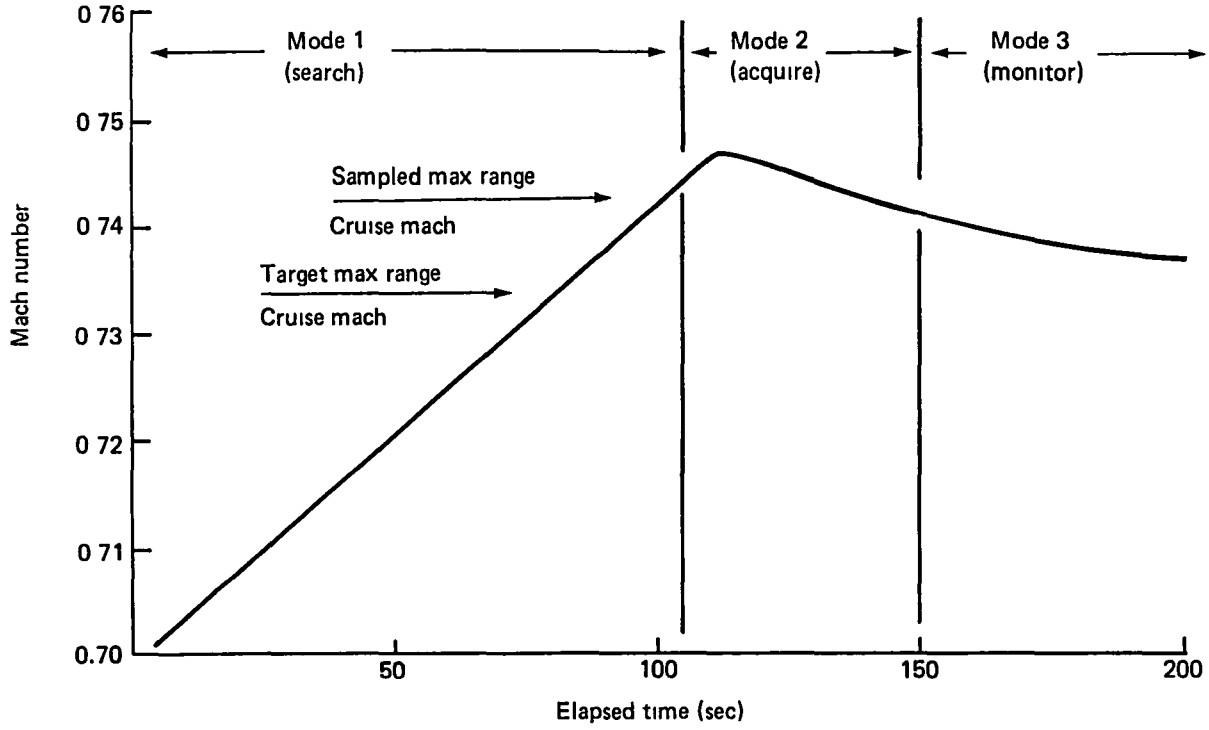

Figure 60. Cruise Simulation Mach Number

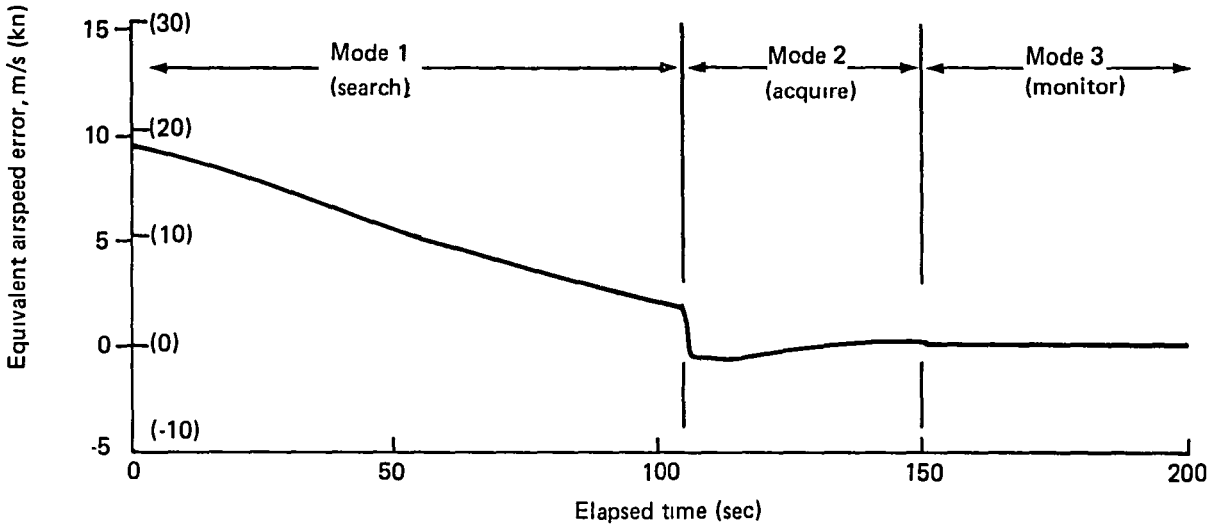

Figure 61. Cruise Simulation Autothrottle Airspeed Error Signal

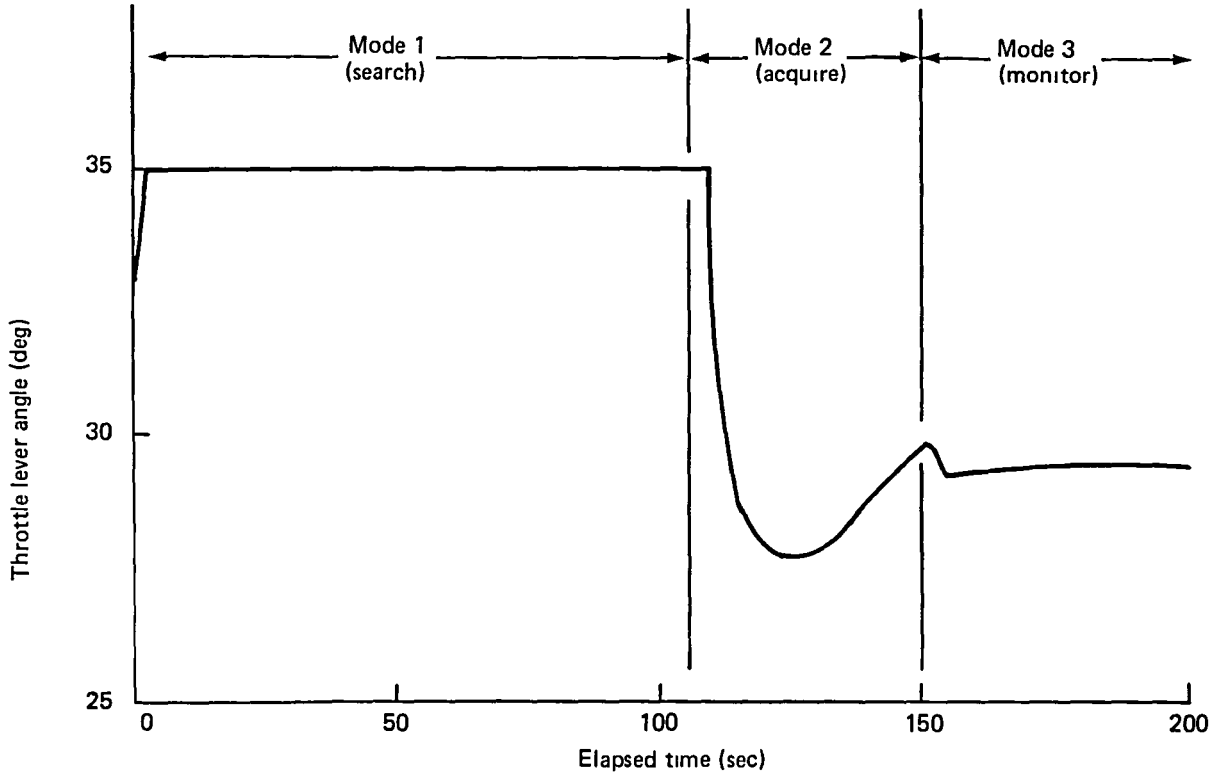

Figure 62. Cruise Simulation Throttle Lever Angle

Table 6. Medium-Range Flight Time, Distance, Fuel Comparison

Flight phase	Reference flight			IEM flight		
	Time, sec	Dist, km (nmi)	Fuel, kg (lb)	Time, sec	Dist, km (nmi)	Fuel, kg (lb)
Accelerate and climb	966	217 6 (177.5)	1633 (3601)	678	142.4 (76.9)	1252 (2760)
Cruise	2991	717.8 (387.6)	2873 (6333)	3720	815 8 (440.5)	3172 (6992)
Descend and decelerate	729	163 0 (88.0)	371 (817)	862	140 2 (75 7)	209 (461)
Total flight above 3048m (10 000 ft)	4686	1098 4 (593.1)	4877 (10 751)	5260	1098.4 (593.1)	4633 (10 213)

The IEM simulation results show a fuel savings of 244 kg (538 lb) compared to the reference flight (about 5%), at an increase of almost 10 min (about 12%) in flight time. These figures only apply to operations at or above base altitude. Fuel savings by flight segment are:

- Climb 89 kg (197 lb), 1.8% of trip fuel
- Cruise 82 kg (180 lb), 1.7% of trip fuel
- Descent 73 kg (161 lb), 1.5% of trip fuel

4.8 INTEGRATED ENERGY MANAGEMENT BENEFITS ASSESSMENT

This section summarizes the quantified fuel savings of the IEM algorithms as determined by simulation of the selected short- and reference medium-range flights. These results are then extrapolated to the 80 flights in the measured sample of 727-200 operations; nonquantified benefits also are indicated.

4.8.1 Short-Range Flight Benefits

The short-range flight selected and described in Section 4.2.4 was simulated for both the flight measured and IEM profiles. Due to computer cost and flow time, the short-range flight was simulated in a simplified point-mass, steady-state version of the 727-200 model. Only the summary results of this flight segment analysis are presented. The time, distance and fuel totals for the short-range flight category for both the selected short range and IEM flight simulations, are summarized in Table 7.

Table 7. Short-Range Flight Time, Distance, Fuel Comparison

Flight phase	Selected short-range flight			IEM flight		
	Time, sec	Dist, km (nmi)	Fuel, kg (lb)	Time, sec	Dist, km (nmi)	Fuel, kg (lb)
Accelerate and climb	646	140 2 (75 7)	1180 (2601)	683	139.3 (75 2)	1092 (2408)
Cruise	300	75 6 (40 8)	406 (896)	361	73 7 (39.8)	356 (784)
Descend and decelerate	387	82 8 (44.7)	166 (366)	547	85.6 (46.2)	124 (274)
Total flight above 3048m (10 000 ft)	1333	298.5 (161 2)	1752 (3863)	1591	298.5 (161.2)	1572 (3466)

As with the medium-range flight simulation, the simulations were adjusted to guarantee identical initial and final altitudes and velocities and total distance in all operations above base altitude. The net fuel saved for the short-range flight was 180 kg (397 lb), approximately 10% of the fuel consumed for the selected short-range flight simulation. The time increase was slightly over 4 minutes, or almost 20% over that of the selected short-range flight time above base altitude.

To determine the savings of fuel by flight phase, a portion of cruise fuel and distance was included in the climb and descent segments for the energy runs. Table 8 summarizes these fuel savings by each flight phase for the selected short-range and IEM flights. The savings were 83 kg (183 lb) in climb, 40 kg (89 lb) in cruise and 57 kg (125 lb) in descent, which were equivalent to 7%, 10.3% and 31.3%, respectively. The savings as a percentage of total fuel used above base altitude were 4.7% for climb, 2.3% for cruise and 3.2% for descent for a total trip fuel savings of 10 2%.

4.8.2 Medium-Range Flight Benefits

Comparable data developed for the medium-range flight results are shown in Table 9. As with the short-range flight, the basic time, distance and fuel values from Table 6 were adjusted to provide comparable range values for each flight phase. The resultant fuel savings for the medium-range (reference) flight were 89 kg (197 lb) in climb, 82 kg (180 lb) in cruise, and 73 kg (161 lb) in descent. As a percentage of fuel consumed in each flight phase, the savings were 5.5%, 2.9% and 19.7%, respectively. As a percentage of total flight fuel above base altitude the savings were 1.8% for climb, 1.7% for cruise and 1.5% for descent. This represents a total savings of 5.0% of trip fuel.

Table 8. Short-Range Flight Fuel Savings

Flight phase	Selected short-range flight			IEM flight			Fuel savings		
	Time, sec	Dist, km (nmi)	Fuel, kg (lb)	Time, sec	Dist, km (nmi)	Fuel, kg (lb)	kg (lb)	Flight seg fuel, %	Total fuel, %
Accelerate and climb	646	140.2 (75 7)	1180 (2601)	688	140.2 (75.7)	1097 (2418)	83 (183)	7	4.7
Cruise	289	72.8 (39 3)	391 (863)	356	72 8 (39.3)	351 (774)	40 (89)	10 3	2.3
Descend and decelerate	398	85.6 (46.2)	181 (399)	547	85 6 (46.2)	124 (274)	57 (125)	31.3	3.2
Total flight	1333	298.5 (161.2)	1752 (3863)	1591	298 5 (161.2)	1572 (3466)	180 (397)		10 2

Table 9. Medium-Range Flight Fuel Savings

Flight phase	Reference flight			IEM flight			Fuel savings		
	Time, sec	Dist, km (nmi)	Fuel, kg (lb)	Time, sec	Dist, km (nmi)	Fuel, kg (lb)	kg (lb)	Flight seg fuel, %	Total fuel, %
Accelerate and climb	966	217 6 (117.5)	1633 (3601)	1021	217 6 (117 5)	1544 (3404)	89 (197)	5.5	1 8
Cruise	2991	717.8 (387.6)	2873 (6333)	3274	717 8 (387 6)	2791 (6153)	82 (180)	2.9	1 7
Descend and decelerate	729	163.0 (88 0)	370 (817)	966	163 0 (88 0)	298 (656)	73 (161)	19.7	1.5
Total flight	4686	1098 4 (593 1)	4877 (10 751)	5261	1098 4 (593 1)	4633 (10 213)	244 (538)		5.0

4.8.3 Long-Range Flight Benefits

An extrapolation of the two evaluated flight fuel savings to long-range flights is illustrated in Figure 63. The long-range flight consisting of 2222 km (1200 nmi) above base altitude, produced fuel savings of about 4%.

A composite saving of 4.8% was derived for all 727-200 flights by combining fuel consumption weighting factors, percent of fuel savings and flight range frequencies for the short-, medium- and long-range flight categories. The fuel consumption weighting factor is a ratio of average total fuel consumed for a given flight category, divided by the medium-range flight average fuel consumption. Factors of 1.0 for the medium-range flight, 0.35 for the short-range flight, and 1.90 for the long-range flight were determined from the UA data. The composite savings factors are summarized in Table 10.

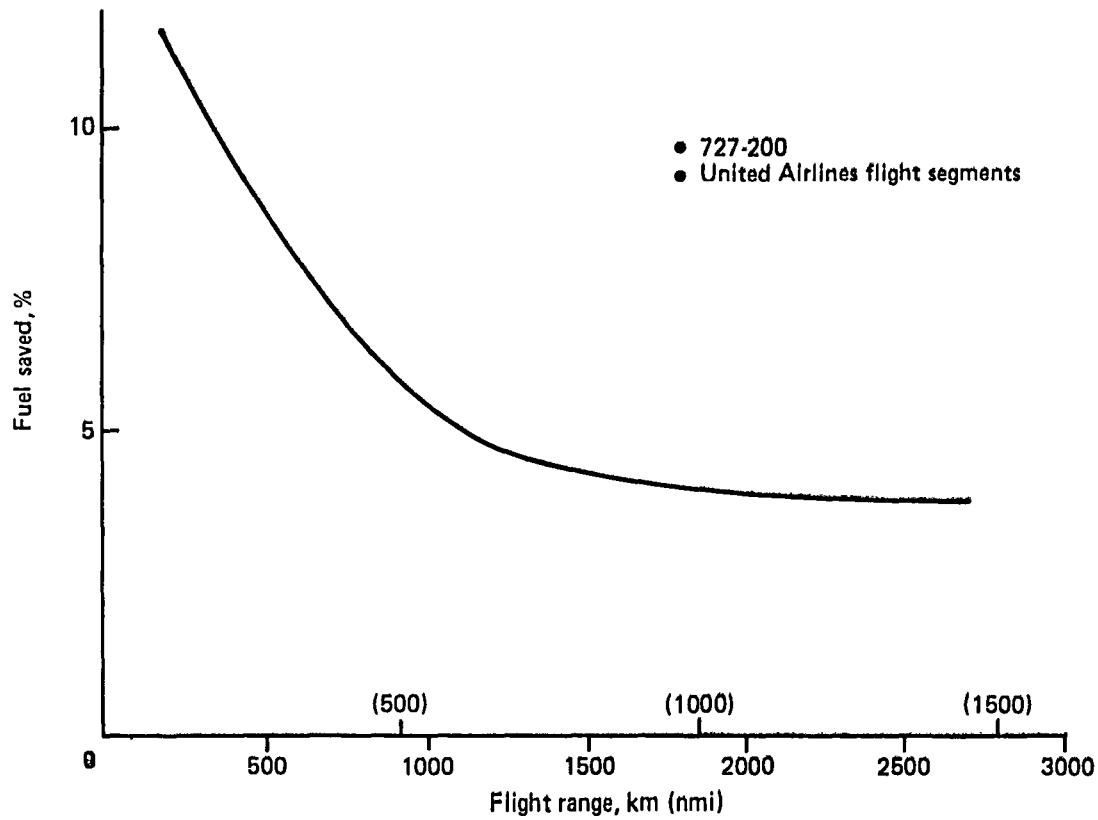

Figure 63. Fuel Savings as a Function of Flight Distance

Table 10. Fleet Fuel Savings Factors

Range	Relative fuel consumption weighting	Frequency	Saving per flight, %
Short	0 35	0.50	10 2
Medium	1 00	0.30	5 0
Long	1.90	0 20	4.1
Composite		1 00	4 8

4.8.4 Method Assessment

The benefits potentially available, using the IEM algorithms as developed in this study, are based only on improved airspeed and throttle guidance and improved controls. No credit has been taken for other benefits that would accrue from the on-board installation of additional capabilities such as altitude optimization and improved point-of-descent prediction

The optimization of initial cruise altitude and the determination of step climb strategies would provide further gains. For the short-range flight, for example, it was determined that an additional 18 kg (40 lb) of fuel (1% of trip fuel) could be saved by continuing the climb to 8230m (27 000 ft). The altitude optimization problem, while straight-forward from a theoretical point of view, is complex with regard to operational problems and ATC considerations. Climbing cruise trajectories at best altitude and speed are not realistic in the U.S. airspace environment.

Similarly, substantial fuel savings are derived from improved point-of-descent prediction. Figure 64 shows an estimate of fuel penalty in kilograms (pounds) as a function of point-of-descent error in kilometers (nautical miles), for one set of descent assumptions. In the IEM study, the lack of groundspeed and ground distance data precluded an assessment of how precisely the conventional procedures predicted point-of-descent, thus, the probable gains are not reflected in the benefit numbers.

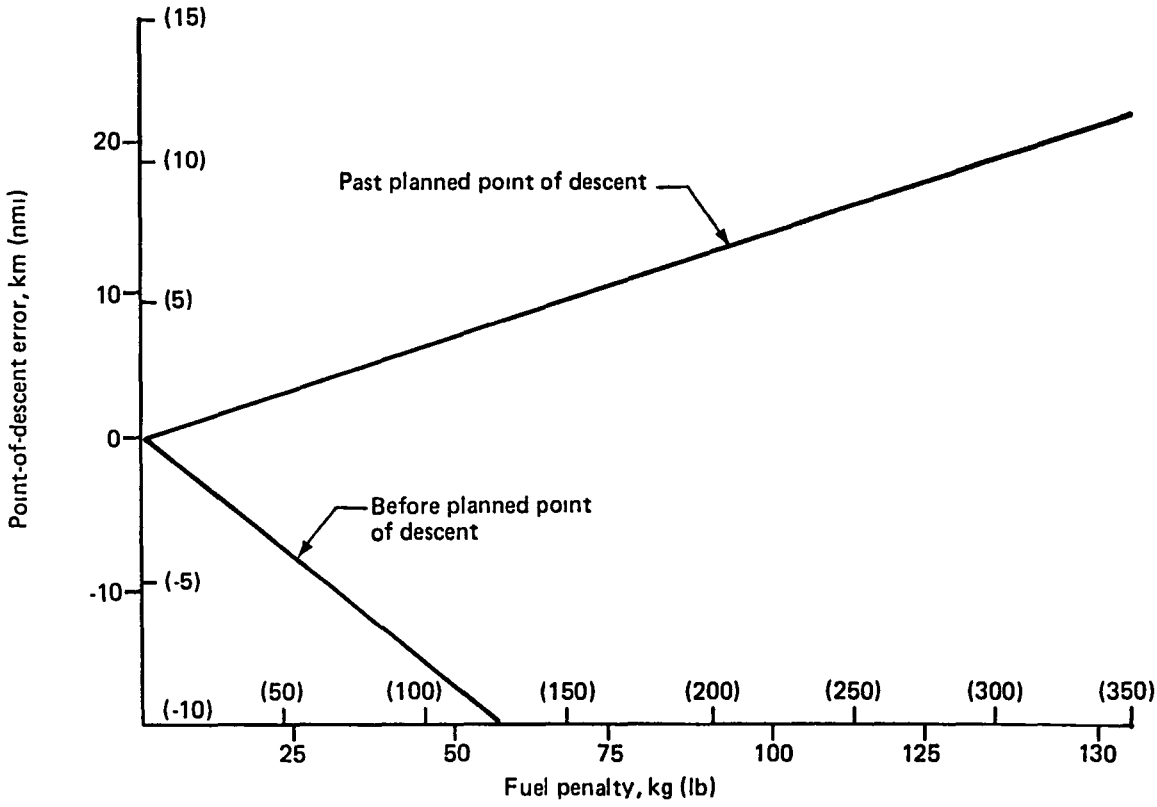

Figure 64. Fuel Penalty for Point of Descent Error

5.0 CONCLUSIONS

The Integrated Energy Management Study provided the following conclusions:

- The aircraft energy guidance and control techniques investigated in this study indicate a significant fuel savings available to a typical mid-range transport aircraft over conventional (handbook reference data and pilot control) profiles and procedures. The 5% fuel savings of the reference medium-range flight was achieved at an increase in trip time of 12%. Significant fuel gains were realized in each of three flight phases (climb, cruise and descent). A savings of 4.8% of fuel was projected for the sample of 80 727-200 flights flown by United Airlines in their route system.

- As a percentage of trip fuel, the savings for the shorter range flights are greater than the longer range flights with correspondingly greater percentage increases in trip time. Further savings from altitude optimization, improved point of descent prediction, etc. would accrue from an IEM system.

- The specific energy guidance algorithms developed show substantial savings over handbook schedules, but much smaller savings compared to best airspeed/Mach schedules. In addition, the IEM concept provides further advantages in terms of operational flexibility, such as the potential to assess off-nominal performance. Further gains are available with more sophisticated optimization techniques, but their computational complexity, data requirements, and relatively small increase in performance weigh against their mechanization employing current technology.

- In climb and descent, the selected energy guidance concept requires stored performance data. For climb and descent, the rate of change of optimal energy state with altitude does not allow sufficient time for on-board determination of the best speed schedule.

- The closed-loop energy guidance algorithm developed for cruise indicated fuel savings of close to 3% for the reference flight in the study simulation. The cruise algorithm searches for the optimum operating state, acquires the desired state and monitors operations to determine when a new search should be initiated. The algorithm employs an altitude-hold-mode autopilot and an airspeed-hold mode autothrottle.

- The IEM study determined that a closed-loop energy management system is feasible and practical for transport aircraft, and provides the basis for industry to proceed with development and implementation of the concept.

6.0 REFERENCES

1. Energy Approach to the General Aircraft Performance Problem, Edward S. Rutowski, Douglas Aircraft Co., Inc., *Journal of the Aeronautical Sciences*, March 1954.

2. Energy State Approximation and Minimum-Fuel Fixed Range Trajectories, Zagalsky, et al, Honeywell Systems and Research Center, *Journal of Aircraft*, Vol. 8, No. 6, June 1971.

3. Fixed-Range Optimum Trajectories for Short-Haul Aircraft, Erzberger, et al, Ames Research Center, NASA TN D-8115, December 1975.

4. Energy Management Techniques for Fuel Conservation in Military Transport Aircraft, The Analytic Sciences Corporation for the Air Force Flight Dynamics Laboratory, AFFDL-TR-75-156, February 1976.

APPENDIX A

STANDARD SIMULATION MODEL OF THE 727-200

This appendix describes seven of the basic models of the 727-200 Standard Simulation Model (SSM) used in the IEM evaluation. The models discussed are:

1) The atmosphere model
2) The aerodynamic model
3) The engine model
4) The rigid body equations of motion
5) The trim computation
6) The autopilot, and
7) The EAS-hold autothrottle

Atmosphere Model

This routine determined air data parameters for a given altitude. Air data values generated were based on the 1962 United States Standard Atmosphere. The capability to input nonstandard static temperatures was included.

Atmosphere parameters computed included:

1) Atmospheric density
2) Static temperature for standard day
3) Nonstandard static temperature
4) Speed of sound
5) Static pressure for standard day
6) Total temperature
7) Total pressure for standard day
8) Total temperature ratio
9) Total pressure ratio, and
10) Density ratio.

Aerodynamic Model

The aerodynamic model consists of equations for the aerodynamic coefficients and their arguments. The stability axis coefficient data are in tabular form; their arguments, or independent variables, are computed from the rate and position data from the rigid body equations of motion module. The independent variables for the total lift and pitching moment coefficients are:

1) Mach number
2) Altitude
3) Load factor
4) Pitch rate
5) Angle of attack
6) Angle of attack rate
7) Center of gravity
8) Stabilizer angle
9) Elevator angle
10) Thrust.

The drag coefficient is a function of the lift coefficient and the Mach number.

Additional parameters are calculated within the aerodynamic module for use in other program modules, such as:

1) Calibrated airspeed
2) Equivalent airspeed
3) Dynamic pressure
4) Impact pressure

Engine Model

The engine model related thrust lever position, engine pressure ratio, and engine RPM to resultant thrust and fuel flow. The model represented three engines, each having its own throttle system. The model data represented the Pratt & Whitney JT8D-9 pod installed engines without aircraft service bleed. The engine model computations included:

1) Cross-shaft angle position as a function of thrust lever angle
2) Engine surge bleed valve position
3) Commanded EPR for a given cross-shaft angle
4) Engine acceleration/deceleration dynamics
5) EPR limit checks
6) Resultant rotational speed of the engine low-speed compressors
7) Gross thrust, and
8) Fuel flow as a function of operating state.

The engine model was driven by thrust lever angle input, autopilot commanded thrust lever angle or commanded EPR schedule

Rigid Body Equations of Motion

This program module contained the basic rigid body equations for a vehicle having three degrees of freedom. External forces acting on the vehicle were resolved into the body axis system, and resultant inertial accelerations with respect to the body axes were generated from a conventional set of Newtonian-coupled translational and rotational velocity equations. Transformation and integration of the resulting angular velocity produced an Euler angle that determined aircraft attitude with respect to the local horizon Specific parameters computed in this routine included

1) Aerodynamic force component in the body axis system
2) Engine force component in the body axis system
3) Total moment about the y-body axis due to aerodynamic forces
4) Total moment about the y-body axis due to engine thrust
5) Gravitational components in the body axis system
6) Inertial linear accelerations and velocities in the body axis system
7) Accelerations at the center of gravity with normal load factor
8) Inertial angular accelerations and velocity terms
9) Local Euler angle and Euler rate terms

10) Body axis to earth axis transformation
11) Transformation of inertial velocity components from body to earth axis
12) Altitude
13) Flight path angle, and
14) Range

Trim Computation

This routine was used with the standard equations of motion to establish initial acceleration conditions within specified tolerances. The accelerations were derived in the body axis system for a given input flight condition.

Autopilot and Autothrottle Modules

This section describes the Flight Controls/Autothrottle logic and modes employed in the 727 modeling. The pitch axis control mode of the 727 as modeled in the SSM was extended as shown in Table A-1 to provide IAS Hold, Mach Hold, Vertical Speed Hold, and Altitude Select Capture, in addition to the Pitch Hold and Altitude Hold modes. The pitch axis control logic incorporated the elevator and stabilizer control modeling. In addition to the Flight Control modes, one Autothrottle mode was incorporated, as equivalent-airspeed hold mode for IEM cruise. The description of the uses of these various control modes in flying conventional profiles and the Integrated Energy Management profiles is contained in sections 4.4 and 4.7, respectively.

The Mod Block V pitch autopilot employed in the energy management modeling provided for automatic changes in control law as a function of pitch selector switch position, vertical speed wheel position, "ALT SEL" switch position and flight condition. Table A-1 summarizes the control law options that were available.

The flight controls modeling included a determination of the elevator position and the threshold detector logic for the stabilizer.

The autothrottle logic incorporated in the model was based on an equivalent airspeed acquire and hold mode autothrottle. Inputs to the autothrottle included an equivalent-airspeed error signal (target minus current EAS) and longitudinal acceleration. Forward and aft limits of autothrottle travel were selected consistent with cruise mode operation. The autothrottle output was throttle rate, which, when integrated, provided throttle position.

Table A-1. IEM Autopilot Modes

ALT SEL switch position (flight conditions)	Pitch selector switch position				
	MACH HOLD	IAS HOLD	PITCH HOLD	VERT SPEED	
				v/s wheel in detent	v/s wheel not in detent
1. ALT SEL not selected	MACH HOLD	IAS HOLD	PITCH HOLD	ALT HOLD	VERT SPEED
2. ALT SEL selected ($\lvert\Delta h\rvert < 1000$ ft) ($9.8\dot{h} + \Delta h < 0$)	ALT SEL CAPTURE	ALT SEL CAPTURE	ALT SEL CAPTURE		ALT SEL CAPTURE
3. ALT SEL selected (v/s wheel in detent) ($\lvert\Delta h\rvert \leq 30$ ft) ($9.8\dot{h} + \Delta h < 0$)	ALT HOLD				
4. ALT SEL selected, condition 2 not satisfied	MACH HOLD	IAS HOLD	PITCH HOLD		VERT SPEED

APPENDIX B

ENERGY GUIDANCE ALTERNATIVES

Four alternative approaches to energy guidance trajectory formulations were considered. The approaches included (1) handbook schedules, (2) optimized CAS/Mach schedules, (3) optimized specific energy trajectories, and (4) calculus of variation optimization techniques. From these alternatives, the optimized specific energy approach was selected as the basis for the development of the IEM algorithms. The advantages and limitations of the selected approach are reviewed in Section 4.5.

Handbook Schedules

The 727 Operations Manual presents two climb and three descent speed schedules that can be used in normal operations. All schedules consist of flying constant calibrated airspeed or constant Mach segments. En route climbs are done with all flaps retracted, gear up and maximum climb thrust. Best rate of climb speed varies with air temperature, altitude, and gross weight. Speed decreases with increasing air temperature or altitude and increases with increasing gross weight. For simplicity, only a single best rate of climb speed is given.

The low-speed climb schedule calls for 144m/sec (280 knots) up to approximately 9266 meters (30 400 ft) and Mach 0.75 above. This speed of 144 m/sec (280 knots) is the average best rate of climb speed with flaps up and is also the recommended turbulent air penetration speed.

High speed climb is at 175 m/sec (340 knots) to approximately 7102 meters (23 300 ft) and Mach 0.78 above. This speed schedule is usually assumed for minimum cost for short range flights at low to medium altitudes. It is used to minimize flight time.

Low speed descent is at Mach 0.80 to approximately 10363 meters (34 000 ft) and then 144 m/sec (280 knots) to 3048 meters (10 000 ft) The low speed descent increases range and is recommended for operation in turbulent air.

Two high speed descent schedules are given. The first is Mach 0.85 to 6401 meters (21 000 ft) and then 201 m/sec (390 knots) to 3048 meters (10 000 ft). The second is Mach 0.85 to 7925 meters (26 000 ft) and then 180 m/sec (350 knots) to 3048 meters (10 000 ft). The high speed descents minimize time.

Optimized CAS/Mach Schedules

The optimization of conventional CAS/Mach profiles provides one method of generating fuel efficient schedules. This technique has been applied in numerous "performance computers" to provide energy guidance. The method assumes as the solution form a constant CAS transitioning to constant Mach climb, cruise (usually at Long Range Cruise Mach for best fuel efficiency), and constant Mach to constant CAS descent. The "best" airspeeds depend on conditions such as weight, selected altitude, temperature, wind, etc. An example of this technique applied to climb is shown in Figure B-1. The figure shows for the specified input conditions, the variation in fuel and time required to climb to cruise altitude and cruise to a common distance of 370 km (200 nmi). The optimized CAS/Mach schedules provide a substantial increase in fuel efficiency over handbook schedules.

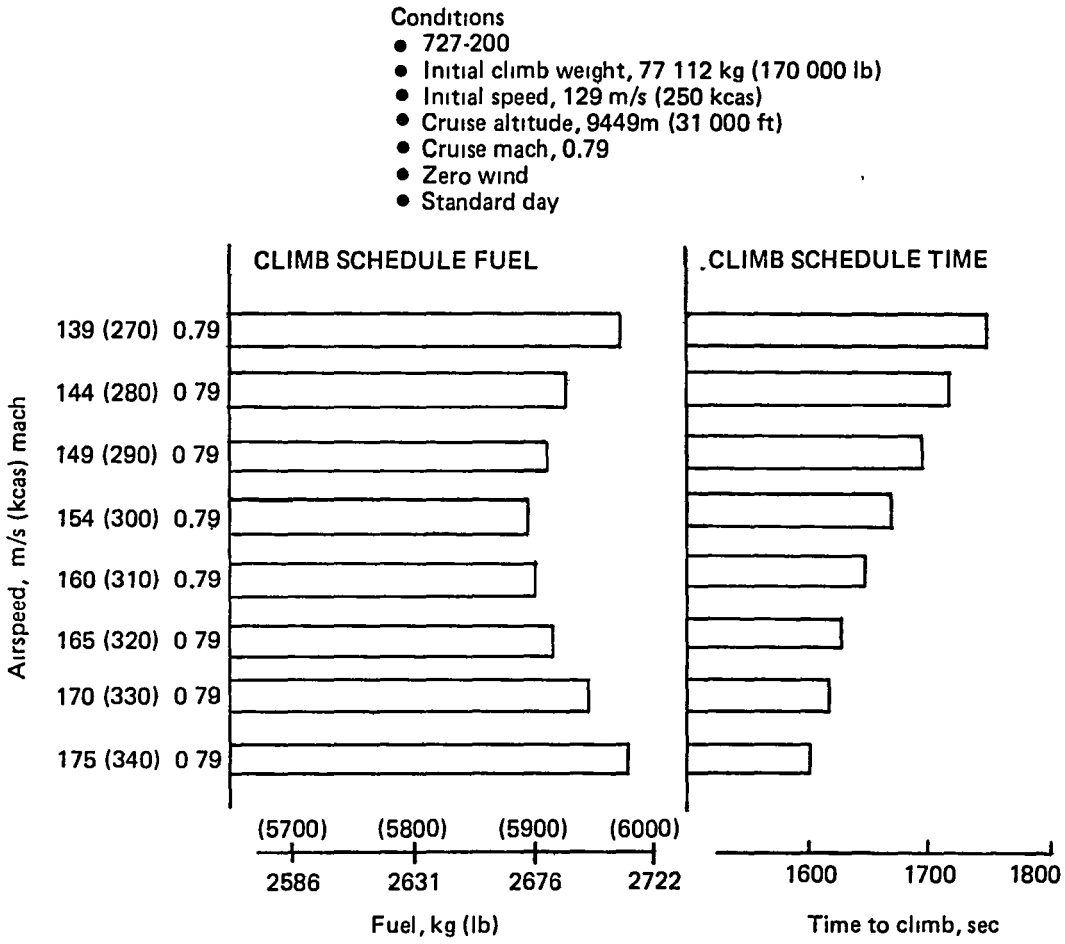

Figure B-1. Time and Fuel for CAS/Mach Schedules

Optimized Specific Energy Schedules

The introduction of the concept of specific energy as a parameter to generate efficient trajectories was formulated in the early 1950s by Rutowski (ref. 1). Specific energy is defined as the sum of the potential and kinetic energies of the aircraft divided by the aircraft weight. The concept was applied to the fixed-range optimization problem in the 1970s (ref 2 and 3)

Various "payoff" functions can be formulated using the specific energy concept and maximized to provide minimum time or fuel trajectories between altitudes, energy states, or to a common distance. For air transport applications, the maximization to a fixed range is the primary objective.

Changes in energy state are related to the primary forces acting on the aircraft: thrust, drag and weight. The flight is divided into three phases. climb, cruise and descent. For each phase

the function to be minimized is the fuel to climb, cruise or descend to a specific range. The velocity and throttle schedules to achieve the objective are formulated as·

Flight Phase	Velocity Schedule	Throttle Schedule
Climb	$\max\left\{\frac{(T - D)/W}{(\sigma \cdot T/V)_{CL} - (\sigma \cdot T/V)_{CR}}\right\}$	$\pi = \pi max$
Cruise	$\min\left\{\sigma \cdot D/V\right\}$	$T = D$
Descent	$\min\left\{\frac{(D - T)/W}{(\sigma \cdot T/V)_{CR} - (\sigma \cdot T/V)_{DS}}\right\}$	$\pi = \pi min$

where
T = thrust
D = drag
W = weight
V = velocity
π = throttle
σ = specific fuel consumption
$(-)_{CL}$ = applies to climb
$(-)_{CR}$ = applies to cruise
$(-)_{DS}$ = applies to descent

The climb function maximizes the excess power, when divided by a term comparing climb fuel mileage to cruise fuel mileage. This function provides maximum rate of change of energy per pound of fuel, subject to the cruise mileage boundary condition As the aircraft climbs to cruise altitude, the term in the denominator assumes greater weight.

The cruise function selects a velocity that maximizes the specific range. The descent function minimizes rate of change of energy per pound of fuel burned subject to the cruise mileage condition. This formulation reduces, for zero thrust and lift equal to drag, to maximizing the ratio of lift to drag on descent.

Figure B-2 shows an example of a specific energy climb schedule for a particular weight and target cruise condition. The contours are lines of constant rate of change of specific energy per pound of fuel. The maximization of these contours at a given altitude determines the optimum velocity schedule.

Figure B-3 shows for one particular weight, the cruise contours of lines of constant specific range ($V/T\sigma$). For any altitude, the maximization of these contours defines the minimum fuel operating Mach number

Figure B-4 shows the optimum specific energy descent schedule for one set of weight and cruise conditions. Again, contours of constant rate of change of specific energy per pound of fuel are shown, and the extreme values of these contours at a given altitude determine the minimum fuel energy schedule.

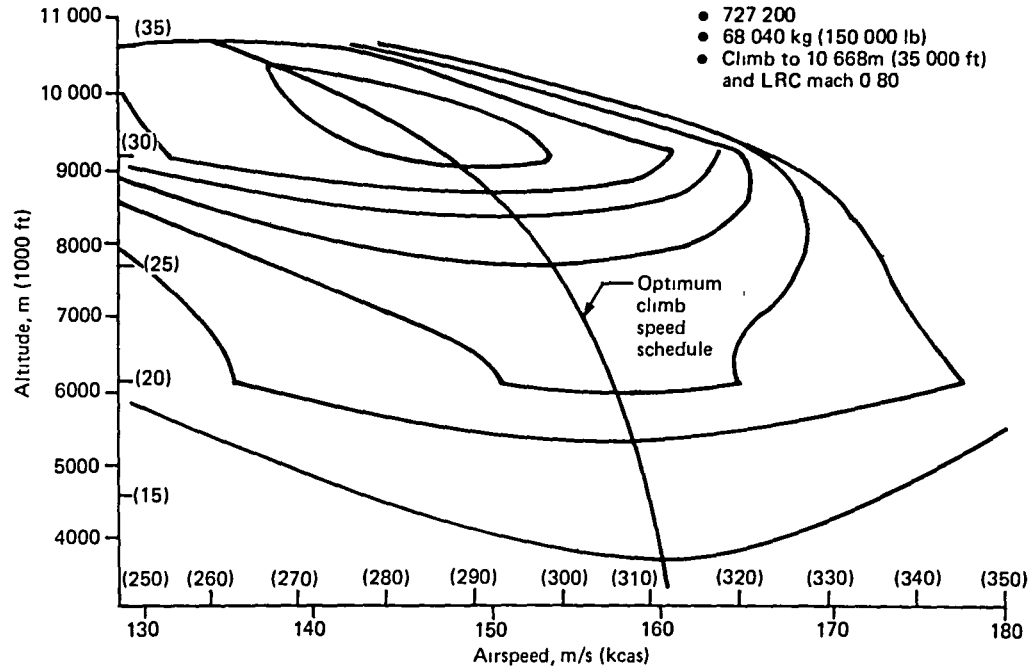

Figure B-2. Climb Energy Speed Schedule

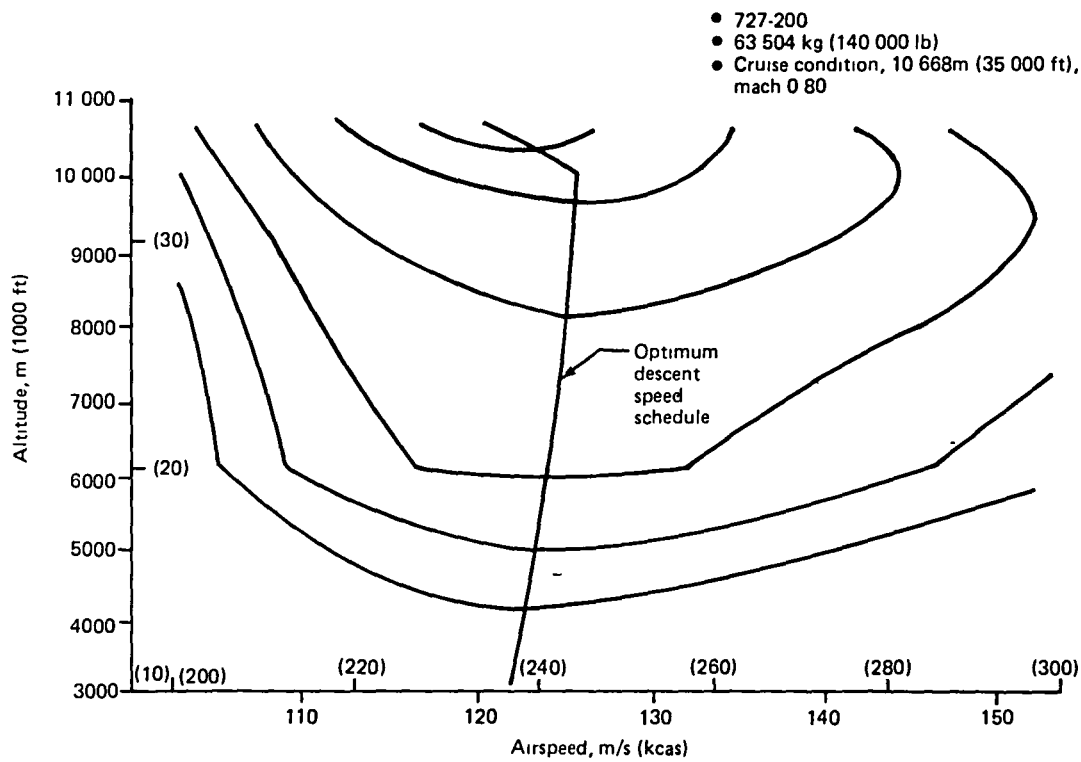

Figure B-3. Cruise Energy Speeds

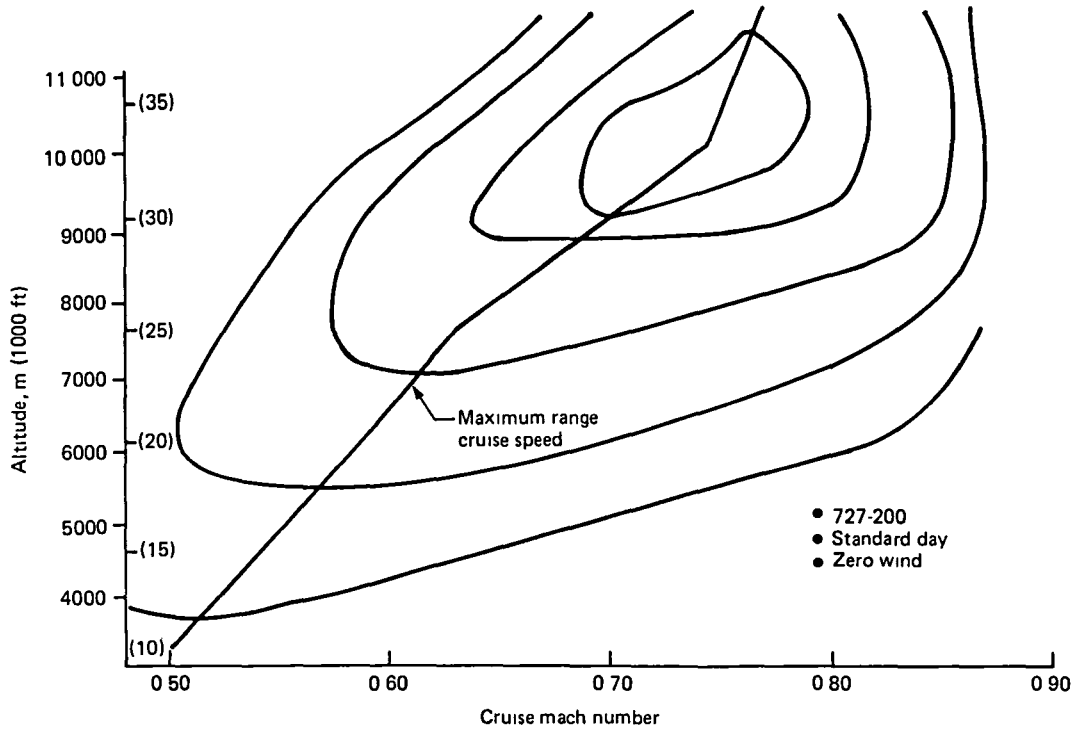

Figure B-4. Descent Energy Speed Schedule

The relatively low descent speed schedule (around 124 m/s (240 kn) calibrated) is slightly higher than the maximum L/D schedule. The insensitivity of fuel burn around the minimum value allows for increased operating speed to 129 m/s (250 kn) calibrated) with a fuel penalty on the order of 4.5 kg (10 lb) If a boundary velocity of 129 m/s (250 kcas) at 3048m (10 000 ft) is imposed, most of this fuel penalty will disappear.

Calculus of Variations Optimized Schedules

The specific energy formulation of rate-of-change of energy neglects the angle of attack term. However, more complex optimization techniques are available, which use angle of attack as a control to generate an optimized schedule. For the purpose of comparison with specific energy and best CAS/Mach schedules, one such technique, the Chebychev Trajectory Optimization Program (CTOP), was applied to a 727-200 to obtain a schedule to minimize fuel in climb to a specific range.

CTOP is a computer program designed to optimize atmospheric vehicle trajectories. It uses a parameter optimization scheme that represents the trajectory by patched Chebychev polynomials. The boundary conditions are satisfied exactly at each iteration and the equations of motion are treated as constraints that are satisfied by means of penalty functions Optimization is by means of a Gauss-Newton method modified in a manner similar to that of Levenberg-

Marquardt. The square root method is used to decompose the second derivative matrix. An adaptive procedure is used to control the iterations.

The equations of motion are written for a point mass vehicle in 3-D flight above a flat earth.

The aircraft is limited to coordinated maneuvers (zero sideslip angle). Control is achieved by modulating the attitude of the vehicle's longitudinal axis. The thrust force is assumed to act along the aircraft's longitudinal axis. The airplane is propelled by an air breathing engine. Maximum engine pressure ratio (EPR) thrust is used in climb.

Values of thrust and specific fuel consumption are input from the flight envelope. Maximum EPR is assumed for climb. At a given Mach number, values of T/δ and σ/θ (where δ is the atmospheric pressure ratio and θ is the atmospheric temperature ratio) are fitted to a cubic polynomial as functions of altitude. The coefficients of the cubic polynomial are then input by tables as functions of Mach number.

The airplane is constrained not to exceed given values for normal load factor, lift coefficient and dynamic pressure.

For minimum fuel problems, CTOP minimizes the sum of the climb fuel plus cruise fuel. The cruise fuel consumption is obtained from:

$$\Delta W = W_T \left[1 - e^{-(R - R_T)/Rf}\right]$$

where W_T = aircraft weight at the end of climb
R_T = range at end of climb
R = total flight range
Rf = range factor
and ΔW = fuel consumed in cruise.

Figure B-5 shows the resultant climb schedule for the minimum fuel trajectory generated by the CTOP program for one set of climb conditions. The CTOP program was not applied to the descent optimization problem in this study.

Evaluation of Alternative Energy Guidance Methods

The approach taken to evaluate alternative climb, cruise and descent strategies is indicated in Figure B-6 which shows the procedure applied to the climb evaluation. Common boundary conditions (weight, altitudes, speeds) and environmental conditions (wind and temperature profiles) are specified. The profiles generated by the alternative procedures discussed in this appendix for these conditions were "flown" through a point-mass, steady-state model of the 727-200. The climb model accelerates, climbs, accelerates and cruises the aircraft to the common distance constraint. Model outputs were time and fuel used. The results of this model were run for various weight and altitude conditions to generate parametric data comparing the alternative techniques.

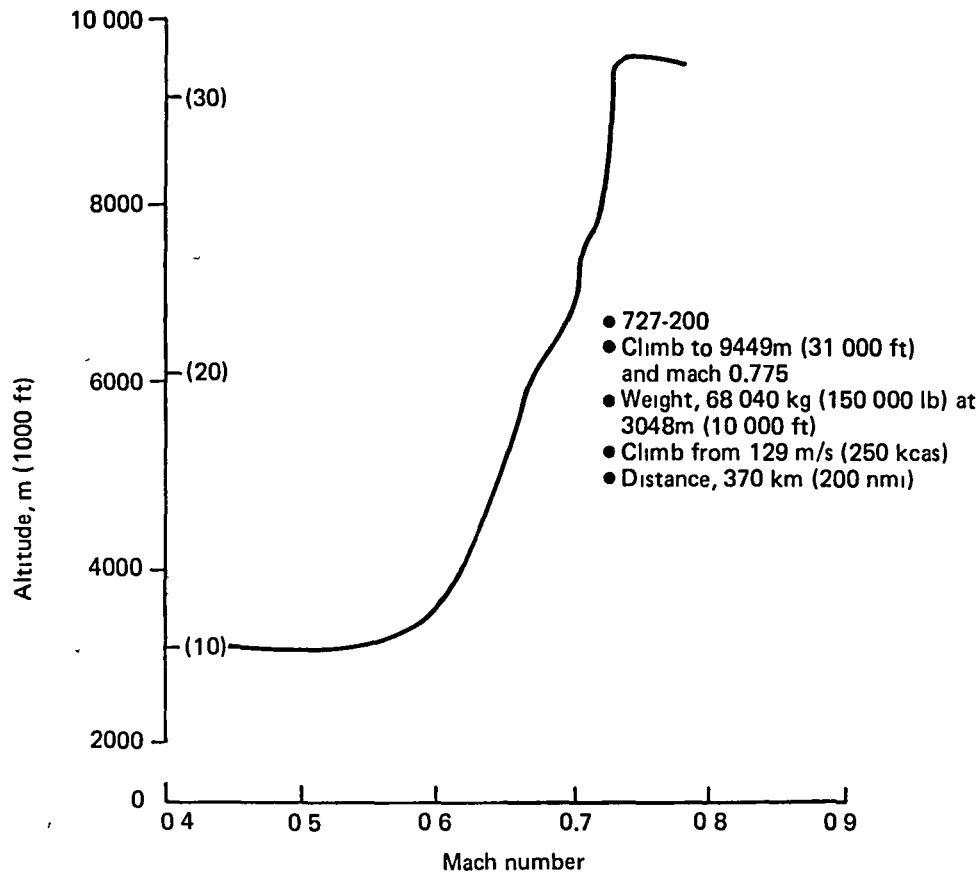

Figure B-5. CTOP Minimum Fuel Climb Schedule

Results of the climb analysis for one set of climb conditions are summarized in Table B-1. The results shown in the table are typical of the results generated over a range of climb weights from 58968 kg (130 000 pounds) through 77112 kg (170 000 pounds) and cruise altitudes from 8230 to 10668 meters (27 000 to 35 000 ft). The best energy, CTOP and best CAS/Mach schedules consistently obtained total climb fuel burns within 0.2%. The handbook climbs required substantially more fuel (0.5 to 2.5%). Descent results showed similar trends. Results for one set of descent conditions are shown in Table B-2. For the descent, a maximum L/D descent profile is included. Optimum CTOP trajectories were not developed for descent. Again, the specific energy, best CAS/Mach and maximum L/D descent fuel burns agree closely. The fuel penalty (both absolute and percentage of segment fuel) was somewhat greater for flying the handbook schedule. The conclusions of this parametric exercise are:

(1) All minimum fuel techniques considered obtained approximately the same fuel burns, although the specific trajectories and time costs differed somewhat.

(2) All minimum fuel techniques showed substantial improvement in fuel burn over handbook schedules.

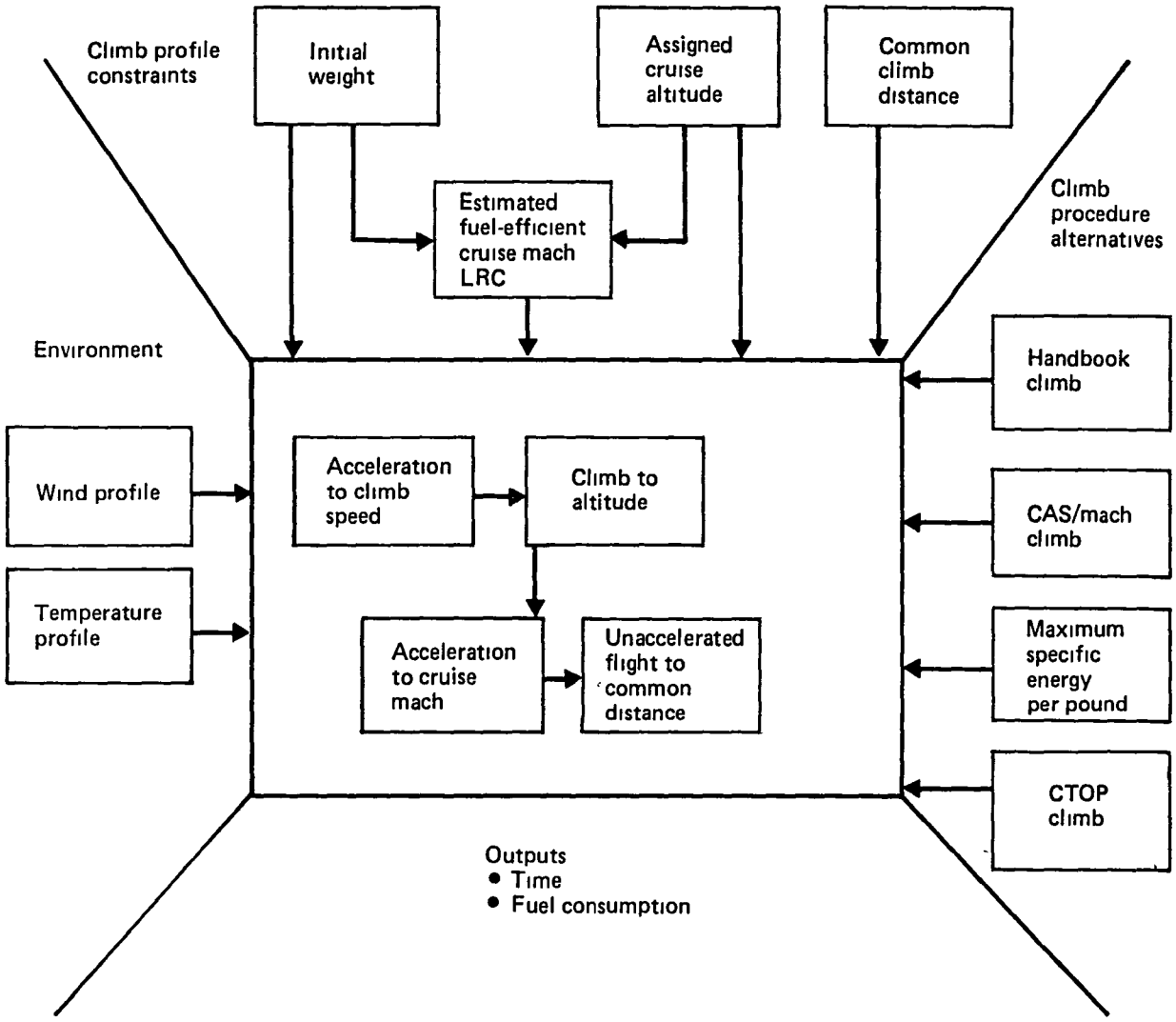

Figure B-6. Fuel-Efficient Procedure Evaluation (Climb)

Table B-1. Energy Guidance Potential Benefits—Handbook Performance Climbs

Strategy	Fuel, kg (lb)	Δ Fuel, %	Time, sec	Δ Time, %
Best energy	2375 (5236)	Reference	1677	4.3
CTOP	2376 (5239)	0.1	1667	3.7
Best CAS/mach	2379 (5244)	0.2	1685	4.8
Low-speed handbook	2391 (5272)	0.7	1696	5 5
High-speed handbook	2429 (5354)	2 2	1608	Reference

- Altitude, 9449m (31 000 ft)
- Weight, 68 040 kg (150 000 lb)
- All climbs to a common distance
- All climbs based on handbook performance
- Max climb EPR schedule assumed

Table B-2. Energy Guidance Potential Benefits—Handbook Performance Descents

Strategy	Fuel, kg (lb)	Δ Fuel, %	Time, sec	Δ Time, %
Best energy	747 (1646)	Reference	1398	16 1
Max L/D	748 (1648)	0.1	1432	18 9
Best CAS/mach	747 (1647)	0.1	1401	16 4
Low-speed handbook	782 (1723)	4.7	1293	7 4
High-speed handbook	850 (1874)	13.9	1204	Reference

- Altitude, 10 668m (35 000 ft)
- Weight, 63 504 kg (140 000 lb)
- All descents to common distance
- All descents based on handbook performance
- Idle descent thrust assumed

APPENDIX C

INTEGRATED ENERGY MANAGEMENT CRUISE ALGORITHM LOGIC

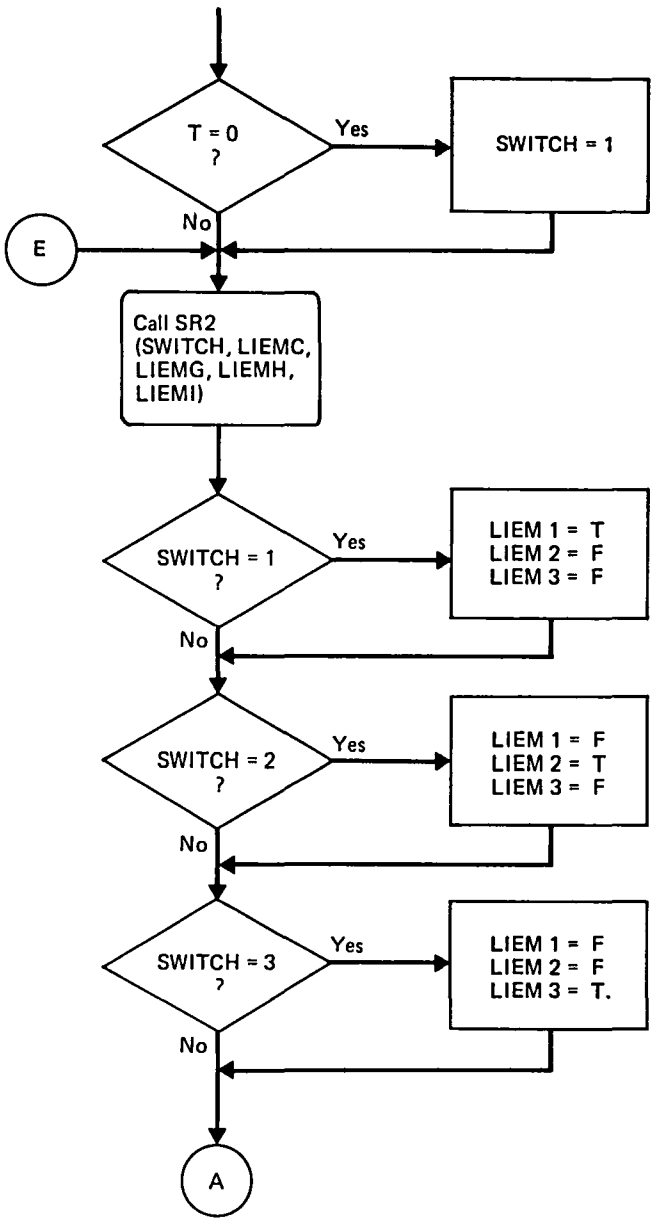

Figure C-1. Mode Control Logic

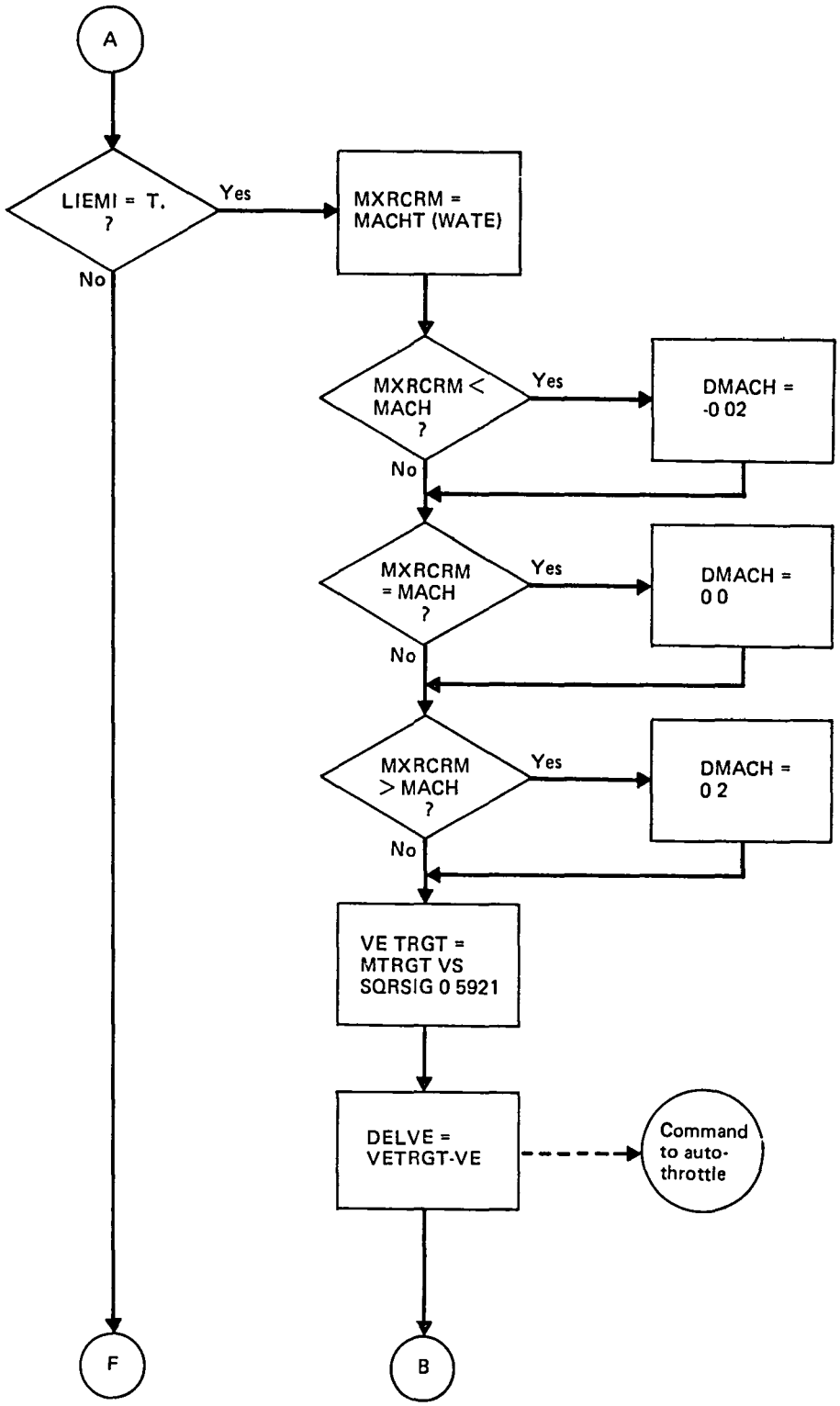

Figure C-2. Search Mode–Autothrottle Command Generation

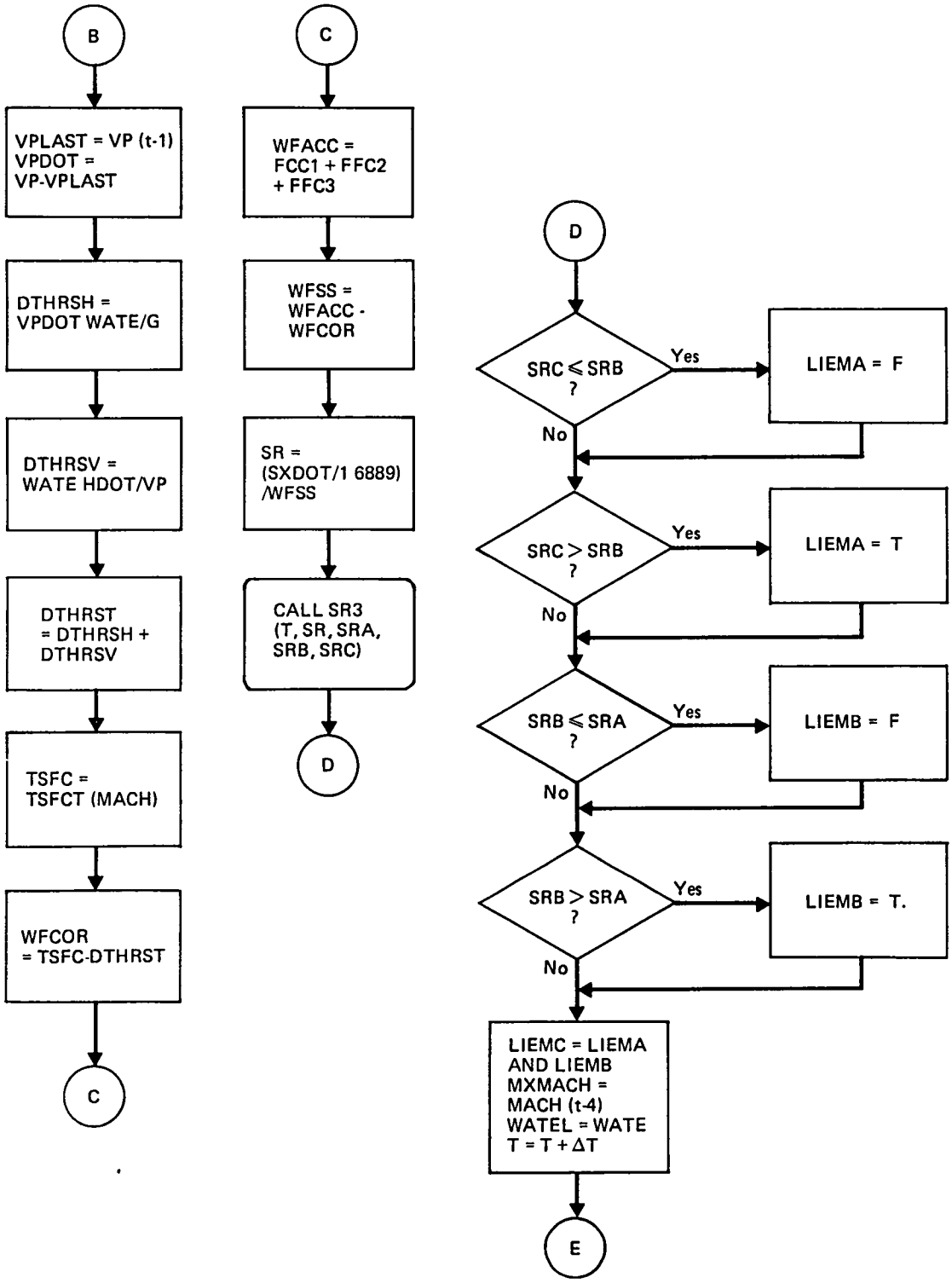

Figure C-3. Search Mode—Specific Range Calculation Adjusted for Acceleration and Switching Logic

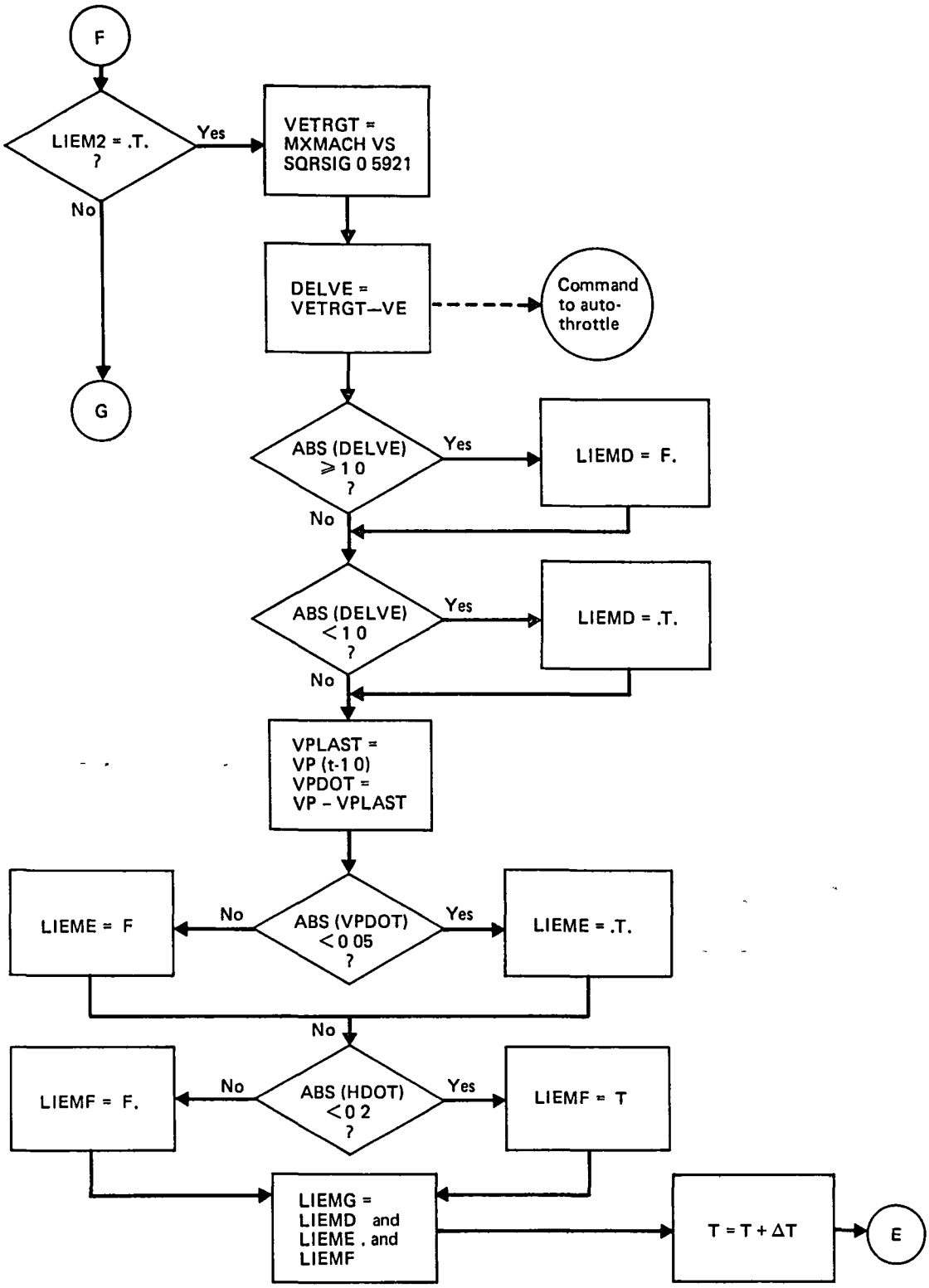

Figure C-4. Acquire Mode–Autothrottle Command Generation and Steady-State Cruise Check

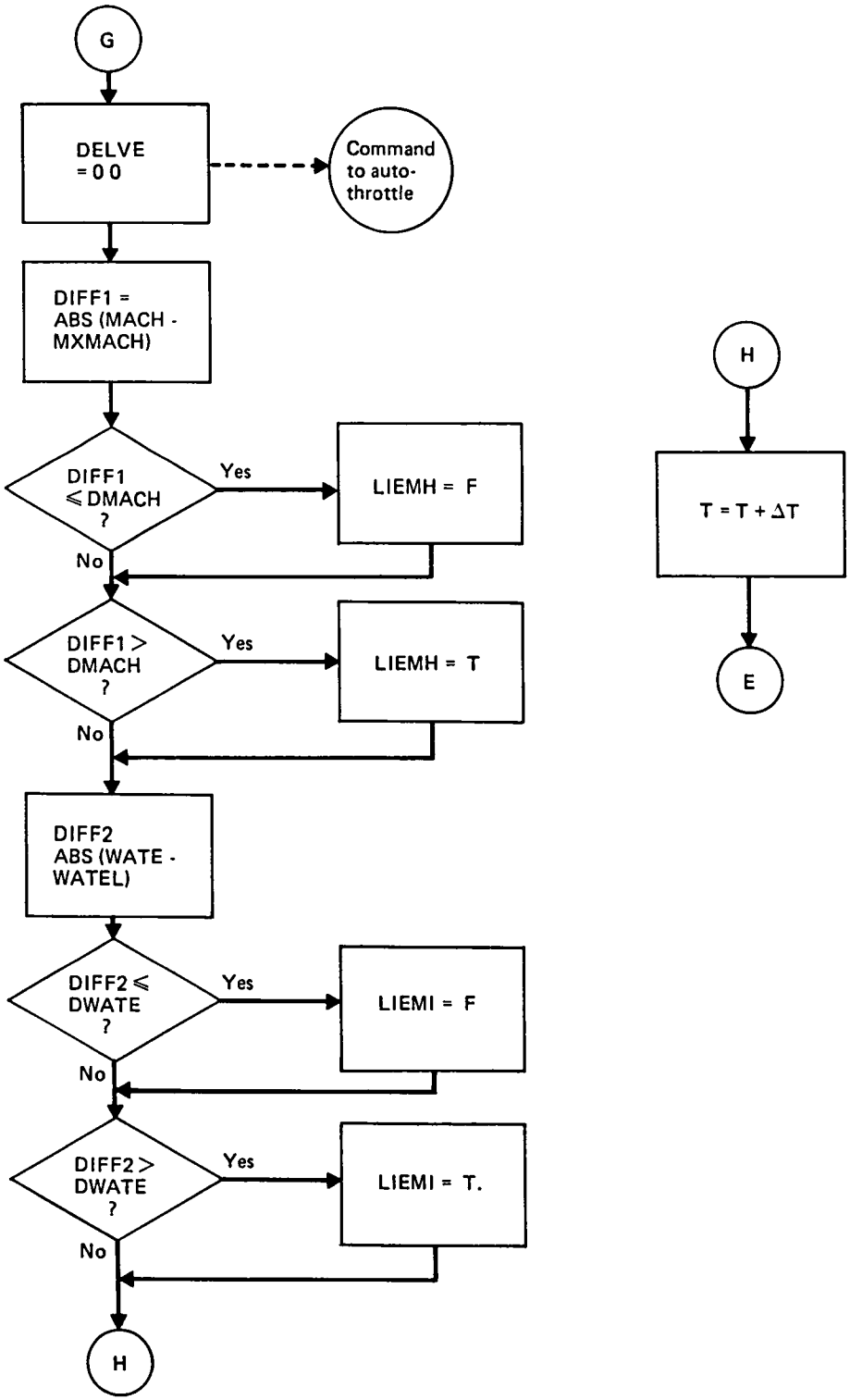

Figure C-5. Throttle Lock and Monitor Mode

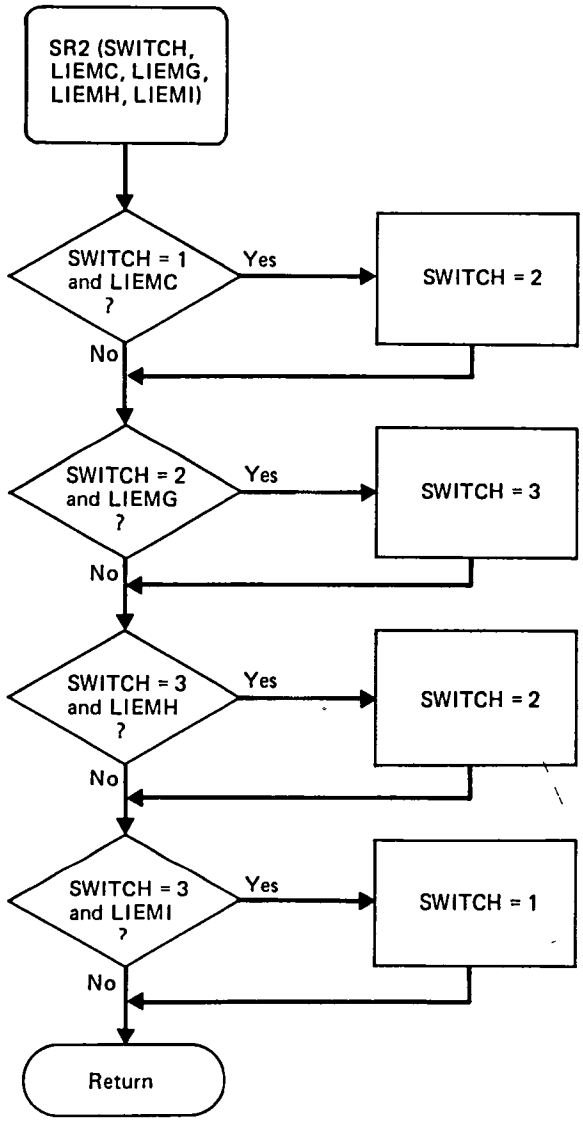

Figure C-6. Mode Switching Logic

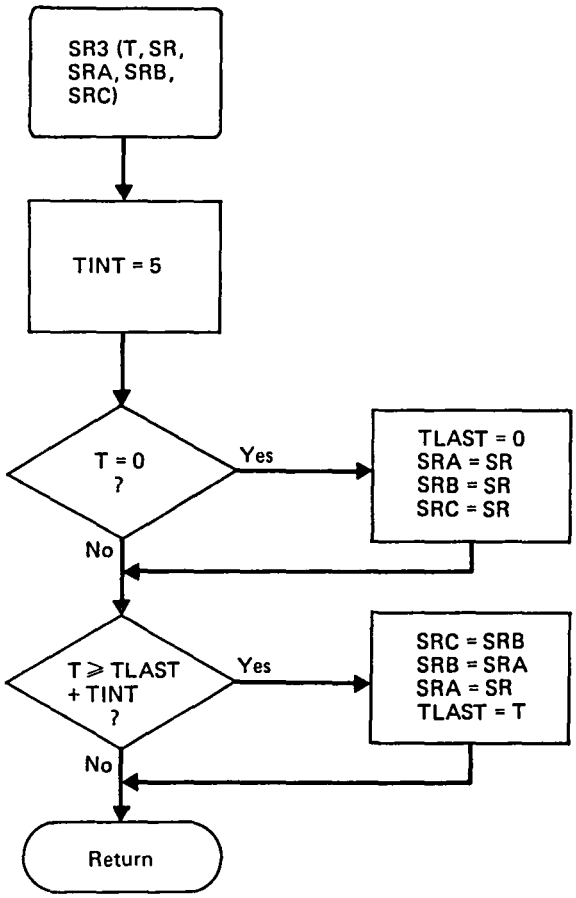

Figure C-7. Specific Range Sampling Logic

Table C-1. Logic Variable Description

SWITCH	Indicates IEM cruise mode· = 1 if search mode operative = 2 if acquire mode operative = 3 if lock/monitor mode operative
LIEM 1	Logical variable true when in search mode
LIEM 2	Logical variable true when in acquire mode
LIEM 3	Logical variable true during lock/monitor mode
DWATE	Weight change threshold to reinitialize search
DMACH	Mach change allowed in monitor mode
MXRCRM	Estimated maximum range cruise mach
DELMACH	A Δ-mach interval added to MXRCRM as a speed target
MTRGT	A target mach number for autothrottle in search mode
VETRGT	Equivalent airspeed value (in knots) of MTRGT
DELVE	Equivalent airspeed error signal to autothrottle
VPLAST	Value of flight path velocity at T - 1 sec
VPDOT	Flight path acceleration (ft/sec^2)
DTHRSH	Along path force components
DTHRSV	Vertical force component
DTHRST	Total accelerating forces
TSFC	Estimated specific fuel consumption
WFLOR	Estimated fuel flow to provide acceleration
FFC1, 2, 3	Measured fuel flows for engines 1, 2, 3
WFACC	Total fuel flow
WFSS	Estimated fuel flow at altitude, mach number for steady state (unaccelerated) flight
SR	Estimated steady-state specific range (nmi/lb)
SRA	Estimated SR at T - ΔT
SRB	Estimated SR at T - 2ΔT
SRC	Estimated SR at T - 3ΔT
LIEMA	Logical variable true when SRC >SRB
LIEMB	Logical variable true when SRB >SRA
LIEMC	Logical variable true when LIEMA and LIEMB are both true
MXMACH	Mach number at maximum estimated SR
WATEL	Weight at maximum estimated SR
LIEMD	Logical variable true when I DELVG I 1 0
LIEME	Logical variable true when I VPDOT I 1 0
LIEMF	Logical variable true when I HDOT I 1 0
LIEMG	Logical variable true when LIEMD, LIEME, LIEMF all true
DIFF1	Difference between target and actual mach number
DIFF2	Difference between current and beginning weight
LIEMH	Logical variable true when DIFF1 exceeds DMACH
LIEMI	Logical variable true when DIFF2 exceeds DWATE
MACHT	Table containing estimated maximum range cruise Mach values
TSFCT	Table containing estimated TSFC values

1 Report No	2 Government Accession No	3 Recipient's Catalog No
CR-158980		

4 Title and Subtitle	5 Report Date
Integrated Energy Management Study	March 1979
	6 Performing Organization Code

7 Author(s)	8 Performing Organization Report No
BCAC System Technology Staff and the Preliminary Design Department	D6-46700
	10 Work Unit No

9 Performing Organization Name and Address	11 Contract or Grant No
Boeing Commercial Airplane Company (BCAC) P.O. Box 3707 Seattle, Washington 98124	NAS1-14742
	13 Type of Report and Period Covered Contractor Final Report 8-10-77—7-1-78

12 Sponsoring Agency Name and Address	14 Sponsoring Agency Code
National Aeronautics and Space Administration Washington, D.C. 10546	

15 Supplementary Notes

This report covers work conducted under one of five tasks included in Contract NAS1-14742.

16 Abstract

The Integrated Energy Management (IEM) Study investigated the practicality and feasibility of a closed-loop energy management system for transport aircraft. The study involved (1) instrumentation and collection of in-flight data for a United Airlines 727-200 flying 80 revenue flights throughout the United Airlines network, (2) analysis of the in-flight data to select representative city pairs and establish operational procedures employed in flying a reference flight profile, (3) simulation of the reference profile in a fast-time model to verify the model and establish performance values against which to measure IEM benefits, (4) development of IEM algorithms, and (5) assessment of the IEM concept.

17 Key Words (Suggested by Author(s))		18 Distribution Statement
Energy management	Real-time flight optimization	[redacted]
Specific energy	Maximum specific range	
Closed-loop system	Fuel conservation	

19 Security Classif (of this report)	20 Security Classif (of this page)	21 No of Pages	22 Price*
Unclassified	Unclassified		

*Available: NASA's Industrial Applications Centers

End of Document